2-4-2020 1:00 PM

Mitochondrial Permeability Regulates Cardiac Graft Ischemia-Reperfusion Injury and Allograft Rejection

Adnan Qamar, *The University of Western Ontario*

Supervisor: Zhang, Zhuxu, *The University of Western Ontario*
Co-Supervisor: Jevnikar, Anthony, *The University of Western Ontario*
A thesis submitted in partial fulfillment of the requirements for the Master of Science degree in Pathology and Laboratory Medicine

ABSTRACT

The clinical relevance of ischemia-reperfusion injury (IRI) in the context of organ transplantation is well-established. IRI is associated with various forms of programmed cell death (PCD), of which necroptosis is particularly significant. Necroptosis is an inflammatory form of PCD that promotes alloimmunity and adversely affects allograft viability and function. We have recently shown the role of cyclophilin D (CypD), a critical mediator of mitochondrial permeability transition pore (mPTP) formation, in necroptosis. In this study, we investigated the downstream mechanism of hypoxia/reoxygenation-induced necroptosis and the effect of CypD inhibition in mitigating IRI-induced allograft injury and the subsequent alloimmune response in a clinically relevant model of cardiac transplantation. Our data indicate that inhibition of caspases during cold hypoxia-reoxygenation injury decreases apoptosis but increases necroptosis and that inhibition of CypD attenuates hypoxia/reoxygenation-induced necroptosis ($n=3$; $p\leq0.001$). Interestingly, we found that hypoxia/reoxygenation-induced necroptosis involves apoptosis-inducing factor (AIF) translocation to the nucleus and that AIF silencing also attenuates hypoxia/reoxygenation-induced necroptosis ($n=3$; $p\leq0.001$). Our *in vivo* studies confirm that CypD deficiency in ischemia-treated donor hearts mitigates IRI and allograft rejection ($n=8$; $p=0.008$). Our findings suggest that CypD inhibition following transplantation substantially attenuates necroptosis and mitigates allograft injury and the subsequent alloimmune response. Our data also indicate that AIF may be the downstream effector molecule that executes IRI-induced DNA damage in necroptosis. As such, targeting mitochondrial permeability may be a plausible approach in formulating therapeutic strategies aimed at improving allograft viability and function.

LAY SUMMARY

Organ transplantation is essential for patients with end-stage organ disease. However, the procedure itself carries its own set of risks. One of the most pertinent risks is damage to the donor organ after its blood supply is cut off. This type of injury is associated with cell death and is called ischemic injury. It may be severe enough to render the donor organ unusable. Despite stringent protocols and guidelines for organ procurement, preservation and transportation, current strategies aimed at reducing ischemic injury are insufficient. Therefore, targeting cell death pathways in ischemic injury may be a better approach. Before such strategies can be developed, a thorough understanding of the cell death pathways in ischemic injury is required. In this study, we investigated a type of cell death called necroptosis. Necroptosis is a severe form of cell death that triggers the recipient's immune response against the donor organ. Hence, inhibiting necroptosis can help prolong donor organ survival following transplantation.

Although necroptosis is involved in ischemic injury, the precise cellular mechanism(s) involved are not yet clear. According to recent research, a specialized cellular structure called mitochondrion that generates the cells' energy may be involved in necroptosis. Our data from this study indicate that mitochondrial components called 'Cyclophilin D' and 'Apoptosis-Inducing Factor' play essential roles in necroptosis. We used pharmacological agents and genetic engineering techniques to inhibit the function of Cyclophilin D and Apoptosis-Inducing Factor in individual cells and found that it protects against ischemic injury. We then extended our findings to an experiment simulating real-life conditions using mice hearts. We found that inhibiting Cyclophilin D and Apoptosis-Inducing Factor provides protection against

ischemic injury and helps promote donor heart survival. We hope to extend our findings to clinical studies and believe that our research will make the organ transplantation process better.

KEYWORDS

Ischemia-Reperfusion Injury (IRI), Mitochondrial Permeability Transition Pore (mPTP), Necroptosis, Cardiac Transplantation, Endothelial Cells

CO-AUTHORSHIPMENT STATEMENT

The following people contributed to the work undertaken as part of this research project:

- Dr. Jifu Jiang at the Matthew Mailing Centre for Translational Transplant Studies in London Health Sciences Centre performed the murine heterotopic cardiac transplantation surgeries.
- Xuyan Huang at the Matthew Mailing Centre for Translational Transplant Studies in London Health Sciences Centre collected and prepared the tissue specimens for histology.
- Winnie Liu at the University of Western Ontario processed the tissue specimens for histology and immunohistochemistry.
- Dr. Aaron Haig at the London Health Sciences Centre evaluated the tissue specimens and performed the histopathological analyses.

ACKNOWLEDGEMENTS

Firstly, I would like to thank my supervisors, Dr. Zhu-Xu Zhang and Dr. Anthony Jevnikar, for their support, guidance, and mentorship throughout my time in the Matthew Mailing Centre. I would like to thank past lab members Benjamin Fuhrmann and Ingrid Gan, and current lab members Shilpa Balaji and Alex Dionne for their companionship and advice. I would also like to thank Dr. Jacqueline Arp, Patrick McLeod Dr. Yuexia Ma and Xuyan Huang for assisting me with troubleshooting many different aspects of my project, and for providing valuable insights. I would like to thank the administrative staff at the Matthew Mailing Centre, including Punya Bose, Catherine Fraser and Pam Gardener. Lastly, I would like to thank my Advisory Committee members Dr. Tianqeng Peng and Dr. Martin Duennwald for their advice and guidance throughout my studies.

TABLE OF CONTENTS

LIST OF ABBREVIATIONS

ΔΨm: mitochondrial transmembrane potential

ACR: acute cellular rejection

AIF: apoptosis-inducing factor

AMR: antibody-mediated rejection

ANT: adenine nucleotide translocator

Apaf-1: apoptotic protease activating factor 1

APC: antigen presenting cell

ATP: adenosine triphosphate

BAK: Bcl-2 homologous antagonist killer

BAX: Bcl-2 associated X protein

BH4: tetrahydrobiopterin

BID: BH3 interacting-domain death agonist

CAV: cardiac allograft vasculopathy

CD: cluster of differentiation

cDAMP: cellular damage-associated molecular pattern

CHF: congestive heart failure

cIAP1/2: cellular inhibitors of apoptosis 1 and 2

c-FLIP: cellular FLICE-like inhibitory protein

CsA: cyclosporine A

CYLD: cylindromatosis

CypA: cyclophilin A

CypD: cyclophilin D

Cyt C: cytochrome C

DAMP: damage-associated molecular pattern

DIABLO: direct IAP binding protein with low pI

Drp1: dynamin-related protein 1

Endo G: endonuclease G

eNOS: endothelial nitric oxide synthase

ER: endoplasmic reticulum

GLUD1: glutamate dehydrogenase 1

H&E: Hematoxylin and Eosin

HLA: human leukocyte antigen

Hq mice: Harlequin mice

HSP-70: heat-shock protein 70

ICAM-1: intercellular adhesion molecule-1

ICC: immunocytochemistry

IFNγ: interferon-gamma

IGF-1: insulin-like growth factor-1

IHC: immunohistochemistry

IL: interleukin

IMM: inner mitochondrial membrane

IRI: ischemia-reperfusion injury

LFA-1: leukocyte function-associated antigen-1

LUBAC: linear ubiquitin chain assembly complex

MAC: membrane attack complex

Mac-1: macrophage-1 antigen

MCP-1: monocyte chemoattractant protein 1

Mdivi-1: mitochondrial division inhibitor 1

MHC: major histocompatibility complex

MLKL: mixed lineage kinase domain-like protein

MnSOD: mitochondrial superoxide dismutase

MOMP: mitochondrial outer membrane permeabilization

mPTP: mitochondrial permeability transition pore

mTOR: mammalian target of rapamycin

NET: neutrophil extracellular traps

NF-κB: nuclear factor-kappa B

NK cell: natural killer cell

NLRP3: NLR Family Pyrin Domain Containing 3

NO: nitric oxide

OMM: outer mitochondrial membrane

PCD: programmed cell death

PDGF: platelet-derived growth factor

PECAM-1: platelet endothelial cell adhesion molecule-1

PGAM5: serine/threonine-protein phosphatase 5

PGD: primary graft dysfunction

PRA: panel-reactive antibody

PRR: pattern recognition receptor

RHIM: RIP homotypic interaction motif

RIPK1/3: receptor-interacting serine/threonine protein kinase 1/3

ROS: reactive oxygen species

SMAC: second mitochondria-derived activator of caspases

tBID: truncated BH3 interacting-domain death agonist

TGFα/β: transforming growth factors α and β

TLR: toll-like receptor

TNFα: tumor necrosis factor-alpha

TNF-R1: TNF-receptor 1

TRADD: TNF receptor-associated death domain protein

TRAF2/5: TNF-receptor associated factors 2 and 5

TRAIL: TNF-related apoptosis-inducing ligand

VCAM-1: vascular cell adhesion molecule-1

VDAC: voltage-dependent anion channel

LIST OF FIGURES

Chapter 1

INTRODUCTION

1.1 – Current Challenges in Cardiac Transplantation

Congestive heart failure (CHF) is a significant public healthcare burden and affects 37.7 million people worldwide [1, 2]. Common underlying causes of CHF include coronary artery disease, valvular dysfunction, cardiac arrhythmias, cardiomyopathy and congenital heart disease [1, 3]. The prevalence of CHF is predicted to rise further because of improvements in the clinical management of CHF patients, an increase in predisposing conditions (diabetes, hypertension), and population expansion and ageing [4, 5]. Despite marked improvements in medical therapy and mechanical circulatory support devices, cardiac transplantation is the preferred treatment option for unresponsive, end-stage CHF patients [6, 7, 8]. Compared to end-stage CHF patients on optimal medical and device therapy, transplant recipients have improved physical function, enhanced quality of life and prolonged survival [7, 8].

Advances in human leukocyte antigen (HLA) matching, biopsy procedures, surgical techniques, and post-transplantation immunosuppressive protocols have increased the 1-year survival rate of patients undergoing cardiac transplantation to ~90% [7, 8, 9]. However, various limitations and challenges still exist. Postoperative management of patients undergoing cardiac transplantation is challenging. It includes monitoring for and addressing numerous complications with potentially significant impact on patient morbidity and mortality. These include graft failure/dysfunction (primary and late), allograft rejection, cardiac allograft vasculopathy, and adverse effects related to chronic immunosuppressive drugs (malignancy, infection) [7, 8, 10]. Despite the marked improvement in the 1-year survival rates,

complications related to chronic immunosuppression, chronic rejection and late graft failure are significant obstacles to long-term survival [7, 8, 10, 11]. Currently, the successful management of these significant post-transplantation complications is limited, and a thorough understanding of these conditions needs to be developed for improving long-term graft survival and function [7, 8, 10].

1.2 – Ischemia-Reperfusion Injury in Organ Transplantation

Ischemia-reperfusion injury (IRI) is an inevitable consequence of organ transplant procedure (Figure 1) that can have life-threatening consequences in the immediate postoperative period, such as primary graft failure or dysfunction. IRI has also been shown to have deleterious long-term effects on graft survival and can contribute to graft rejection (Figure 3) [4, 8, 12].

1.2.1 – Pathophysiology of Ischemia Injury – Ischemia occurs with the cessation of arterial blood flow during organ procurement. It is a period of insufficient oxygen and nutrients supply that disrupts the electron transport chain (ETC) and oxidative phosphorylation, which induces anaerobic metabolism [13, 14]. This ultimately leads to the depletion of adenosine triphosphate (ATP) and profoundly affects cellular homeostasis. Failure of ATP-dependent membrane pumps such as the Na^+/K^+ ATPase pump leads to intracellular sodium overload, causing cellular edema, followed by cell swelling and altered ionic composition [13, 15]. Potassium ions move out of the cell while calcium ions accumulate within the cytoplasm due to reduced extracellular efflux by Ca^{2+} pumps and limited uptake by the endoplasmic reticulum (ER). The accumulation of intracellular calcium activates calcium-dependent proteases (e.g., calpains) and phospholipases, which results in injury to various cellular components [13, 14, 15, 16]. Anaerobic metabolism leads to lactic acid accumulation, intracellular acidosis and decreased

activity of many cellular enzymes. ATP depletion and cellular edema also result in detachment of the ribosomes from the rough ER (RER) and disruption of the cell's protein-synthesizing machinery [13, 14, 15, 17]. Ionic and metabolic alterations can be reversed; however, once there is damage to the plasma membrane, lysosomes and mitochondria, irreversible widespread cellular injury occurs, and cell death follows (Figure 2) [13, 18].

1.2.2 – Pathophysiology of Reperfusion Injury – Although the restoration of blood is imperative to limit the degree of ischemic injury, it can have detrimental consequences. Injury induced by the restoration of blood supply is called reperfusion injury and occurs following reimplantation of the donor organ into the recipient. Reperfusion injury can damage previously unaffected cells and exacerbate injury caused by ischemia [13, 18]. Due to dysfunctional ETC activity and impaired cellular/mitochondrial enzymes, incoming oxygen is incompletely reduced and results in the generation of reactive oxygen species (ROS) [13, 14, 17]. ROS contribute to oxidative stress and avidly attack many biological molecules, including proteins, lipids, and nucleic acids [13, 17, 18, 19]. ROS-mediated cellular damage is exacerbated by the reduced antioxidant and ROS scavenging capacity of the cell. Restoration of blood flow further increases the intracellular accumulation of calcium ions transiently. The excess calcium ions are transported into the mitochondrial matrix by the mitochondrial Ca^{2+} uniporter [13, 17, 18]. Along with ROS, the excess calcium may induce the formation of the mitochondrial permeability transition pore (mPTP), which disrupts the proton motive force (PMF) and the mitochondrial transmembrane potential ($\Delta\Psi m$) causing further depletion of ATP [13, 17, 20]. mPTP formation also leads to augmented osmotic pressure within the mitochondria, followed by mitochondrial swelling and rupture, releasing various mediators involved in cell death pathways (Figure 2) [13, 20].

1.2.3 – IRI-Associated Inflammatory Response – The pathological changes induced by IRI trigger a non-specific inflammatory response that contributes to the immunogenicity of the allograft and adversely affects allograft survival and function [21, 22]. This inflammatory response is initiated and perpetuated by ROS-mediated cell damage that alters several endogenous molecules. The altered molecules are called damage-associated molecular patterns (DAMPs) and include extracellular ATP, DNA fragments, uric acid (DNA breakdown product), heat shock proteins, heparan sulphate, and many others [21, 23, 26]. DAMPs are recognized by cellular pattern recognition receptors (PRRs) present on circulating leukocytes, endothelial cells, and epithelial cells [21, 26]. Ligation of PRRs activates the cytoplasmic protein called NLR Family Pyrin Domain Containing 3 (NLRP3), which in turn assembles a multiprotein cytosolic complex called the inflammasome. The inflammasome recruits and activates caspase-1, which processes various proinflammatory cytokines, including potent inflammatory mediators such as interleukins-1β (IL-1β) and -18 (IL-18) [21, 24, 25]. The engagement of PRRs, particularly toll-like receptors 2 and 4 (TLR-2 and 4), by DAMPs also activates nuclear factor-kappa B (NF-κB), a transcription factor that translocates to the nucleus and upregulates the expression of several proinflammatory cytokines and chemokines [21, 26]. The important upregulated proinflammatory cytokines include tumor necrosis factor-alpha (TNFα), interferon-gamma (IFNγ), IL-1, and IL-6, while the important chemokines include IL-8 and monocyte chemoattractant protein 1 (MCP-1). These chemokines belong to the C-X-C (e.g., IL-8) and C-C chemokine (e.g., MCP-1) groups and are secreted by leukocytes and endothelial cells. The expression of proinflammatory cytokines and chemokine signaling promotes leukocyte infiltration and the activation of the complement system, thereby initiating the innate immune response [21, 26, 27].

All cells of the innate immune system express PRRs and are capable of sensing DAMPs; however, neutrophils and monocytes are principally responsible for acute inflammatory injury associated with IRI [21, 28, 29]. Neutrophils are the first leukocytes to infiltrate the site of injury. DAMPs and IL-8 from resident tissue macrophages, dendritic cells, and endothelial cells serve as potent neutrophil chemokines [21, 28]. Neutrophil-mediated graft injury involves the production and release of proteases, hydrolytic enzymes, neutrophil extracellular traps (NETs), and ROS [21, 30]. Moreover, in the presence of TNFα, neutrophils release various proinflammatory cytokines and chemokines that recruit additional leukocytes, including monocytes [21, 28]. Once recruited to the site of injury, monocytes differentiate into macrophages and can undergo the proinflammatory M1 or the anti-inflammatory M2 polarization. TNFα and IFNγ stimulation and engagement of macrophage PRRs, particularly TLR2 and TLR4, by DAMPs promote M1 polarization [21, 31, 32, 33, 34]. Activated M1 macrophages produce ROS and several proinflammatory cytokines like IL-1, IL-6, IL-17, IL-23, TNFα, and IFNγ that mediate graft injury via diverse pathways, including the induction of programmed cell death pathways [35, 36, 37, 38, 39]. Macrophage recruitment also results in significant injury to the microvasculature and activation of the adaptive alloimmune responses [21, 31, 32]. Natural Killer (NK) cells have also been shown to play crucial roles in mediating acute and chronic allograft injury. Several studies have shown that NK cells are capable of 'directly' lysing allograft endothelial and epithelial cells [40, 41]. NK cells can also 'indirectly' induce cellular death in the allograft by enhancing cellular and humoral alloimmune responses. NK cell-mediated allograft injury is significant and can occur even in the presence of T cell tolerance but remains an overlooked aspect of the immunosuppressive therapeutic strategies aimed at inducing allograft tolerance [40, 41, 42, 43, 44].

1.2.4 – Role of Endothelial Cells in IRI and Associated Inflammatory Response – Endothelial cells play a crucial role in the inflammatory response associated with IRI. Leukocyte recruitment at the site of injury involves 'endothelial activation' – a process that induces a series of changes in the endothelial cells that facilitate their interaction with leukocytes [45, 46]. TNFα, IL-1, and IL-6 upregulate the expression of adhesion molecules on the surface of endothelial cells via the activation of the NF-κB pathway [46, 47, 48]. The upregulated adhesion molecules include selectins (e.g., E-selectin and P-selectin), intercellular adhesion molecule-1 (ICAM-1), and vascular cell adhesion molecule-1 (VCAM-1). Surface glycoproteins on activated leukocytes called integrins [e.g., leukocyte function-associated antigen-1 (LFA-1) and macrophage-1 antigen (Mac-1)] serve as ligands for endothelial cell adhesion molecules and mediate leukocyte adhesion to the endothelium. This is followed by leukocyte transmigration through the endothelium, which is aided by the adhesion molecule platelet endothelial cell adhesion molecule-1 (PECAM-1), and infiltration into the graft tissue along a chemokine gradient [21, 45, 46, 47, 48, 49].

Endothelial activation can lead to 'endothelial dysfunction' if the inflammatory injury associated with IRI is severe, as is the case with prolonged ischemia times, inefficient organ preservation, or the use of extended-criteria donor organs. Severe inflammation leads to endothelial cell injury and impaired vascular homeostasis due to uncontrolled ROS production, and persistently elevated levels of proinflammatory cytokines, especially TNFα. The central mechanism underlying endothelial dysfunction is decreased nitric oxide (NO) bioavailability due to inhibition of endothelial nitric oxide synthase (eNOS) [46, 50, 51, 52]. Under normal physiological conditions, NO maintains vasodilation, suppresses platelet aggregation, prevents leukocyte adhesion, attenuates vascular smooth muscle cell proliferation, and inhibits the expression of proinflammatory cytokines (via downregulation of the NF-κB pathway) [46, 53,

54, 55]. Thus, the inhibition of eNOS due to oxidative stress and endothelial cell injury/death promotes vasoconstriction and leads to a pro-thrombotic and proinflammatory state [49, 50, 51, 52, 53, 54, 55]. Furthermore, oxidative depletion of eNOS cofactor, tetrahydrobiopterin (BH4), in dysfunctional endothelial cells 'uncouples' eNOS resulting in the incomplete reduction of molecular oxygen and generation of more ROS [49, 56]. Finally, endothelial cell injury/death results in the loss of vascular integrity and increased vascular permeability facilitating leukocyte infiltration into graft tissue and the generation of an alloimmune response [21, 49, 50, 51].

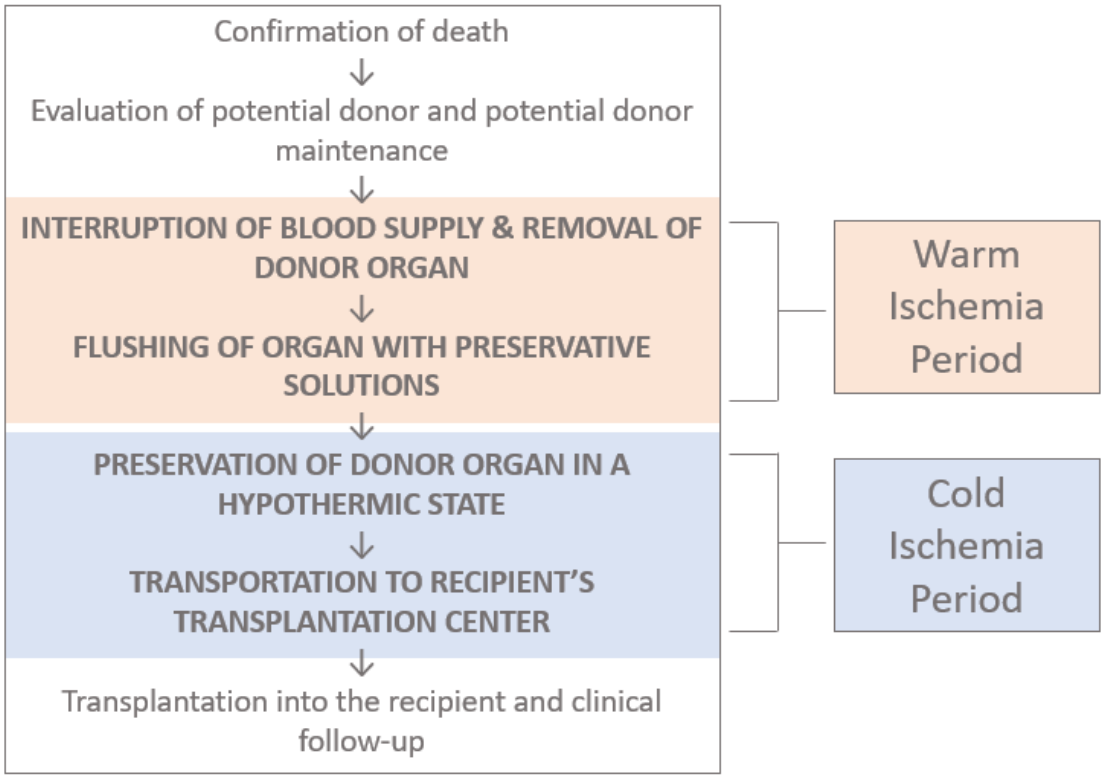

Figure 1 – Ischemia-Reperfusion Injury During Organ Transplantation

In the transplant setting, ischemia occurs in two phases called the 'warm ischemia phase' and the 'cold ischemia phase.' Warm ischemia occurs when the blood supply of the donor organ is interrupted and lasts until the donor organ is flushed with a cold organ preservation solution. Cold ischemia occurs during organ preservation. Currently, the most common method of donor organ preservation is static cold (4°C) storage on ice. The donor organ undergoes another brief period of warm ischemia when it is removed from cold storage until blood flow to the graft is re-established [57, 58, 59].

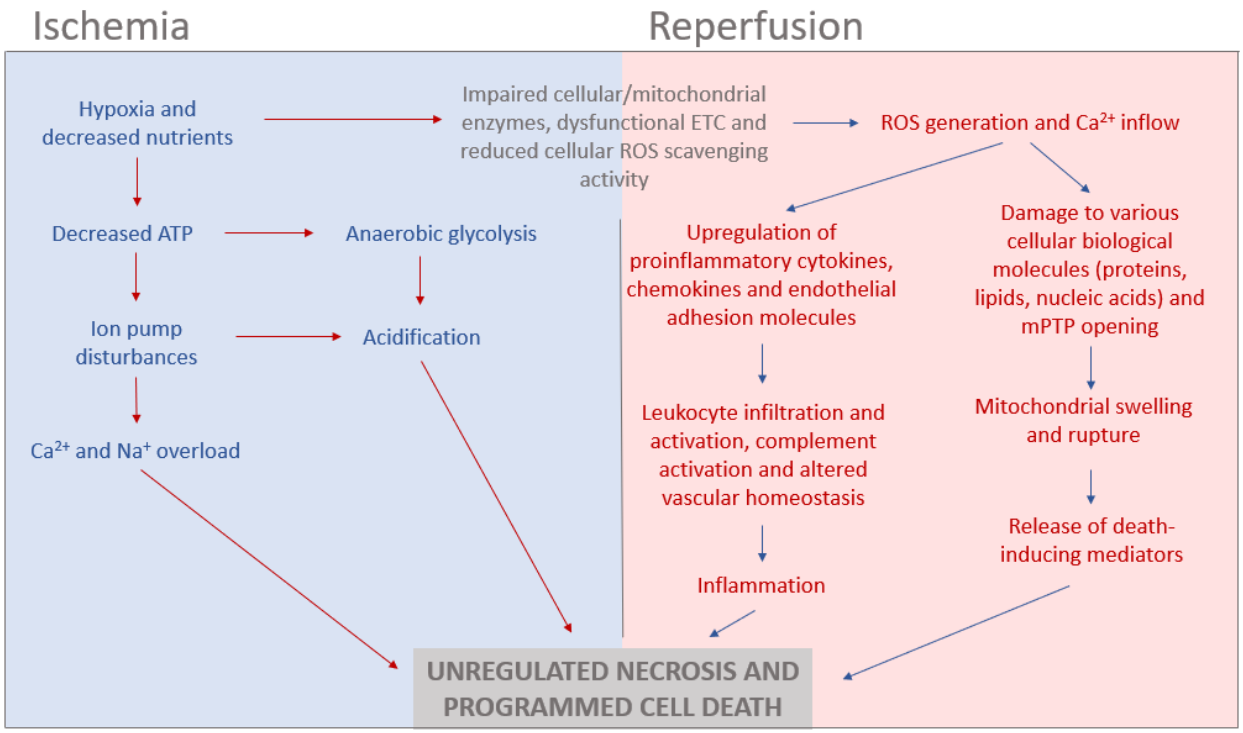

Figure 2 – Cellular Biology of Ischemia-Reperfusion Injury

The most important biochemical abnormality in ischemic cells is the decreased intracellular generation of ATP. Loss of ATP leads to the failure of many energy-dependent cellular systems, including ATP-dependent ion pumps, which results in increased intracellular sodium and calcium. Anaerobic glycolysis leads to lactic acid accumulation, resulting in intracellular acidosis. Ultimately, the failure of the critical energy-dependent systems and altered cellular ionic homeostasis can lead to cell death. During reperfusion, there is increased generation of ROS due to impaired cellular/mitochondrial enzymes, dysfunctional ETC components and reduced cellular ROS-scavenging capacity. The ROS that are generated cause damage to lipids, proteins and DNA and along with increased intracellular calcium induce mPTP formation. mPTP formation leads to loss of PMF, as a result of which there is a further decline in ATP

production. mPTP formation also leads to the release of mitochondrial factors involved in PCD pathways [13, 18, 20].

1.3 – Cardiac Allograft Dysfunction and Rejection

The cumulative pathological changes induced by IRI and the subsequent inflammatory response have a detrimental impact on the outcome of cardiac transplantation. IRI contributes to alloimmune injury and influences short-term as well as long-term allograft survival and function (Figure 3) [8, 10, 11, 12].

1.3.1 – Primary Graft Dysfunction – Amongst the early complications, primary graft dysfunction (PGD) remains the leading cause of mortality in heart transplant recipients, with a 30-day mortality rate of ~30% [8, 60]. PGD presents as the failure of the graft to meet the circulatory requirements of the recipient due to ventricular dysfunction and develops within 24 hours of transplantation. Although PGD is not associated with a discernible cause, numerous studies have postulated IRI as the predominant factor in its development [8, 59, 60, 61].

1.3.2 – Cardiac Allograft Rejection – The inflammatory insult associated with IRI promotes leukocyte recruitment (via endothelial adhesion molecules) and activation (via expression of proinflammatory cytokines/chemokines and release of cDAMPS). Leukocyte infiltration into the cardiac allograft perpetuates graft injury and initiates alloimmune responses, which culminates in allograft transplant rejection. Although the development of novel and effective immunosuppressive agents has significantly reduced the rejection rates, it continues to remain one of the major causes of death after cardiac transplantation [8, 10, 62]. Rejection can be classified as hyperacute, acute cellular (cell-mediated) or humoral (antibody-mediated) rejection [8, 10].

1.3.3 – Hyperacute Rejection – Hyperacute rejection occurs within minutes to hours following transplantation and manifests as severe graft failure with hemodynamic instability. It is

mediated by pre-formed antibodies directed against antigens in the cardiac allograft. The target antigens include human leukocyte antigens (HLA) and ABO blood antigens expressed on the allograft endothelial cells. The binding of the alloantibodies to these antigens activates the complement system, which results in endothelial disruption, thrombosis, hemorrhage, and irreversible rapid destruction of the graft by the recipient's immune system [8, 63, 64]. Histologically, hyperacute rejection manifests as vasculitis and ischemic necrosis of the cardiac allograft due to occlusive thrombosis. The management of hyperacute rejection is complicated and involves pharmacological and mechanical circulatory support, along with intense immunosuppression and plasmapheresis to remove the circulating alloantibodies. Hyperacute rejection has a high mortality rate but is now uncommon due to comprehensive pre-transplant cross-match testing, including panel-reactive antibody (PRA) screening [8, 63, 64, 65].

1.3.4 – Acute Cellular Rejection – Acute cellular rejection (ACR) is the most common type of rejection after cardiac transplantation, with over 60% of the patients experiencing one or more episodes [8, 62, 68, 69]. It generally occurs within the first six months post-transplantation [8, 62, 69]. ACR involves coordination between the innate and the adaptive immune systems, with T cells playing a central role [8, 69, 70, 71]. Alloantigen recognition in ACR can occur via the direct or the indirect pathways. In the direct pathway of alloantigen recognition, recipient T cells recognize 'intact' non-self major histocompatibility complex (MHC) molecules on donor cells within the graft tissue. In the indirect pathway, 'processed' non-self MHC molecules are presented by recipient MHC molecules to recipient T cells [70, 71, 72]. Of the professional antigen presenting cells (APCs), dendritic cells play the most important role in eliciting the alloimmune response by capturing and presenting antigens to the naive T cells in lymph nodes. The resulting primed T cells then migrate to, infiltrate, and attack

the graft tissue by multiple mechanisms, including lysis of graft cells, alloantibody production, complement activation, and recruitment of monocytes and macrophages [70, 72]. Various cytokines orchestrate the ACR response, the most important of which are TNFα, IL-1β, and CD40 [70, 73, 74, 75, 76]. Both CD4+ helper and CD8+ cytotoxic T cells are implicated in ACR [8, 69, 70, 71, 72]. Histologically, ACR is characterized by leukocyte infiltration with a predominance of T cells, edema, hemorrhage, myocyte damage/necrosis, and vasculitis [8, 69, 71]. The incidence and management of ACR have significantly improved in the past few decades due to advancements in biopsy techniques, improved histopathological grading systems, and the development of potent immunosuppressive agents [8, 66, 67].

1.3.5 – Antibody-Mediated Rejection – Antibody-mediated rejection (AMR) typically occurs within the first few months following cardiac transplantation in 10-20% of the patients [77, 78, 79]. Recipient antibodies directed against MHC Class I and Class II molecules on the surface of endothelial cells, activate the complement system, and initiate inflammatory pathways that cause injury to graft tissue [8, 77, 78, 79]. The recipient alloantibodies may be pre-formed and present prior to transplantation or may form following innate immune system activation after transplantation. Complement activation leads to endothelial cell and myocyte lysis via the formation of membrane attack complex (MAC) [66, 79, 80]. Since the primary focus of the recipient alloantibodies is the endothelium, the allograft microvasculature undergoes significant injury resulting in increased vascular permeability and intravascular thrombosis. The complement fragments C3a and C5a induce endothelial activation, and serve as potent chemokines for neutrophils and macrophages, which further augments the inflammatory injury through cytotoxic actions, ROS production and cytokine release [8, 77, 78, 79].

Histologically, AMR was initially described as a "biopsy-negative rejection" due to vasculitis, edema and hemorrhage in the absence of cellular infiltrate in the graft tissue; however, standardized clinical and pathological criteria for the diagnosis of AMR are now available [71, 77, 78, 79]. Myocardial capillaries, venules and arterioles display varying levels of injury depending on the severity of AMR, with vasculitis and leukocyte infiltration indicating an active AMR response. Interstitial edema, hemorrhage and intravascular thrombi may also be seen. AMR necessitates aggressive immunosuppression with more severe cases requiring plasmapheresis and hemodynamic support. Severe or persistent AMR may lead to cardiac allograft vasculopathy [8, 71, 77, 78, 79, 81, 82].

1.3.6 – Cardiac Allograft Vasculopathy – Cardiac allograft vasculopathy (CAV) represents a substantial barrier to the long-term survival of the cardiac allograft. It is the most significant determinant of patient survival after three years of cardiac transplantation and occurs in up to 50% of the patients within ten years of the transplant procedure [8, 65, 83, 84, 85]. CAV is characterized by progressive diffuse concentric intimal hyperplasia and medial disease involving the epicardial and intramural arteries, arterioles, and capillaries with relative sparing of the venules and veins [71, 83, 85, 86]. The pathophysiologic factors involved in the development of CAV are both immunologic and non-immunologic. Immunologic factors include the degree of MHC mismatch between the donor and the recipient, and the severity of the acute rejection episodes, particularly those involving injury to the endothelium (such as AMR) [71, 83, 85]. Non-immunologic factors include age, sex, obesity, dyslipidemia, diabetes mellitus, hypertension, and graft IRI [66, 67, 83, 85]. Both immunologic and non-immunologic factors result in endothelial activation/dysfunction [8, 66, 67, 83, 85].

MHC molecules on the surface of graft endothelial cells activate recipient CD4+ helper and CD8+ cytotoxic T cells, which then orchestrate the graft injury and fibroproliferative repair processes by recruiting inflammatory cells and inducing cytokine secretion [83, 85, 86, 87]. The important cytokines include IL-2, TNFα, and IFNγ. IL-2 promotes T cell proliferation and differentiation while TNFα and IFNγ both increase the expression of MHC molecules and promote endothelial activation/dysfunction [83, 85, 87, 88, 89]. TNFα also has direct cytotoxic effects and IFNγ activates macrophages. The recruited macrophages contribute to graft injury and produce several growth factors such as platelet-derived growth factor (PDGF), insulin-like growth factor-1 (IGF-1) and transforming growth factors α and β (TGFα and β) [83, 88, 89]. These growth factors cause smooth muscle cell migration, proliferation, and extracellular matrix deposition in the intima, resulting in concentric thickening of the vasculature [8, 66, 67, 83, 85, 86, 87, 88, 89, 90].

Clinically, CAV is asymptomatic due to denervation of the transplanted graft and is difficult to detect. It is a progressive disease associated with adverse outcomes and may necessitate surgical intervention for revascularization and re-transplantation in the most severe cases. Furthermore, the current surveillance methods and diagnostic tools for the detection of CAV have significant limitations. Accordingly, prevention is an essential strategy [8, 83, 85, 88, 91]. The use of statins and mammalian target of rapamycin (mTOR) inhibitors provide significant protection against CAV [8, 83, 91, 92]. Addressing the immunologic and non-immunologic factors associated with the development of CAV is also important [8, 66, 83].

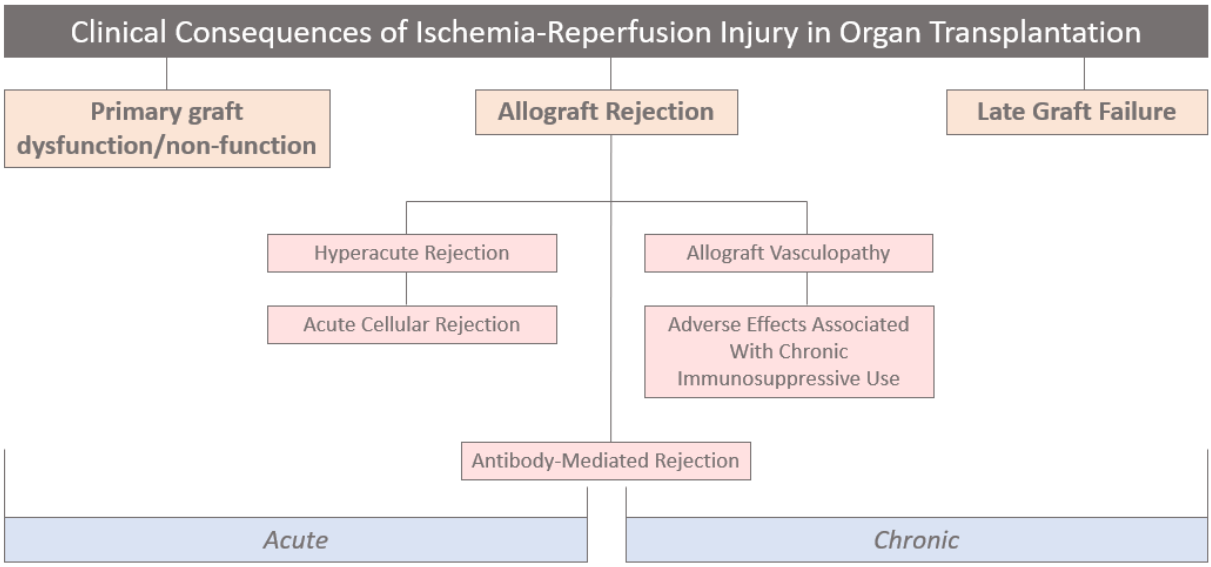

Figure 3 – Clinical Consequences of Ischemia-Reperfusion Injury in Organ Transplantation

The cumulative pathological changes induced by IRI causes cellular death and inflammation with life-threatening consequences in the immediate postoperative period, such as primary graft dysfunction/non-function. IRI contributes to acute and chronic alloimmune injury via cellular and humoral immune responses and has been shown to have deleterious long-term effects on graft survival and contributes to graft rejection. The use of potent immunosuppressive agents to induce graft tolerance is also associated with life-threatening adverse effects such as diabetes, infections and malignancy [8, 10, 12, 65, 66, 67, 77, 90].

1.4 – The Endothelium in Cardiac Transplantation

The endothelium is crucial in maintaining the vascular homeostasis by regulating thrombosis, thrombolysis, platelet adherence, vascular tone, and blood flow. It also plays an active part in immune surveillance by facilitating and limiting the recruitment of leukocytes and stimulating immune reactivity. In transplantation, it represents the first barrier between the graft tissue and the recipient's immune system. The role of the endothelium on the outcome of the transplantation procedure was often overlooked in the past [42, 93, 94]. This was particularly true for cardiac transplantation, where cardiomyocytes were considered more sensitive to IRI and the primary target of the alloimmune response. Several studies have now established that endothelial cells are not only more susceptible to IRI than cardiomyocytes but also perpetuate the graft IRI and play an active role in the subsequent alloimmune response [95, 96].

Endothelial cells undergo many of the pathological changes associated with IRI, including disruption of critical energy-dependent cellular systems, intracellular acidosis, electrolyte imbalances, cellular swelling, and damage to various biological molecules by ROS and degradative enzymes [49, 94, 95]. These changes can induce endothelial activation/dysfunction, injury, and death. Endothelial activation/dysfunction contributes to the inflammatory response associated with IRI by secreting proinflammatory cytokines (IL-1, IL-6, IL-8, TNFα) and upregulating the expression of adhesion molecules (E-selectin, P-selectin, ICAM-1, VCAM-1) that facilitate leukocyte infiltration into the graft tissue [50, 51, 94]. Injury to the endothelial cells generates ROS and cDAMPS that perpetuate IRI and augment the inflammatory response [47, 48, 49, 50, 56]. Endothelial cells express many alloantigens and contribute to the development of alloimmune responses [8, 10, 65, 66, 67, 77, 90]. They also

express MHC molecules (Class I and II) and co-stimulatory molecules, including CD80 and CD86, that can activate naive T cells [97, 98, 99, 100]. Endothelial cells are the primary target in all types of graft rejection [8, 72, 77, 83, 94]. In the chronic setting, they play a crucial role in allograft vascular disease by stimulating the migration of smooth muscle cells to the intimal layer and deposition of fibrous matrix. Significant endothelial cell injury and death results in loss of vascular integrity and tone, increased vascular permeability, and intravascular thromboses, which disrupts blood flow, promotes inflammation and alloimmunity, and ultimately, contributes to graft injury and necrosis [8, 10, 65, 66, 67, 77, 90].

1.5 – Endothelial Cell Death

At the cellular level, the cumulative pathological changes induced by IRI may lead to cell death, which may be unregulated or programmed (Figure 2) [101, 102, 105]. The detrimental effects of cell death on graft injury and alloimmunity have been extensively characterized. Inhibiting cell death in organ transplantation is important for two reasons. Firstly, uncontrolled cell death with insufficient replacement of cells adversely affects graft survival and function [102, 103, 104, 105]. Secondly, the release of cytoplasmic contents and cDAMPs from dying cells triggers and sustains alloimmune responses [13, 18, 20, 21]. Several different forms of programmed cell death (PCD) are now known, broadly classified as apoptosis and regulated necrosis types. The latter includes many further types, including necroptosis, pyroptosis, ferroptosis, and oxytosis, among others. [101, 102, 105]. As the role of these different forms of PCD in organ transplantation becomes increasingly evident, targeting these cell death pathways can potentially present novel therapeutic approaches to preserve graft function and survival. This is especially important considering the limited success of recipient immunosuppression in alleviating alloimmunity and prolonging graft

survival. Amongst the various regulated necrosis types, the detrimental role of necroptosis in inducing graft injury and alloimmunity is best characterized [102, 103, 104, 105].

Endothelial cells are susceptible to the different forms of PCD induced by IRI (Figure 4). Given the central role of the endothelium in developing and sustaining the alloimmune response, preventing endothelial cell death is particularly important. Several studies, including some from our group, have established the role of apoptosis and necroptosis in cardiac and other solid organ transplantation [8, 10, 25, 26, 27, 28, 32, 43, 44]. Understanding the mediators and the signal transduction pathways involved in the induction of endothelial cell necroptosis will help elucidate targets for mechanism-based inhibitors that can help preserve graft survival and function [102, 103, 104, 105].

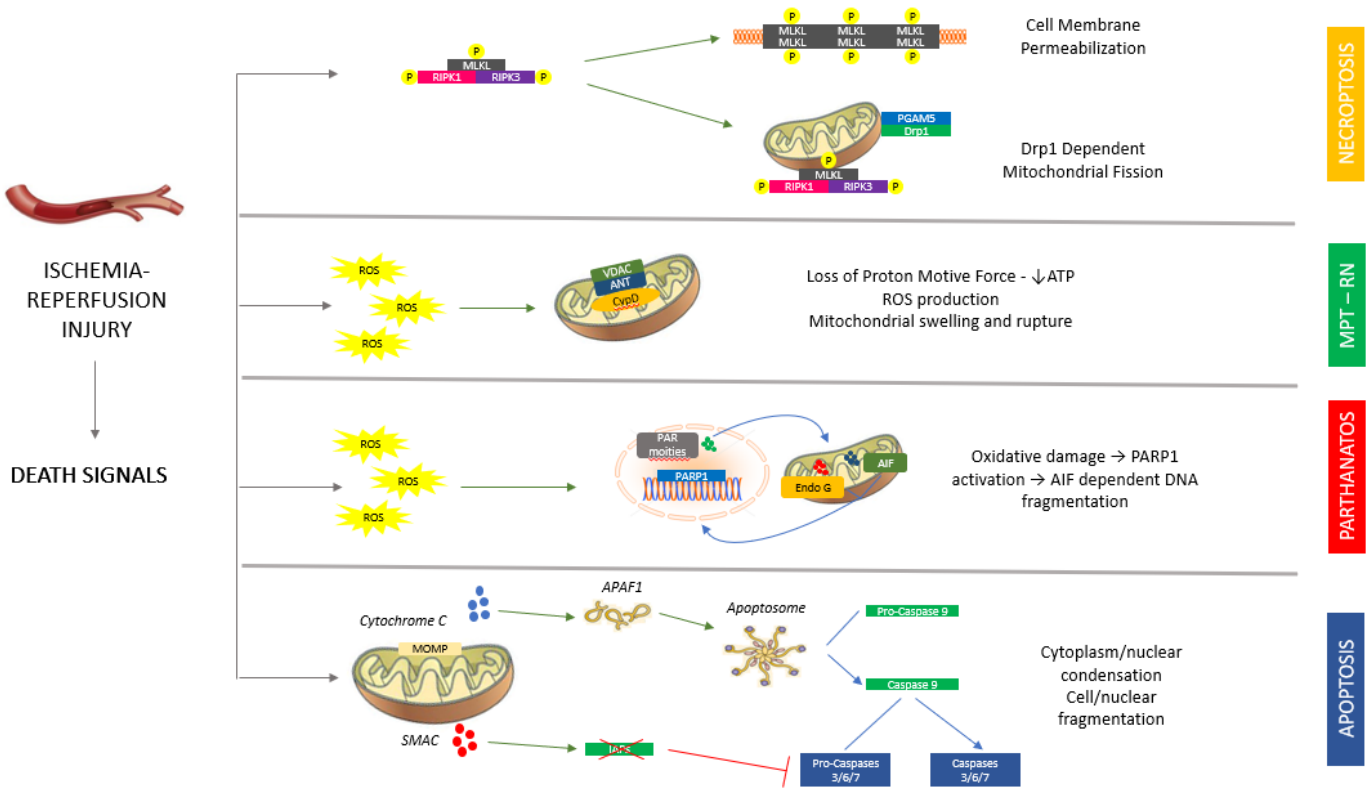

Figure 4 – Programmed Cell Death Pathways Induced by Ischemia-Reperfusion Injury

In the context of IRI, the major PCD pathways studied include apoptosis, necroptosis and parthanatos. The mitochondria play a critical role in inducing all of the PCD pathways associated with IRI. Although the downstream mechanisms involved in necroptosis are not established, most studies strongly support a role for the mitochondria in necroptosis and suggest the involvement of the CypD-mediated mPTP formation [13, 102, 105, 106, 107].

1.6 – Necroptosis

1.6.1 – Shared Upstream Pathway of Apoptosis and Necroptosis – The upstream signaling pathways of apoptosis (extrinsic) and necroptosis are shared (Figure 5). In organ transplantation, apoptosis and necroptosis can both be initiated due to direct and severe injury to the cell or due to proinflammatory cytokines and factors. The ligation of TNFα with TNF-receptor 1 (TNF-R1) mediates the best characterized pathway of necroptosis. Necroptosis can also be initiated by TLR3, TLR4, Fas ligand, and TNF-related apoptosis-inducing ligand (TRAIL) [102, 103, 104, 105, 106]. IRI involves the expression of several of these factors as well as necroptosis-inducing injury to the cells such as ROS-mediated damage and calcium overload [13, 18, 20].

The binding of TNFα to TNF-R1 recruits TNF receptor-associated death domain protein (TRADD), TNF-receptor associated factors 2 and 5 (TRAF2/5), cellular inhibitors of apoptosis 1 and 2 (cIAP1/2), linear ubiquitin chain assembly complex (LUBAC), and receptor-interacting serine/threonine protein kinase 1 (RIPK1). This complex of proteins is called 'Complex I.' cIAP1/2, and LUBAC possess E3 ubiquitin ligase activity and polyubiquitinate RIPK1. This results in signaling through the pro-survival NF-κB pathway and counters the cytotoxic effects of TNFα [102, 103, 104, 105, 106].

In the presence of persistent or severe injury, RIPK1 is deubiquitinated by the enzymes A20 and cylindromatosis (CYLD). CYLD is a deubiquitinase that counters the ubiquitin ligase activities of cIAP1/2 and LUBAC and removes the ubiquitin chains from RIPK1. Deubiquitinated RIPK1 dissociates from Complex I and interacts with FAS-associated Death Domain (FADD), procaspase-8 and cellular FLICE-like inhibitory protein (c-FLIP) to form the 'Death Inducing Signaling Complex' (DISC) or 'Complex IIa.' c-FLIP has three different

splice variants, c-FLIP$_L$, c-FLIP$_S$ and c-FLIP$_R$, which regulate the activity of caspase-8 differently. c-FLIP$_S$ and c-FLIP$_R$ inhibit apoptosis by preventing caspase-8 processing and activation. c-FLIP$_L$ is an enzymatically inert homolog of caspase-8 and its activity is dependent on its expression levels, which in turn is dependent on the extent of cellular injury and the level of NF-κB activation [102, 105, 108].

When expressed at low levels, c-FLIP$_L$ forms a heterodimer with procaspase-8 and activates it. Activated caspase-8 is considered the 'initiator' caspase. It forms homodimers that activate the procaspases-3, -6 and -7 to their 'effector' active forms, which mediate cell death via apoptosis. The c-FLIP$_L$/caspase-8 heterodimer prevents necroptosis by cleaving the crucial necroptotic mediators RIPK1 and RIPK3. The inhibitory effect of c-FLIP$_L$/caspase-8 heterodimer on necroptosis explains why caspase-8 deficient mice are embryonically lethal and why RIPK3 deficiency in these mice rescues them from lethality [102, 107, 108]. This also indicates that, in addition to promoting apoptosis, an important function of caspase-8 is to prevent necroptosis. When expressed at high levels, c-FLIP$_L$ partially processes procaspase-8, the cleavage activity of which is limited to DISC. This partially processed caspase-8 cleaves the DISC associated proteins, including RIPK1 and itself, and prevents both apoptosis and necroptosis [102, 103, 104, 107, 108].

It is important to note that the ubiquitination status of RIPK1 determines cellular fate. RIPK1 ubiquitination promotes cellular survival by restricting the interactions of the pro-apoptotic caspase-8 and the pro-necroptotic RIPK3 with RIPK1. Deubiquitination of RIPK1 promotes cell death by permitting the interaction of caspase-8 and RIPK3 with RIPK1 and activating the downstream death pathways [102, 105, 106, 107, 108].

1.6.2 – The 'Necrosome' – If caspase-8 activity is disrupted (in case of mutation, inhibitory viral proteins or ischemia), RIPK1 detaches from DISC and interacts with RIPK3 via the RIP homotypic interaction motif (RHIM) domains. RIPK1 and RIPK3 then auto- and trans-phosphorylate each other to form the 'necrosome' or 'Complex IIb.' The necrosome-associated, phosphorylated RIPK3 then phosphorylates mixed lineage kinase domain-like protein (MLKL), which initiates the downstream signaling in necroptosis. When overexpressed, RIPK3 can also phosphorylate MLKL independent of RIPK1 [102, 105, 106, 109, 110].

1.6.3 – Downstream Pathway of Necroptosis – It is now established that necrosome formation and phosphorylation of MLKL are essential for necroptosis; however, the precise pathway downstream of necrosome formation is unclear. Several studies have been conducted to elucidate the downstream pathway involved in necroptosis with contradictory results. However, most studies have suggested that the mitochondria, in one form or another, play a pivotal role in necroptosis [102, 105, 106].

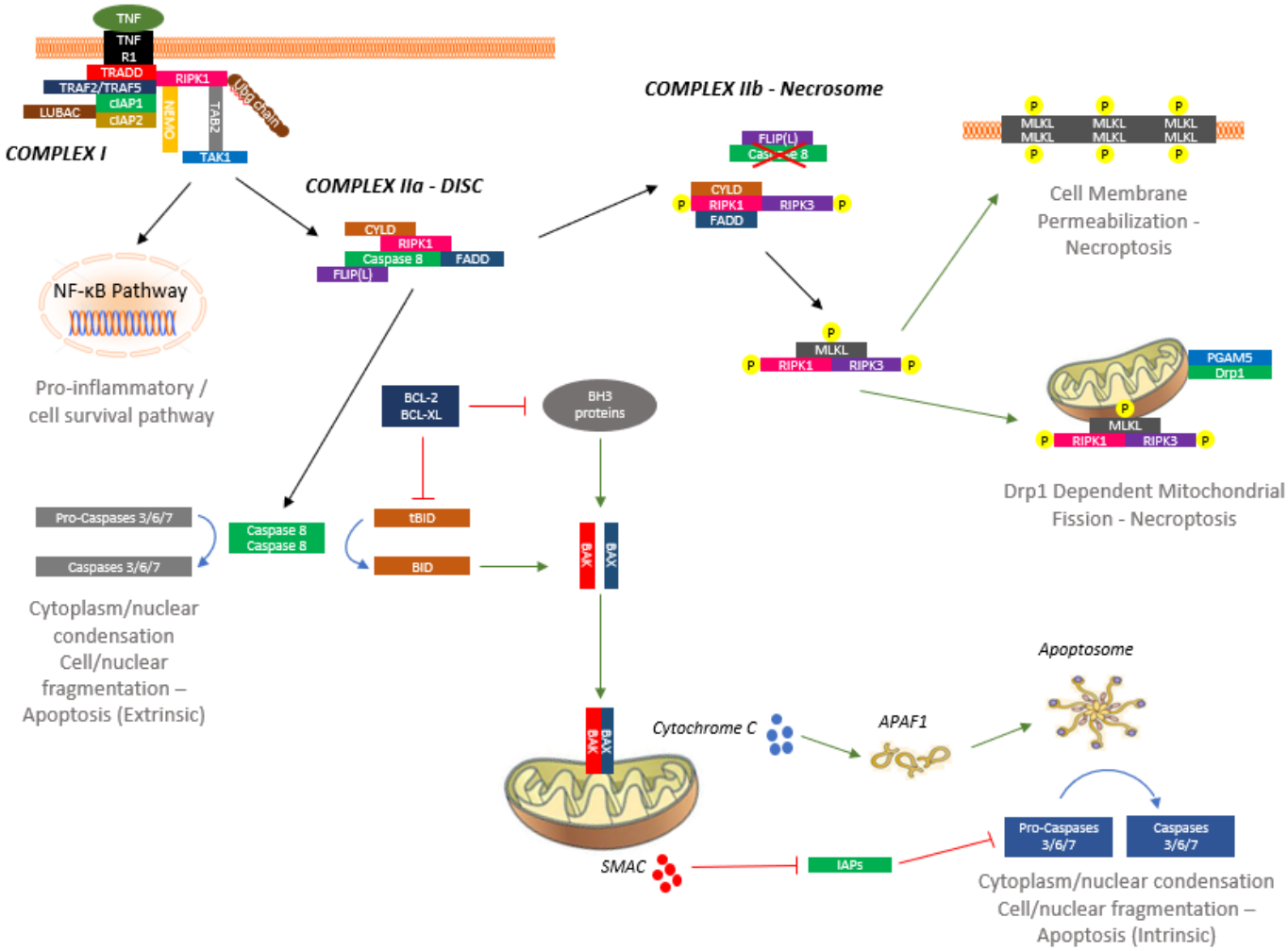

Figure 5 – Necroptosis Mediators and Signaling Pathway

The best-characterized pathway of necroptosis involves the ligation of TNFα with TNF-R1, which recruits TRADD, TRAF2/5, cIAP1/2, LUBAC and RIPK1 to form Complex I. cIAP1/2 and LUBAC then polyubiquitinate RIPK1 which results in signaling through the pro-survival NF-κB pathway. Persistent/severe injury results in RIPK1 deubiquitination by the enzymes A20 and CYLD. Deubiquitinated RIPK1 interacts with FADD, procaspase-8 and c-FLIP$_L$ to form Complex IIa. c-FLIP$_L$ differentially regulates the activation/inhibition of caspase-8 depending on its expression levels. Activated caspase-8 induces apoptosis via activation of

caspases-3, -6 and -7; however, if caspase-8 activity is disrupted, RIPK1 interacts with RIPK3 to form Complex IIb. RIPK1 and RIPK3 then auto- and trans-phosphorylate each other and also phosphorylate MLKL, which initiates the downstream signaling in necroptosis [102, 105, 106, 109, 110].

1.7 – Mitochondria in Cell Death

Mitochondria are highly dynamic organelles that have vital roles in cellular bioenergetics, metabolism, biosynthesis, and regulation of diverse signals that determine the fate of the cell. Cellular injury leads to mitochondrial dysfunction that disrupts the mitochondrial functions integral to the survival of the cell and activates signals that promote cell death. Although mitochondria are involved in several forms of PCD, their role in apoptosis and necroptosis is most relevant to IRI (Figures 5 and 7) [104, 106, 111, 112, 113].

1.7.1 – Role of Mitochondria in Apoptosis – Apoptosis can be initiated through two different pathways - extrinsic (via death receptor stimulation) and intrinsic. Although mitochondria are involved in both pathways, they have a more critical role in the intrinsic pathway of apoptosis (Figure 5) [111, 112, 113]. Pathological changes associated with cell injury such as ROS-mediated oxidative damage, intracellular calcium overload, and DNA damage (all of which may result from IRI) can initiate the intrinsic pathway of apoptosis by permeabilization of the outer mitochondrial membrane (OMM). Mitochondrial outer membrane permeabilization (MOMP) is normally tightly regulated by the B cell lymphoma 2 (Bcl-2) family of pro- and anti-apoptotic members. Following an apoptotic stimulus, the pro-apoptotic Bcl-2 associated X protein (BAX) and Bcl-2 homologous antagonist killer (BAK) undergo conformational changes and form homo-oligomers that form pores in the OMM. Permeabilization of the OMM releases pro-apoptotic proteins such as Cytochrome C (Cyt C) and second mitochondria-derived activator of caspases (SMAC)/direct IAP binding protein with low pI (DIABLO) [111, 112, 113, 114]. Cyt C is an essential ETC component that interacts with apoptotic protease activating factor 1 (Apaf-1), procaspase-9 and dATP to form the apoptosome. The apoptosome activates procaspase-9 to the 'initiator' caspase-9 that cleaves procaspases-3, -6 and -7 to their

active forms. SMAC/DIABLO promotes apoptosis by neutralizing the inhibitory effect of IAPs on caspases [102, 111, 112, 113, 114].

The extrinsic pathway of apoptosis, triggered by death receptor stimulation, is linked to the intrinsic pathway of apoptosis by the pro-apoptotic Bcl-2 protein, BH3 interacting-domain death agonist (BID). Caspase-8 cleaves BID into its truncated form, tBID, which promotes the OMM permeabilization by BAX and BAK and release of Cyt C and SMAC/DIABLO [111, 112, 113, 114].

1.7.2 – Role of Mitochondria in Necroptosis – As explained earlier, most studies suggest a role for mitochondria in necroptosis. However, even for the studies indicating a mitochondrial role, the precise signaling pathway is a point of contention (Figures 5 and 7) [106]. The earliest studies done to investigate the mitochondrial role in necroptosis suggested that the involvement of ROS generation is secondary to mitochondrial damage and ETC disruption [115, 116, 117, 118, 119]. These studies have shown the formation of necrosome and its translocation to the mitochondria along with pMLKL following TNFα signaling [106, 115, 116, 117, 120, 121, 122, 123]. Furthermore, the use of the antioxidant butylated hydroxyanisole prevented ROS generation and TNFα-induced necroptosis [115, 116]. In other studies, the ROS generated were determined to be mitochondrially derived. Inhibiting cytoplasmic ROS generation by the enzyme NADPH oxidase did not inhibit TNFα-induced necroptosis; however, suppression of the ETC complex I and the use of the mitochondria-specific ROS scavenging enzyme, mitochondrial superoxide dismutase (MnSOD), did [115, 116, 122]. There is also evidence suggesting the involvement of the mitochondrial enzyme glutamate dehydrogenase 1 (GLUD1) in TNFα-induced ROS production and necroptosis [121].

The involvement of the mitochondrial factors serine/threonine-protein phosphatase 5 (PGAM5) and Dynamin-related protein 1 (Drp1) in necroptosis have also been studied [123, 124]. According to these studies, following necroptosis induction, the necrosome and pMLKL translocate to the mitochondria, where they activate PGAM5. PGAM5 then recruits and activates Drp1 by dephosphorylation of serine 637 of Drp1. Activated Drp1 induces mitochondrial fragmentation, resulting in necroptosis. In support of these findings, Drp1 inhibition (with Mdivi-1) and deficiency have been shown to reduce TNFα-induced necroptosis. Furthermore, coimmunoprecipitation assays have indicated a direct interaction between necrosome and PGAM5 following TNFα signaling [123, 124].

Among the proposed mitochondrial mediators of necroptosis, evidence for the role of mPTP is the strongest [104, 106]. As explained earlier, IRI induces the formation of mPTP, which leads to cellular demise via $\Delta\Psi m$ dissipation, ATP depletion, ROS production, and mitochondrial swelling and rupture, releasing various cell death mediators [20]. Genetic experiments involving cells and mice deficient for cyclophilin D (CypD), a critical regulator of mPTP opening, have shown resistance to cell death induced by necroptotic mediators. Furthermore, these experiments have also shown that the protection conferred by CypD inhibition or ablation is not additive to that conferred by blocking the upstream signaling pathway in necroptosis [125, 126, 127].

It is important to note that some studies have indicated that necroptosis can occur independently of mitochondria. In a study investigating the role of mitochondria in necroptosis, widespread mitochondrial depletion via mitophagy did not prevent TNFα-induced necroptosis [128]. The role of mitochondrial ROS, PGAM-Drp1 axis and mPTP formation in necroptosis is also disputed and not fully established. Several studies have shown that treatment with a

variety of antioxidants did not attenuate cell death following ROS production in response to TNFα signaling. Similarly, necroptosis was observed in cells despite PGAM5 and Drp1 knockdown [128, 129, 130, 131]. Although evidence for the role of mPTP in necroptosis is strongest, findings from one study have questioned its role. This study reveals that simultaneous RIPK3 and CypD ablation provides greater protection against necroptosis than separate RIPK3 and CypD depletions in the context of renal IRI [132]. The most compelling studies disputing the role of mitochondria in necroptosis indicate that necrosome formation is followed by phosphorylation and oligomerization of MLKL. Oligomerized pMLKL complexes then translocate to the plasma membrane, where they compromise its integrity by forming holes [133, 134, 135, 136].

1.8 – Mitochondrial Permeability Transition Pore

The outer and inner membranes of the mitochondria are different from each other in several aspects. OMM is relatively permeable due to the presence of the voltage-dependent anion channels (VDAC), which form general diffusion pores for ions and hydrophilic molecules between the mitochondria and cytosol. The inner mitochondrial membrane (IMM), on the other hand, is highly impermeable and effectively separates the mitochondrial matrix from the cytosol. Movement of ions and metabolites across IMM involves specialized membrane transporters [20, 137, 138]. The ETC complexes are embedded within IMM and are responsible for establishing the $\Delta\Psi m$ by creating a proton gradient across IMM. This proton gradient is used by the 'F1/F0 ATP synthase' to generate ATP. Increased permeability of IMM disrupts the proton gradient and the $\Delta\Psi m$, resulting in decreased ATP synthesis. It also enables the loss of ETC components, which results in the incomplete reduction of oxygen and ROS production [140, 141]. The loss of mitochondrial antioxidants compromises the ROS

neutralizing ability of the mitochondria and further augments oxidative damage. The 'pore' responsible for the increased permeability of the IMM is the entity termed 'mPTP' (Figure 6) [20, 137, 138, 139, 140, 141]. mPTP formation also results in the influx of metabolites (<1.5 kDa) and water into the mitochondrial matrix leading to osmotic swelling. Swelling of the mitochondrial matrix may not compromise the integrity of IMM because of cristae unfolding, but it exerts pressure on OMM and ruptures it. This releases cell death mediators, such as the pro-apoptotic ETC component Cyt C, resulting in cellular demise [20, 137, 138, 139].

1.8.1 – Structural Components of mPTP – While the pathological consequences of mPTP formation are well established, its exact structural components are still disputed. According to the classical model, mPTP spans the mitochondrial intermembrane space and comprises of VDAC in OMM and adenine nucleotide translocator (ANT) in IMM, besides the regulatory component, CypD, in the mitochondrial matrix. Although genetic tests do not fully support the roles of VDAC and ANT, the role of CypD in regulating mPTP formation is well established. [106, 137, 138]. CypD regulation of mPTP formation occurs even in the absence of VDAC and ANT [20, 106, 137, 138].

Recent studies have suggested that the OMM component of mPTP may be formed by the pro-apoptotic Bcl-2 proteins BAX and BAK that form MOMP in their active oligomerized state [138, 142, 143]. According to this more current model, the IMM component is formed by the c-subunit of F1/F0 ATP synthase. CypD binds with the oligomycin sensitivity-conferring protein (OSCP) of F1/F0 ATP synthase and triggers mPTP formation through its dimerization. This model also suggests that the two structural components of mPTP do not form in apposition to form a contiguous pore [142, 143]. The regulation of mPTP occurs at F1/F0 ATP synthase in IMM while MOMP is relatively non-selective. Some studies have also suggested that BAX

and BAK generate a low level of OMM permeability even in their non-oligomerized (inactive) states, although evidence for this is inconclusive (Figure 6) [137, 138, 139, 142, 143].

1.8.2 – Formation of mPTP in IRI – Under physiological conditions, brief and abrupt mPTP formation (mPTP flickering) is considered a mitochondrial calcium efflux mechanism and maintains calcium homeostasis [137, 144]. IRI results in ROS generation and increased intracellular calcium, the two most potent triggers of prolonged and pathological mPTP formation [13, 106, 139, 140, 141]. As explained earlier, ischemia results in insufficient ATP levels, increased intracellular sodium and calcium and decreased intracellular pH. Although ischemia is associated with increased intracellular calcium, mPTP formation is not observed. This may be due to the hydrogen ions competing with the calcium ions at the trigger site. Reperfusion is associated with the additional generation of ROS, further calcium overload and restoration of the intracellular pH. The removal of the accumulated hydrogen ions enables the increased intracellular calcium to trigger the formation of mPTP. ROS-mediated oxidative damage promotes mPTP formation by sensitizing mPTP to increased calcium levels and by increasing CypD interaction with the IMM component of mPTP (Figure 5) [13, 18, 20].

1.8.3 – Role of mPTP in Necroptosis – As explained earlier, evidence supporting the role of mitochondria in necroptosis is most indicative of mPTP formation (Figure 5). Recent studies have suggested that the precise mechanism of necroptosis may involve the release of pro-necroptotic mediators following mPTP formation [104, 145, 146]. The putative mitochondrial pro-necroptotic mediators currently being investigated are apoptosis-inducing factor (AIF) and endonuclease G (Endo G). AIF and Endo G are mitochondrial proteins that translocate to the nucleus following their release into the cytosol and mediate DNA fragmentation, a characteristic finding observed in necroptosis [145, 146]. According to a recent study, CypD

inhibition prevents AIF and Endo G translocation to the nucleus [145]. Furthermore, as with RIPK1 and RIPK3 inhibition, CypD and AIF/Endo G silencing are protective against IRI, suggesting their role in necroptosis [147, 148]. mPTP formation in IRI may also lead to ROS generation, another potential mediator of necroptosis and ATP depletion that ultimately leads to unregulated necrosis (Figure 7) [13, 18, 20, 106].

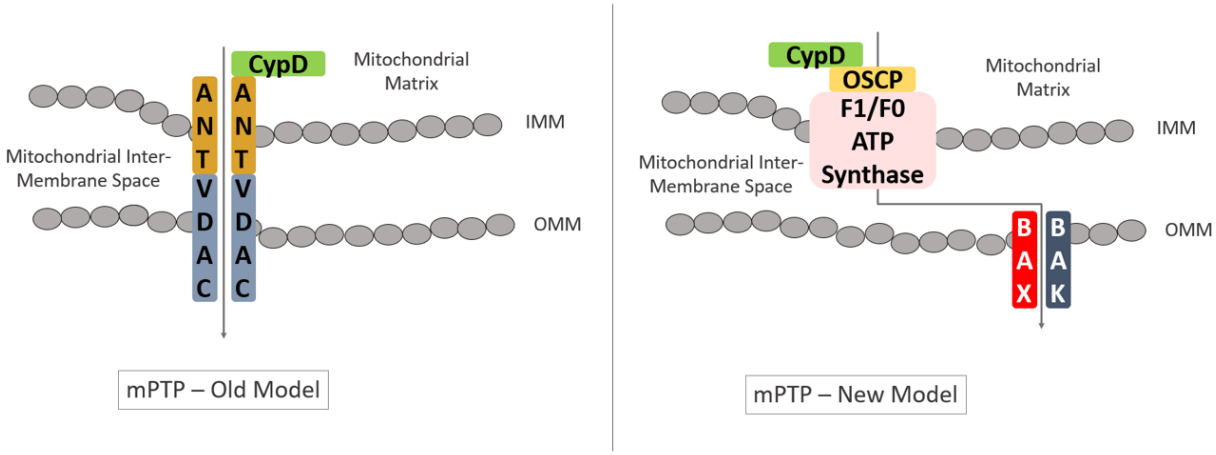

Figure 6 – Mitochondrial Permeability Transition Pore Components and Structure

The classical model of mPTP involves VDAC in the OMM, ANT in the IMM and the regulatory component CypD in the mitochondrial matrix. Although genetic tests do not fully support the roles of VDAC and ANT, CypD regulation of mPTP formation occurs even in the absence of VDAC and ANT. According to the current model of mPTP, the OMM component of mPTP may be formed by the pro-apoptotic Bcl-2 proteins BAX and BAK that form MOMP in their active oligomerized state while the IMM component is formed by F1/F0 ATP synthase. CypD binds with OSCP of F1/F0 ATP synthase and triggers mPTP formation through its dimerization. This model also suggests that the two structural components of mPTP do not form in apposition to form a contiguous pore. The regulation of mPTP occurs at F1/F0 ATP synthase in IMM, while MOMP is relatively non-selective [137, 138, 142, 143].

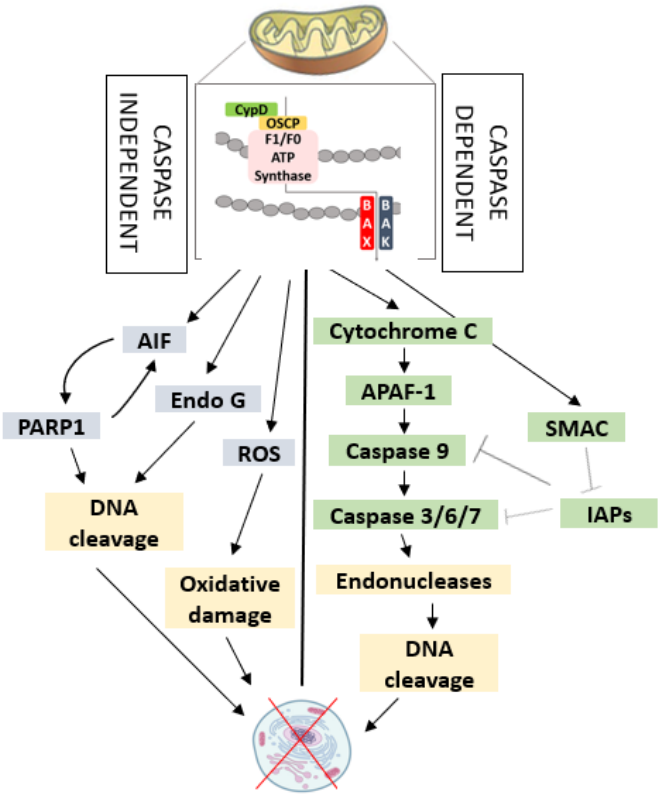

Figure 7 – Role of Mitochondria in Programmed Cell Death Pathways

Mitochondria play a critical role in unregulated necrosis and PCD. MOMP formation contributes to apoptosis via the release of Cyt C, cIAP1/2 and SMAC/DIABLO. Following cellular injury (especially IRI), mPTP formation may contribute to ROS production, which have a role in inducing necroptosis in several cell types. mPTP formation also facilitates the release of AIF/Endo G, which then translocate to the nucleus and mediate DNA fragmentation, a characteristic finding observed in necroptosis and parthanatos. Finally, persistent mPTP formation results in loss of PMF and $\Delta\Psi m$, resulting in failure of critical energy-dependent cellular systems and cell death via unregulated necrosis [13, 18, 20, 104, 106, 111, 145, 146, 147, 148, 149].

1.9 – Apoptosis-Inducing Factor

AIF is a mitochondrial flavoprotein that, under physiological conditions, has essential pro-survival functions. AIF has oxidoreductase activity and is crucial for the biogenesis and stabilization of key ETC components, Complex I and Complex III [147, 148]. Harlequin (Hq) mice, which have a hypomorphic AIF mutation (80% reduction) due to proviral insertion at the X-linked *Aifm1* (AIF gene) locus, display phenotypic changes characteristic of mitochondrial diseases and disruption in energy metabolism. These mice develop severe neuromuscular mitochondriopathies and exhibit progressive hair loss, neurodegeneration, ataxia and blindness due to retinal degeneration [147, 148, 149]. Cardiac and skeletal muscle-specific AIF knockout results in cardiomyopathy and skeletal atrophy [146, 147, 148, 151]. Consistent with these findings, *in vitro* experiments indicate that cells lacking AIF have high lactic acid production due to ETC disruption and anaerobic glycolysis [145, 146, 147, 148, 149].

Although mitochondrion-localized AIF has pro-survival functions, extra-mitochondrial AIF is involved in PCD (Figure 8). Following its release into the cytoplasm, AIF translocates to the nucleus and triggers caspase-independent cell death by inducing DNA damage. AIF-mediated DNA degradation has been shown to occur in response to several types of pathologic insults, including IRI. Mitochondria purified following IRI show a decrease in their AIF content and presence of AIF in the nucleus [147, 148]. There is limited evidence suggesting that inhibition of the upstream necroptotic pathway and blocking mPTP formation restricts AIF-mediated DNA fragmentation [145, 148]. Furthermore, mitochondrial calcium overload, a potent trigger for mPTP formation, also induces AIF release [145, 147, 148].

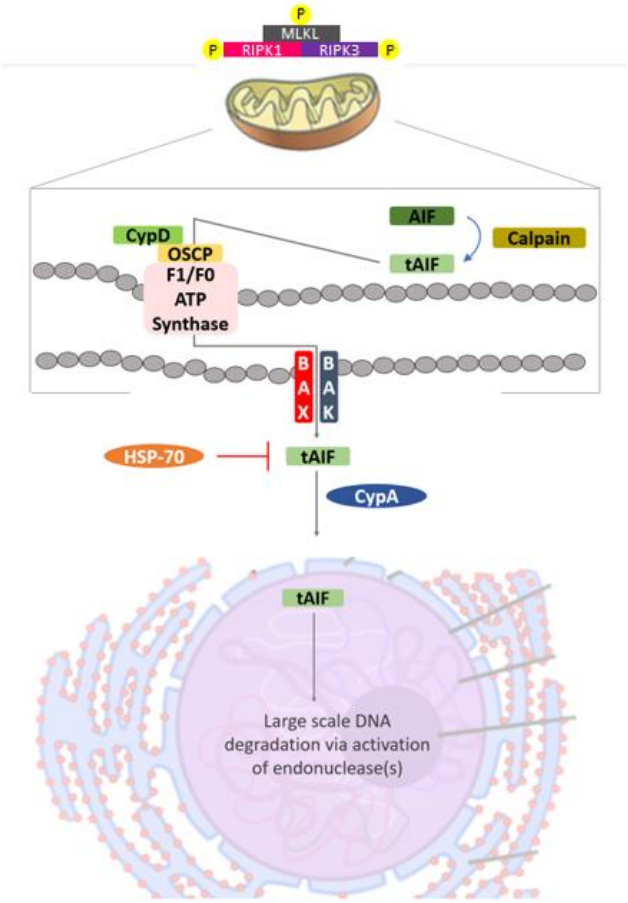

Figure 8 – Role of Apoptosis-Inducing Factor in Programmed Cell Death

Mitochondrion-localized AIF has essential pro-survival functions in cellular bioenergetics; however, extra-mitochondrial AIF is involved in PCD. Following its release into the cytoplasm by a death-inducing signaling event, AIF is cleaved to its truncated form and translocates to the nucleus where it mediates large-scale DNA fragmentation via activation of an unidentified endonuclease. Recent studies have suggested that mPTP formation may facilitate the release of AIF from the mitochondria. AIF translocation to the nucleus is inhibited by HSP-70 and facilitated by CypA [145, 146, 147, 148].

1.10 – Study Rationale

A growing body of evidence indicates that necroptosis is a highly inflammatory form of PCD that contributes to IRI-mediated allograft injury and promotes recipient alloimmune responses [102, 105]. As such, it represents a relevant therapeutic target in the clinical management involving organ transplantation. Previous studies from our lab suggest that necroptosis contributes to kidney IRI and promotes cardiac and renal allograft rejection [103, 104]. We have also shown that inhibition of RIPK3 and CypD prevents necroptosis in murine microvascular endothelial cells, thereby establishing the significance of these mediators in the necroptotic pathway. In our previous studies, inhibition of RIPK3 and CypD attenuated allograft rejection and promoted graft survival [103, 104]. Although the upstream signaling molecules and pathways involved in necroptosis are well-established, the role of mitochondria and the downstream mediators involved are mostly unknown [102, 106]. The main objective of this study was to investigate the precise role of CypD-mediated mPTP formation in promoting mitochondrial damage and release of mediators involved in DNA fragmentation associated with hypoxia/reoxygenation-induced necroptosis. We also translated findings from our previous studies supporting the role of CypD inhibition in promoting graft survival to a clinically relevant model involving prolonged cold ischemic organ storage followed by heterotopic transplantation.

1.11 – Hypothesis

We hypothesize that ischemia-reperfusion injury induces mitochondrial damage, release of mitochondrial factors, and activation of the downstream mechanisms of nuclear fragmentation, thus promoting allograft injury and transplant rejection.

1.12 – Study Aims

1. To determine the role of CypD in endothelial cell death following *in vitro* cold hypoxia-reoxygenation injury.
2. To determine the effectiveness of CypD inhibition in attenuating IRI-aggravated transplant rejection and prolonging graft survival.
3. To investigate the mitochondrial mechanism(s) involved in mediating DNA fragmentation in hypoxia/reoxygenation-induced endothelial cell necroptosis.
4. To determine the effectiveness of inhibiting the mitochondrial mechanism(s) involved in mediating DNA fragmentation in attenuating IRI-mediated transplant rejection and prolonging graft survival.

Chapter 2

MATERIALS AND METHODS

2.1 – Mice

Wild-type (WT) C57BL/6 (B6), BALB/c and B6 CypD$^{-/-}$ mice were purchased from the Jackson Laboratory (Bar Harbor, ME, USA). The mice were maintained in the Animal Care and Veterinary Services facility at Western University. All animal use protocols and experimental procedures were approved by the institutional Animal Care Committee.

2.2 – Cardiac Transplantation and Post-Operative Monitoring

Donor hearts from WT and CypD$^{-/-}$ mice were heterotopically transplanted into the abdominal region of BALB/c mice. The mice were anesthetized with a mixture of ketamine/xylazine before the transplantation procedures. Donor hearts were removed after clamping the aortae, vena cavae and pulmonary arteries and veins. They were then flushed with cold normal saline and stored in Lactated Ringer's buffer (Baxter International Inc., Deerfield, IL, USA) at 4°C for 4 hours before heterotopic transplantation into the abdominal cavity in recipient mice. Aortae from the donor hearts were sutured to the recipient mice abdominal aortae and the donor heart pulmonary arteries were sutured to the recipient mice inferior vena cavae. The vena cavae and pulmonary veins in the donor hearts were sutured shut. The hearts were observed for spontaneous contractions following transplantation before the recipient mice were sutured close. Cardiac transplantation experiments were performed by experienced microsurgeons at the Matthew Mailing Centre for Translational Transplantation Studies at the London Health Sciences Centre according to institutionally approved protocols.

Following the transplantation procedure, the immunosuppressive sirolimus (rapamycin; LCL Laboratories, Woburn, MA, USA) at 1 mg/kg was given from the operative day to postoperative day 9. Graft survival was monitored daily by abdominal palpation for pulse detection. Cessation of or significant drop in pulsation was considered as graft rejection and confirmed by histopathological analysis.

2.3 – Histology and Immunohistochemistry

Cardiac allografts in the recipient mice were collected on the day of rejection or at 21 days post-transplantation for pathological analysis. The recipient mice were anesthetized with a mixture of ketamine/xylazine before the abdominal cavities were opened and the allografts removed. The isolated cardiac allografts were then flushed with normal saline, fixed with 10% neutral buffered formalin and embedded in paraffin for sectioning. The tissue sections were then stained with Hematoxylin & Eosin (H&E) and Verhoeff–Van Gieson elastic stain to evaluate damage to microvasculature, neointima formation and fibrosis. The tissue sections were also stained with anti-CD3 and anti-CD68 antibodies (eBioscience, San Diego, CA, USA) to evaluate and quantify T cell and macrophage infiltration, respectively. Tissue sectioning and staining was done by a laboratory technician according to the manufacturers' protocols. Graft injury was evaluated based on the change in endothelium and leukocyte infiltration compared to naïve tissue by a pathologist in a blinded manner. The following changes were evaluated and quantified: damage to microvasculature, neointima formation, fibrosis, and leukocyte infiltration. The criteria used scored the injury on a scale of 0-4 as follows – 0: no change, 1: 0-24% change, 2: 25-49% change, 3: 50-74% change, and 4: >75% change.

2.4 – Endothelial Cell Culture

Endothelial cells were isolated as per the established protocol described previously [103]. Endothelial cells were isolated from the ventricles of 3-4 weeks old WT and CypD$^{-/-}$ mice. The major vessels (aortae, pulmonary veins and vena cavae) and atrial tissue were cut out and discarded. The ventricles were washed thoroughly with Dulbecco's Phosphate Buffered Saline (PBS; Thermo Fisher Scientific, Mississauga, ON, Canada) and minced before incubation in D-Hank's digestion buffer containing Collagenase II (1 mg/mL) and Dispase II (2 mg/mL) (Thermo Fisher Scientific, Mississauga, ON, Canada) at 37°C for 40 mins. The cell suspension was filtered using a 100 μm nylon mesh filter and then incubated with anti-CD31 coated Dynal magnet beads (Invitrogen, Burlington, ON, Canada) for 30 mins. The isolated CD31-positive cells were then washed and grown in Endothelial Cell Growth Basal Medium-2 (EBM-2; Lonza, Mississauga, ON, Canada) containing 5% fetal bovine serum (FBS), 0.04% hydrocortisone, 0.4% human fibroblast growth factor (hFGF), 0.1% vascular endothelial cell growth factor (VEGF), 0.1% R3-insulin-like growth factor-1 (R3-IFG-1), 0.1% ascorbic acid, 0.1% human epidermal growth factor (hEGF) and 0.1% gentamicin-sulfate amphotericin 1000 (GA-1000). The phenotype of isolated endothelial cells was confirmed by flow cytometry analysis of CD31, CD102 and CD105 (eBioscience, San Diego, CA, USA). The positively staining cells were then immortalized by origin-defective SV40-plasmid transfection.

Normal cell culture medium used to grow endothelial cells was prepared by supplementing 1 g/L glucose Dulbecco's Modified Eagle Medium (DMEM; Thermo Fisher Scientific, Mississauga, ON, Canada) with 10% FBS and 1% penicillin/streptomycin. Cells were passaged a maximum of ten times with 0.25% trypsin (Life Technologies, Burlington, ON, Canada) before being discarded.

CypD$^{-/-}$ endothelial cells did not display any phenotypic changes as compared to WT endothelial cells. The growth and baseline turnover of the CypD$^{-/-}$ endothelial cells were comparable to the WT endothelial cells.

2.5 – RNA Interference Silencing

WT endothelial cells were seeded on 6-well plates and grown to 60-80% confluency in normal cell culture medium. The cells were washed with PBS before transfection with ON-TARGETplus Mouse *Aifm1* siRNA (Dharmacon, Lafayette, CO, USA) using EndoFectin™ Max transfection reagent (Genecopoeia, Rockville, MD, USA) in Opti-MEM® media (Invitrogen, Carlsbad, CA, USA). ON-TARGETplus Mouse *Aifm1* siRNA was used at various concentrations from 100 nM – 800 nM. siRNA-induced silencing of *Aifm1* expression was confirmed by quantitative reverse transcription-polymerase chain reaction (RT-qPCR) and Western Blot, respectively at 24-, 48-, 72- and 96-hours post-transfection. Based on RT-qPCR and Western Blot results, the manufacturer-recommended dose of 200 nM was used for this study. The AIF-silenced cells were harvested at 48-hours post-transfection by 0.25% trypsin for cell death assays.

2.6 – RT-qPCR

siRNA-induced silencing of *Aifm1* expression was confirmed by RT-qPCR at 24-, 48-, 72- and 96-hours post-transfection. Total RNA from scrambled siRNA-transfected cells and *Aifm1* siRNA-transfected cells was extracted using TRIzol Reagent (Invitrogen, Carlsbad, CA, USA). The concentration and purity of the isolated RNA was measured using the NanoDrop™ 2000 Spectrophotometer (Thermo Fisher Scientific, Mississauga, ON, Canada). cDNA was generated from RNA using SuperScript™ II Reverse Transcriptase (Thermo Fisher Scientific,

Mississauga, ON, Canada). RT-qPCR was performed using Brilliant II SYBR® Green QPCR Master Mix (ABM, Vancouver, BC, Canada) and CFX Connect™ Real-Time PCR Detection System (Bio-Rad, Hercules, CA, USA). The *Aifm1* primers used are as follows: *Aifm1* forward primer (5' – 3') GTA GAT CAG GTT GGC CAG AAA CTC and *Aifm1* reverse primer (5' – 3') GGA TTA AAG GCA TGT GCC AAC ACG. *β-actin* was used as endogenous control for gene expression analysis. *β-actin* primers used are as follows: *β-actin* forward primer (5' – 3') CCA GCC TTC CTT CCT GGG TA and *β-actin* reverse primer (5' – 3') CTA GAA CAT TTG CGG TGC A. The ΔCt values for *Aifm1* and *β-actin* were used to calculate the $2^{-\Delta\Delta Ct}$ to get the expression fold change.

2.7 – Western Blots

siRNA-induced silencing of AIF protein expression was confirmed by Western Blot analysis at 24-, 48-, 72- and 96-hours post-transfection. Total protein from scrambled siRNA-transfected cells and *Aifm1* siRNA-transfected cells was extracted using RIPA Lysis and Extraction Buffer (Thermo Fisher Scientific, Mississauga, ON, Canada) with Thermo Scientific™ Pierce Protease Inhibitor Cocktail Tablets (Thermo Fisher Scientific, Mississauga, ON, Canada). The concentration and purity of the isolated protein was measured by Bradford Dye Protein Assay using GENESYS™ 10S UV-Vis Spectrophotometer (Thermo Fisher Scientific, Mississauga, ON, Canada). The isolated protein samples were denatured by boiling in a loading buffer (4% SDS, 5% 2-mercaptoethanol, 20% glycerol, 0.004% bromophenol blue, 0.125 M Tris-HCl; pH adjusted to 6.8) at 95°C for 5 minutes. The protein samples were then equally loaded (30-40 μg) in the wells of 10% SDS-PAGE gel and the gel was run at 100 V for ~1.5 hours in the electrophoresis apparatus with 1X running buffer (25 mM Tris base, 192 mM glycine, 0.1% SDS; pH adjusted to 8.3). The separated protein samples were transferred

onto polyvinylidene fluoride (PVDF; activated with methanol) membrane in a transfer apparatus filled with ice-cold 1X transfer buffer (25 mM Tris base, 192 mM glycine, 20% methanol; pH adjusted to 8.3). The transfer cassette was prepared with the PVDF membrane, filter paper and fiber pads and the transfer apparatus was placed in ice and run at 70 V for ~1.5 hours. Once the protein samples were transferred onto the PVDF membrane, the membrane was blocked with 5% bovine serum albumin (BSA) in TBS-T (20 mM Tris base, 150 mM NaCl, 0.1% Tween-20) on a standard analogue shaker (VWR, Mississauga, ON, Canada) at room temperature for 1 hour. After blocking, the PVDF membrane was incubated with primary rabbit anti-mouse AIF antibody (Cell Signaling Technology, Danvers, MA, USA) at 1:1000 dilution in 2.5% BSA in TBS-T overnight at 4°C. The PVDF membrane was then washed with TBS-T 3X for 15 minutes each time before incubation with HRP-conjugated secondary goat anti-rabbit antibody (Cell Signaling Technology, Danvers, MA, USA) at 1:1000 dilution in 2.5% BSA in TBS-T at 4°C for 1 hour. The PVDF membrane was then washed with TBS-T 3X for 10 minutes each time before it was developed for protein visualization using the HRP chemiluminescent substrate (EMD Millipore, Burlington, MA, USA) and imaged in the FluorChem M Imaging System. The housekeeping proteins, β-actin and/or GAPDH, were used as loading controls. Murine anti-mouse β-actin antibody (MilliporeSigma, Etobicoke, ON, Canada) was used to detect β-actin and rabbit anti-mouse GAPDH antibody (Abcam, Cambridge, UK) was used to detect GAPDH.

To detect the expression of pMLKL in endothelial cells undergoing necroptosis, endothelial cell cultures (in 6-well plates) were subjected to the *in vitro* cold hypoxia-reoxygenation injury model described earlier. The reoxygenation phase was limited to 12-18 hours at which point, the total protein was isolated and analyzed as described earlier. The primary antibody used to detect pMLKL was rabbit anti-mouse pMLKL (S345) antibody

(Abcam, Cambridge, UK). The primary antibody used to detect MLKL was rat anti-mouse MLKL antibody (MilliporeSigma, Etobicoke, ON, Canada).

2.8 – *In Vitro* Cold Hypoxia-Reoxygenation Injury Model

To model ischemia injury, endothelial cell cultures were incubated in oxygen-depleted, glucose-free DMEM under hypoxic condition in Whitley H45 Hypoxystation (Don Whitley Scientific, United Kingdom) or anaerobic GENbags (BioMérieux, France). For cold hypoxia, the Hypoxystation was set at 10°C for 24 hours and the GENbags were placed in a refrigerator set at 4°C. To model reperfusion injury, the endothelial cell cultures were removed from the hypoxic environment and the oxygen-depleted, glucose free DMEM was replaced with normal cell culture medium in a normoxic incubator. Human TNFα (hTNFα; PeproTech, Rocky Hill, NJ, USA) at 50-100 μg/mL and recombinant mouse IFNγ (PeproTech, Rocky Holl, NJ, USA) at 50-100 μg/mL were added during both the hypoxia and the reoxygenation phases to simulate the IRI microenvironment *in vitro*. Pan-caspase inhibition was achieved by adding the pan-caspase inhibitor N-Benzyloxycarbonyl-Val-Ala-Asp(O-Me) fluoromethyl ketone (z-VAD-fmk; BD Biosciences, Mississauga, ON, Canada) at 30 μM. RIPK1 inhibition was achieved by adding the RIPK1 specific kinase inhibitor necrostatin-1s (Nec-1s; Merck Millipore, Etobicoke, ON, Canada) at 10 μM. CypD mediated mPTP formation was inhibited by Cyclosporin A (CsA; Sigma-Aldrich, Oakville, ON, Canada) at 0.5-20 μM. The immunosuppressive FK-506 (Sigma-Aldrich, Oakville, ON, Canada), which is a calcineurin inhibitor but not a CypD inhibitor was used as CsA control. The ROS scavengers used include the superoxide dismutase mimetic 1-oxyl-2,2,6,6-tetramethyl-4-hydroxypiperidine (TEMPOL; Sigma-Aldrich, Oakville, ON, Canada) at 5-20 μM, the glutathione precursor N-acetyl-L-cysteine (NAC; Sigma-Aldrich, Oakville, ON, Canada) and the mitochondrion-

specific superoxide dismutase mimetic mito-TEMPOL (Sigma-Aldrich, Oakville, ON, Canada) at 5-20 μM. To inhibit Drp1-mediated mitochondrial division, the Mitochondrial Division Inhibitor 1 (Mdivi-1; Sigma-Aldrich, Oakville, ON, Canada) was used at 10-40 μM. The CypA inhibitor, Alisporivir (DebioPharm, Lausanne, Switzerland) was used at 0.25-4 μM to prevent AIF translocation. Based on available literature and dose-response curves indicating maximum reduction in hypoxia/reoxygenation-induced cell death, a dose of 1 μM for Alisporivir was chosen for the study. The PARP-1 inhibitor, 3-aminobanzamide (3-ABA; MilliporeSigma, Etobicoke, ON, Canada) at 10-100 μM was used to inhibit parthanatos. The inhibitors were added during both the hypoxia and the reoxygenation phases. Endothelial cells from $CypD^{-/-}$ mice and AIF-silenced endothelial cells were also subjected to the *in vitro* cold hypoxia-reoxygenation injury model.

2.9 – Cell Death Assay

Cell death was detected and quantified by real-time imaging in the IncuCyte ZOOM® Live Cell Analysis System (Essen Bioscience, Ann Arbor, MI, USA). SYTOX™ Green Nucleic Acid Stain (Thermo Fisher Scientific, Mississauga, ON, Canada) at 100 nM was used to indicate dead cells. SYTOX™ Green is impermeable to live cells but crosses the compromised plasma membranes of dead cells and stains the nucleic acid. It is excited with 488 nm laser light in the IncuCyte and fluoresces green which helps in distinguishing dead cells from live cells. Cell death was also detected with propidium iodide (PI) or annexin V labeling (BD Bioscience, Mississauga, ON, Canada) and analyzed by flow cytometry (Beckman Coulter, Mississauga, ON, Canada).

2.10 – Immunocytochemistry

To show AIF translocation to the nucleus from the mitochondria in endothelial cells undergoing necroptosis, endothelial cell cultures (in 96-well plates) were subjected to the *in vitro* cold hypoxia-reoxygenation injury model described earlier. The reoxygenation phase was limited to 24 hours at which point, the cells were fixed with 4% paraformaldehyde in PBS (pH 7.4) for 30 minutes at room temperature. The cells were washed 3X for 5 minutes each time with PBS and then incubated with 0.1-0.25% Triton™ X-100 non-ionic surfactant in PBS for 10 minutes at room temperature for permeabilization. The cells were washed again 3X for 5 minutes each time with PBS. To reduce non-specific antigen binding and background fluorescence, the cells were incubated in a blocking solution (1% BSA, 22.52 mg/mL glycine and 0.1% Tween 20) for 30-45 minutes at room temperature. Following blocking, the cells were incubated with primary rabbit anti-mouse AIF antibody diluted in 1% BSA in PBS with 0.1% Tween-20 at 1:1000 concentration ratio for 1 hour at room temperature in a humidified chamber. The cells were then washed 3X for 5 minutes each time and then incubated with secondary donkey anti-rabbit PE-conjugated antibody (Abcam, Cambridge, United Kingdom) diluted in 1% BSA in PBS at 1:60 concentration ratio for 1 hour at room temperature in a dark humidified chamber. The cells were washed again 3X for 5 minutes each time with PBS. For nuclear counterstaining, the cells were incubated with 300 nM DAPI staining solution (Thermo Fisher Scientific, Mississauga, ON, Canada) for 5 minutes at room temperature in a humidified chamber and then washed 3X for minutes each time with PBS. Nikon Inverted Research Microscope ECLIPSE Ts2R (Nikon, Tokyo, Japan) was used to capture fluorescent images at 20-40X magnification.

2.11 – DNA Gel Analysis

To analyze AIF-mediated DNA degradation into ~50 kbp fragments, endothelial cell cultures (in 6-well plates) were subjected to the *in vitro* cold hypoxia-reoxygenation injury model described earlier. The reoxygenation phase was limited to 12-18 hours at which point, DNA was isolated using the Qiagen Blood & Cell Culture DNA Mini Kit (Qiagen, Hilden, Germany). The concentration and purity of the isolated DNA was measured using the NanoDrop™ 2000 Spectrophotometer (Thermo Fisher Scientific, Mississauga, ON, Canada). The size of the isolated DNA fragments was characterized by electrophoretic separation using 0.3% agarose gel run at 3-4 V/cm. For DNA visualization, the agarose gel was stained with SYBR™ Safe DNA Gel Stain and imaged in the FluorChem M Imaging System.

2.12 – Statistical Analysis

The experimental values are expressed as mean ± SD. Data was analyzed using the Student's t-test for unpaired values, and 1- and 2-way ANOVA with Tukey's post-hoc corrections test. The Mantel-Cox Log Rank test was used to determine graft survival differences. Differences were considered significant when p-value ≤ 0.05.

Chapter 3

RESULTS

3.1 – *In Vitro* Cold Hypoxia-Reoxygenation Injury Promotes Necroptosis in Endothelial Cells

Endothelial cells from WT B6 mice were isolated and subjected to the *in vitro* cold hypoxia-reoxygenation injury model described earlier. TNFα, IFNγ, z-VAD-fmk and Nec-1s were added during the hypoxia as well as the reperfusion phases. Murine TNFα (mTNFα) can bind to both TNF-R1 and TNF-R2 [225, 226, 227]. While TNF-R1 signaling induces cell death, TNF-R2 signaling promotes cell survival [223, 224]. To ensure signaling through the TNF-R1, human TNFα (hTNFα) was used, which specifically binds to murine TNF-R1 (with limited TNF-R2 binding) [225, 226, 227]. SYTOX™ Green staining was used to indicate and measure cell death in the IncuCyte. Treatment of endothelial cells with the proinflammatory cytokines hTNFα and IFNγ increased cell death compared to untreated cells (Figure 9). The addition of z-VAD-fmk to hTNFα + IFNγ treated cells increased cell death compared to cells treated only with hTNFα + IFNγ. z-VAD-fmk is a pan-caspase inhibitor and prevents apoptosis; therefore, the increase in cell death following treatment with z-VAD-fmk was suggestive of necroptosis. This was confirmed with the addition of the RIPK1 inhibitor Nec-1s. The addition of Nec-1s significantly reversed the cell death observed in the hTNFα + IFNγ + z-VAD-fmk treated cells.

Cell death during and immediately following the cold hypoxia phase was minimal and progressively increased during the reperfusion phase in all treatment groups (Figure 9A). Cell

death in the first 36 hours was negligible in the absence of cold hypoxia-reoxygenation injury in all treatment groups

.

A

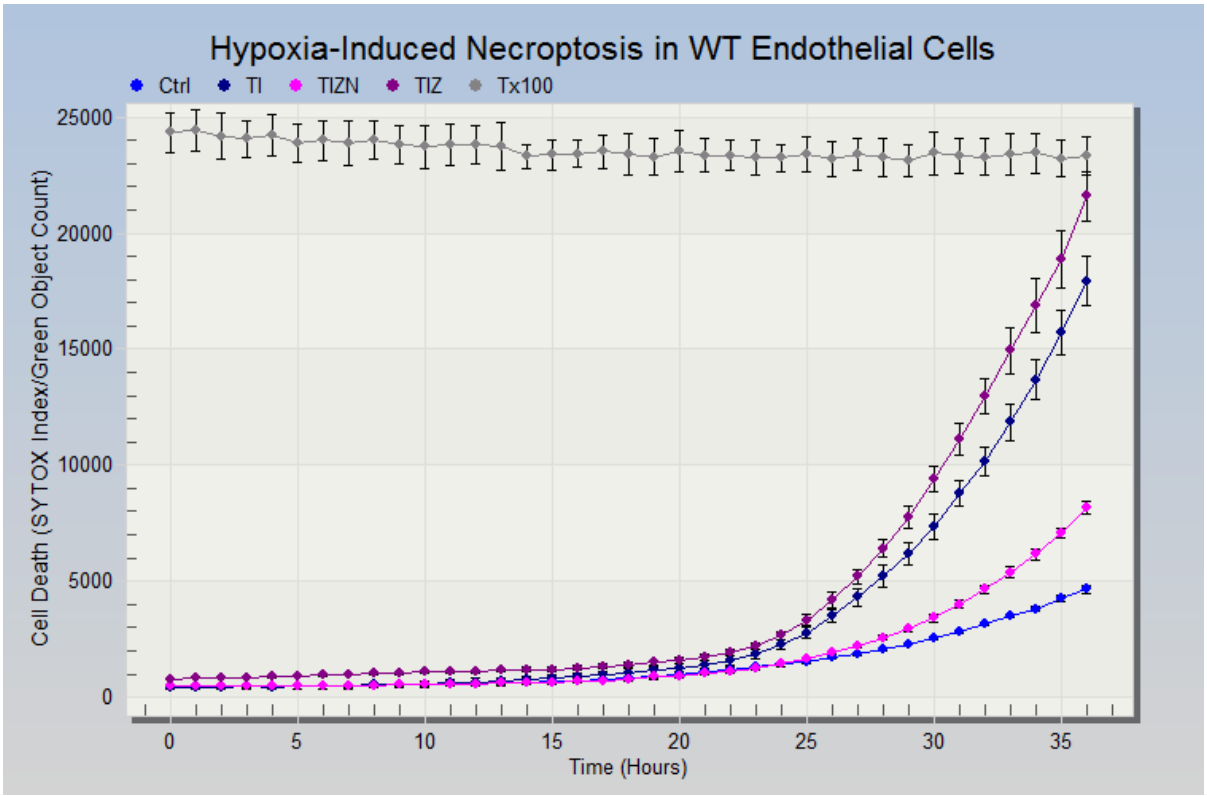
Hypoxia-Induced Necroptosis in WT Endothelial Cells
Ctrl
TI
TIZN
TIZ
Tx100
Cell Death (SYTOX Index/Green Object Count)
25000
20000
15000
10000
5000
0
0
5
10
15
20
25
30
35
Time (Hours)

B

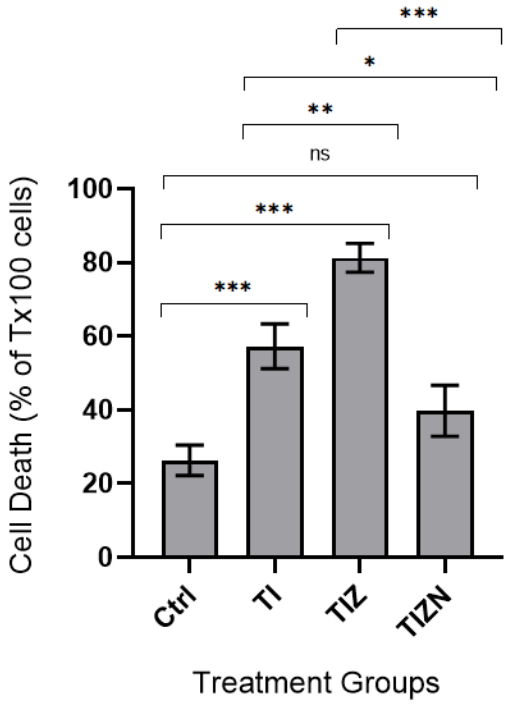
***
*
**
ns
***
***
Cell Death (% of Tx100 cells)
100
80
60
40
20
0
Ctrl
TI
TIZ
TIZN
Treatment Groups

Figure 9 – Cold Hypoxia-Reoxygenation Injury Promotes Necroptosis in Endothelial Cells

(A) WT B6 endothelial cells were seeded in a 96-well plate in triplicates at 70-80% confluency. To model *in vitro* ischemia injury, endothelial cell cultures were incubated in oxygen-depleted, glucose-free DMEM during hypoxia. The cell culture plates were subjected to cold hypoxia for 24 hours in anaerobic GENbags placed in a refrigerator set at 4°C. To model *in vitro* reperfusion injury, the endothelial cell cultures were removed from the hypoxia environment and the oxygen-depleted, glucose free culture medium was replaced with normal cell culture medium before the endothelial cell cultures were transferred to a normoxic incubator set at 37°C, 20% O_2 and 5% CO_2. hTNFα (T) at 100 μg/mL, IFNγ (I) at 100 μg/mL, z-VAD-fmk (Z) at 30 μM and Nec-1s (N) at 10 μM were added during both the hypoxia and the reoxygenation phases to simulate the IRI microenvironment *in vitro*. SYTOX™ Green Nucleic Acid Stain at 100 nM was used as a nuclear counterstain to indicate dead cells. Cell death (during the reoxygenation phase; time in hours on X-axis represents reoxygenation time following 24 hours of cold hypoxia at 4°C) was detected and quantified in the IncuCyte ZOOM® Live Cell Analysis System. For positive control, 1% Triton™ X-100 (Tx100) non-ionic surfactant was used to induce 100% cell death and used to calculate percent cell death in all the treatment groups. **(B)** Data at 36 hours post-reperfusion are shown as mean ± SD and representative of at least 3 independent experiments; n = 3; ***$p \leq 0.001$, **$p \leq 0.002$, *$p \leq 0.033$, ns = non-significant (p value ≥ 0.05); 1-way ANOVA; Tukey's multiple comparisons test.

3.2 – PGAM5-Drp1 Axis and ROS Do Not Contribute to Hypoxia/Reoxygenation-Induced Necroptosis in Endothelial Cells

The potential mitochondrial mediators of necroptosis include the PGAM5-Drp1 axis and ROS [106, 115, 116, 117, 118, 119, 123, 124]. ROS are also generated following mPTP formation [13, 18, 20, 106, 125, 127]. To determine the role of the PGAM5-Drp1 axis in necroptosis, the Drp1 inhibitor, Mdivi-1, was used. The addition of Mdivi-1 to hTNFα + IFNγ + z-VAD-fmk treated cells did not reverse the hypoxia/reoxygenation-induced necroptosis (Figure 10A). This finding ruled out the role of the PGAM5-Drp1 axis in endothelial cell necroptosis following cold hypoxia-reoxygenation injury.

The generation of ROS and ROS-mediated injury have been the most crucial focus of basic and clinical research studies aimed at understanding the molecular mechanisms of reperfusion injury. The role of ROS-mediated cellular injury in inducing apoptosis in the setting of IRI has been extensively documented [13, 18, 110, 111, 112, 113, 114]. As explained earlier, the role of ROS in inducing necroptosis has been studied in several cell types following various types of injuries but particularly IRI [102, 103, 104, 105, 106, 109, 154, 156, 157, 158, 194, 195, 196]. These studies, however, have yielded conflicting results indicating that the role of ROS in necroptosis is dependent on cell-type and the cause of injury.

To determine the role of ROS in hypoxia/reoxygenation-induced necroptosis in endothelial cells, the ROS scavengers, TEMPOL and NAC were used. The addition of TEMPOL or NAC to hTNFα + IFNγ + z-VAD-fmk treated cells did not reverse necroptosis following the *in vitro* cold hypoxia-reoxygenation injury (Figure 10B&C). The addition of the mitochondrion-specific ROS scavenger, mito-TEMPOL, to hTNFα + IFNγ + z-VAD-fmk treated cells also did not reverse the hypoxia/reoxygenation-induced necroptosis (Figure 10D).

This finding ruled out the role of ROS in hypoxia/reoxygenation-induced necroptosis in endothelial cells. It also established that mitochondrial ROS (following mPTP formation and ETC dysfunction) did not contribute to hypoxia/reoxygenation-induced necroptosis in endothelial cells.

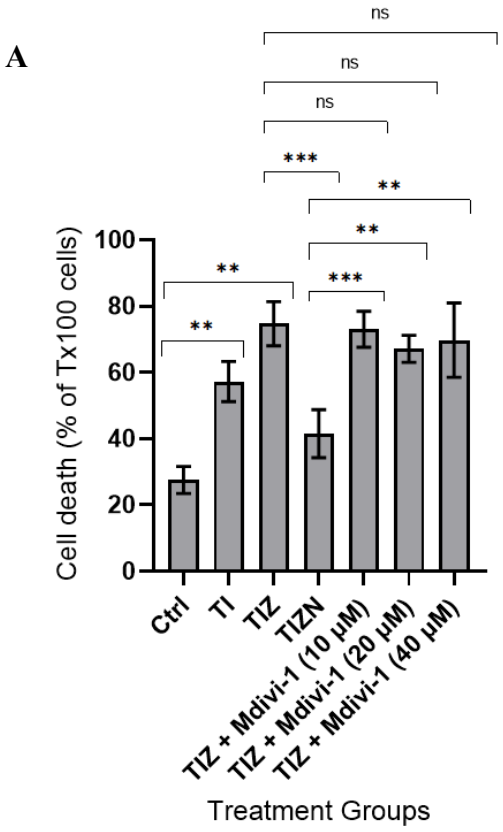
A
ns
ns
ns
***
**
**
**
***
**
Cell death (% of Tx100 cells)
100
80
60
40
20
0
Ctrl
TI
TIZ
TIZN
TIZ + Mdivi-1 (10 μM)
TIZ + Mdivi-1 (20 μM)
TIZ + Mdivi-1 (40 μM)
Treatment Groups

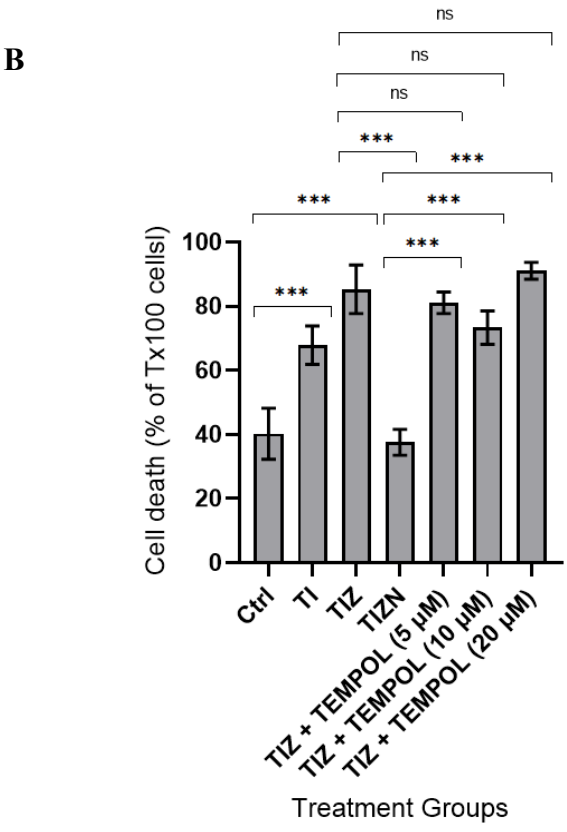
B
ns
ns
ns
***
***
***
***
***
Cell death (% of Tx100 cellsl)
100
80
60
40
20
0
Ctrl
TI
TIZ
TIZN
TIZ + TEMPOL (5 μM)
TIZ + TEMPOL (10 μM)
TIZ + TEMPOL (20 μM)
Treatment Groups

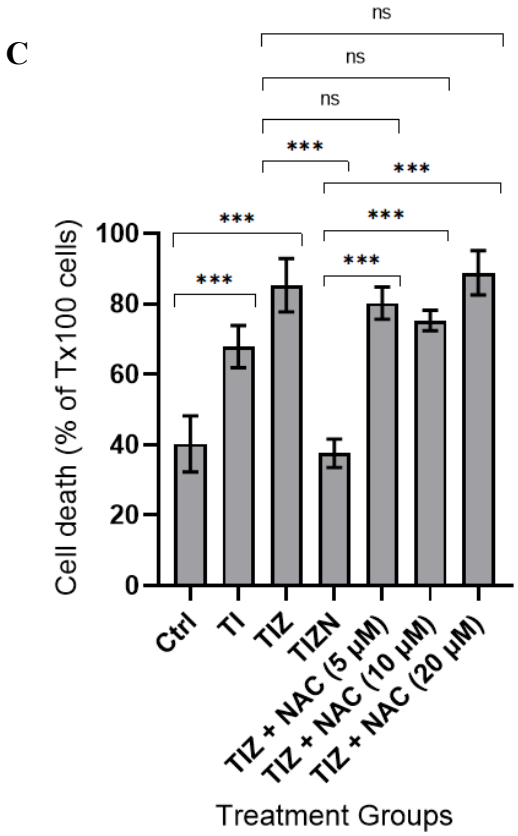
C
ns
ns
ns
***
***
***
***
***
Cell death (% of Tx100 cells)
100
80
60
40
20
0
Ctrl
TI
TIZ
TIZN
TIZ + NAC (5 μM)
TIZ + NAC (10 μM)
TIZ + NAC (20 μM)
Treatment Groups

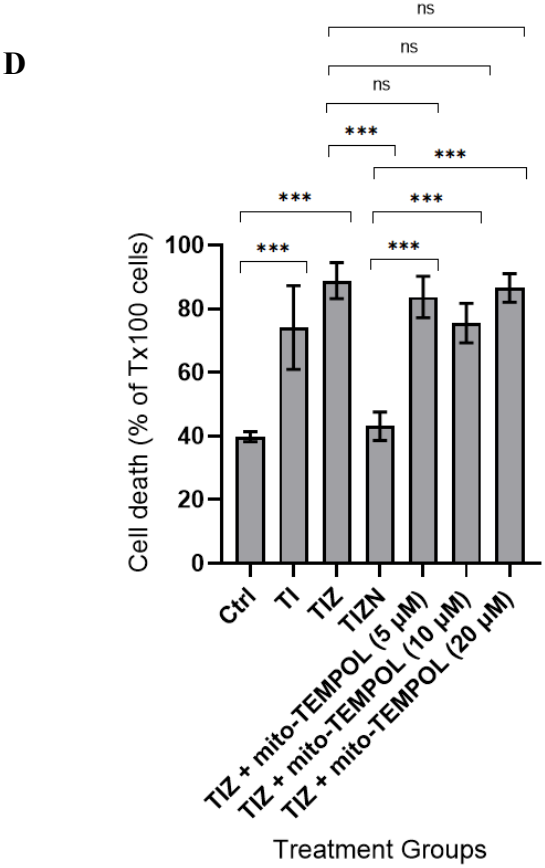
D
ns
ns
ns
***
***
***
***
***
Cell death (% of Tx100 cells)
100
80
60
40
20
0
Ctrl
TI
TIZ
TIZN
TIZ + mito-TEMPOL (5 μM)
TIZ + mito-TEMPOL (10 μM)
TIZ + mito-TEMPOL (20 μM)
Treatment Groups

Figure 10 – PGAM5-Drp1 Axis and ROS Do Not Contribute to Hypoxia/Reoxygenation-Induced Necroptosis in Endothelial Cells

WT B6 endothelial cells were subjected to the *in vitro* cold hypoxia-reoxygenation model and cell death was detected and quantified as described earlier in Figure 9. Data at 36 hours post-reperfusion are shown as mean ± SD and representative of at least 3 independent experiments. **(A)** Drp1 inhibitor – Mdivi-1 at 10 μM, 20 μM and 40 μM was added during both the hypoxia and the reoxygenation phases to inhibit PGAM5-Drp1-induced mitochondrial fragmentation. n = 3; ***p ≤ 0.001, **p ≤ 0.002, *p ≤ 0.033, ns = non-significant (p value ≥ 0.05); 1-way ANOVA; Tukey's multiple comparisons test. **(B)** ROS scavenger – TEMPOL at 5 μM, 10 μM and 20 μM was added during both the hypoxia and the reoxygenation phases to inhibit ROS-mediated cell damage and death. n = 3; ***p ≤ 0.001, **p ≤ 0.002, *p ≤ 0.033, ns = non-significant (p value ≥ 0.05); 1-way ANOVA; Tukey's multiple comparisons test. **(C)** ROS scavenger – NAC at 5 μM, 10 μM and 20 μM was added during both the hypoxia and the reoxygenation phases to inhibit ROS-mediated cell damage and death. n = 3; ***p ≤ 0.001, **p ≤ 0.002, *p ≤ 0.033, ns = non-significant (p value ≥ 0.05); 1-way ANOVA; Tukey's multiple comparisons test. **(D)** Mitochondrion-specific ROS scavenger – mito-TEMPOL at 5 μM, 10 μM and 20 μM was added during both the hypoxia and the reoxygenation phases to inhibit mitochondrial ROS-mediated cell damage and death. n = 3; ***p ≤ 0.001, **p ≤ 0.002, *p ≤ 0.033, ns = non-significant (p value ≥ 0.05); 1-way ANOVA; Tukey's multiple comparisons test.

3.3 – CypD-Mediated mPTP Formation Contributes to Hypoxia/Reoxygenation-Induced Necroptosis in Endothelial Cells

As described earlier, studies have firmly established the role of CypD in regulating mPTP formation [20, 125, 137, 138, 142]. Of the putative mitochondrial mediators involved in necroptosis, the role of CypD-mediated mPTP formation is the most well-studied. As with ROS, studies investigating the role of CypD-mediated mPTP in necroptosis have yielded contradictory results [104, 106, 128, 132, 133, 134, 135, 136]. Persistent/prolonged mPTP formation leads to the incomplete reduction of oxygen and also provides a link to ROS generation, which lead to cellular damage, are a strong trigger for necroptosis and are investigated as the downstream mediators of necroptosis [13, 18, 20, 104, 106, 140, 141].

To study the role of CypD in hypoxia/reoxygenation-induced necroptosis in endothelial cells, CsA was used. CsA is a potent CypD inhibitor and blocks mPTP formation [13, 18, 20, 104, 137, 138, 211]. As with Nec-1s, the addition of CsA to hTNFα + IFNγ + z-VAD-fmk treated cells reversed the hypoxia/reoxygenation-induced necroptosis in endothelial cells (Figure 11A). Besides, blocking mPTP formation, CsA is a calcineurin inhibitor and a potent immunosuppressive drug [211, 212]. To rule out the participation of calcineurin in necroptosis, the non-CypD binding calcineurin inhibitor, FK-506, was used [104, 211]. The addition of FK-506 to hTNFα + IFNγ + z-VAD-fmk treated cells did not inhibit hypoxia/reoxygenation-induced necroptosis in endothelial cells.

Phosphorylation of MLKL is an established event in necroptosis [102, 104, 105, 106]. In the hTNFα + IFNγ + z-VAD-fmk treated cells, which were undergoing hypoxia/reoxygenation-induced necroptosis, pMLKL protein expression was noted (Figure 11B&C). The addition of Nec1s to the hTNFα + IFNγ + z-VAD-fmk treated cells, significantly

reduces the level of hypoxia/reoxygenation-induced necroptosis and the level of pMLKL protein expression (Figure 11B&C).

To confirm the role of CypD in necroptosis, endothelial cells from $CypD^{-/-}$ mice were subjected to the *in vitro* cold hypoxia-reoxygenation injury model. As with CypD inhibition by CsA, $CypD^{-/-}$ endothelial cells resisted hypoxia/reoxygenation-induced necroptosis (Figure 11D). In our study, the level of necroptosis inhibition by Nec-1s is comparable to the level of necroptosis inhibition by CypD inhibition and ablation (Figure 11A&D). This finding confirms that CypD contributes to hypoxia/reoxygenation-induced necroptosis in endothelial cells.

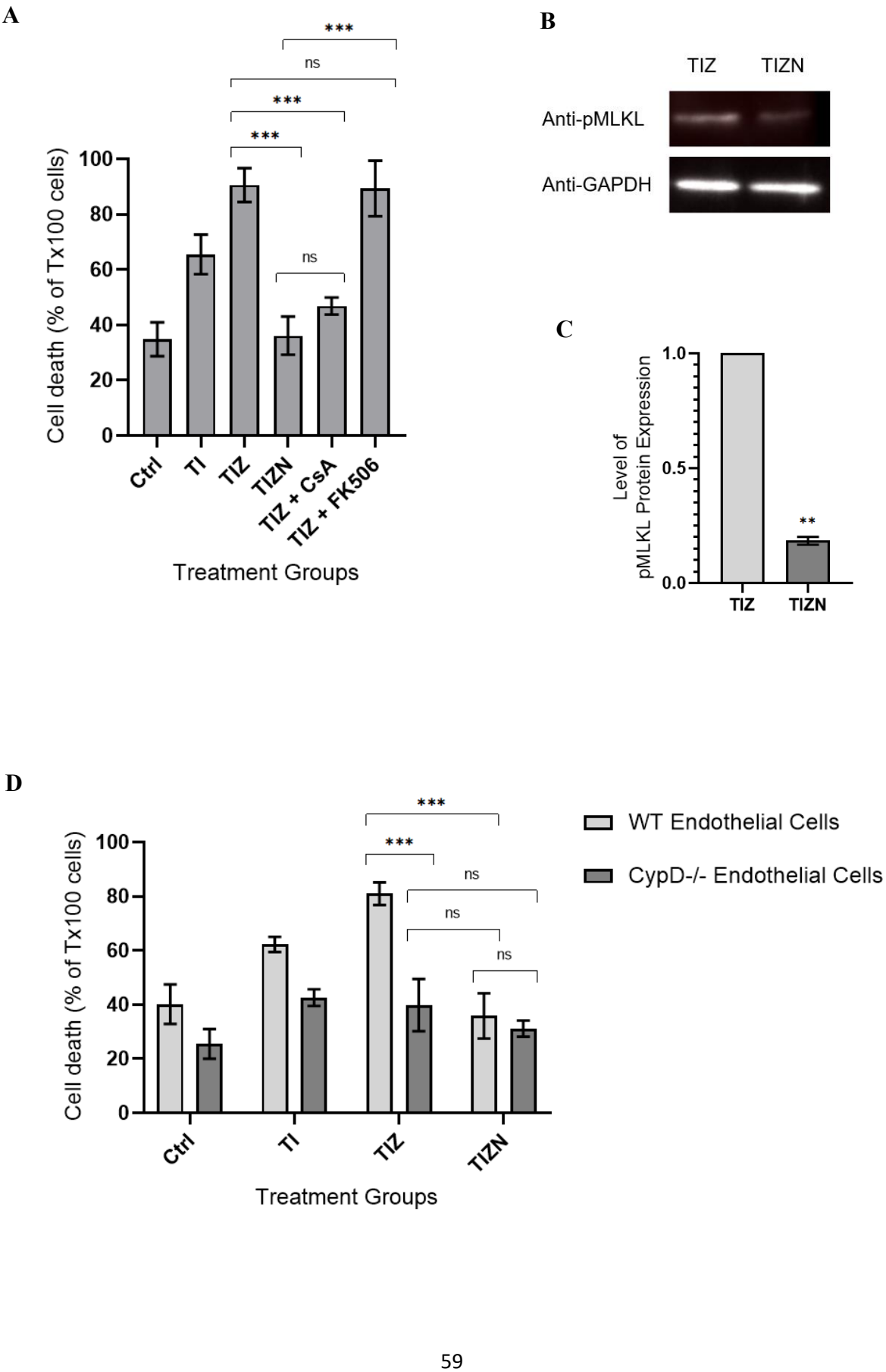
A
***
ns
***
***
ns
Cell death (% of Tx100 cells)
100
80
60
40
20
0
Ctrl
TI
TIZ
TIZN
TIZ + CsA
TIZ + FK506
Treatment Groups
B
TIZ
TIZN
Anti-pMLKL
Anti-GAPDH
C
Level of pMLKL Protein Expression
1.0
0.5
0.0
**
TIZ
TIZN
D
***
***
ns
ns
ns
Cell death (% of Tx100 cells)
100
80
60
40
20
0
Ctrl
TI
TIZ
TIZN
Treatment Groups
WT Endothelial Cells
CypD-/- Endothelial Cells

Figure 11 – CypD Deficiency Prevents Hypoxia/Reoxygenation-Induced Necroptosis in Endothelial Cells

WT and CypD$^{-/-}$ B6 endothelial cells were subjected to the *in vitro* cold hypoxia-reoxygenation model and cell death was detected and quantified as described earlier in Figure 9. Data at 36 hours post-reoxygenation are shown as mean ± SD and representative of at least 3 independent experiments. **(A)** CypD inhibitor – CsA at 10 μM was added during both the hypoxia and the reoxygenation phases. For control, the non-CypD binding calcineurin inhibitor FK506 at 10 μM was during both the hypoxia and the reoxygenation phases. n = 3; ***p ≤ 0.001, **p ≤ 0.002, *p ≤ 0.033, ns = non-significant (p value ≥ 0.05); 1-way ANOVA; Tukey's multiple comparisons test. CsA dose (10 μM) was optimized (dose-response curves showing maximum reduction in cell death following cold hypoxia-reoxygenation injury) after using it at various concentrations from 0.5-20 μM; corresponding doses were used for FK506. **(B)** WT endothelial cells were subjected to the *in vitro* cold hypoxia-reoxygenation injury model described earlier in Figure 9. The reoxygenation phase was limited to 12-15 hours, at which point the total protein was isolated and Western Blot analysis was performed for detection of pMLKL protein. GAPDH was used as loading control. **(C)** The level of pMLKL protein expression was quantified in the TIZ and TIZN groups. n = 3; **p ≤ 0.05; Student's t test for paired values. **(D)** Endothelial cells were isolated from CypD$^{-/-}$ mice and were subjected to the same *in vitro* cold hypoxia-reoxygenation injury model. n = 3; ***p ≤ 0.001, **p ≤ 0.002, *p ≤ 0.033, ns = non-significant (p value ≥ 0.05); 2-way ANOVA; Tukey's multiple comparisons test.

3.4 – AIF Contributes to Hypoxia/Reoxygenation-Induced Necroptosis in Endothelial Cells

Necroptosis exhibits morphological features of unregulated necrosis. Characteristic findings of necroptotic death include cell membrane rupture and permeabilization, oncosis and vacuolization of the cytoplasm and organelles, mitochondrial swelling and DNA fragmentation [102, 105, 109, 110, 157]. Extra-mitochondrial AIF translocates to the nucleus and induces caspase-independent cell death by inducing large-scale DNA fragmentation (~50 kbp fragments) [147, 148]. AIF-mediated DNA degradation has been shown to occur in response to several types of pathologic insults, including IRI [145, 146, 147, 148, 173, 174, 175, 176, 177, 178]. Recent studies have also indicated that mPTP formation facilitates AIF release from the mitochondria by serving as a morphological conduit [145, 177]. Therefore, we decided to investigate the role of AIF in hypoxia/reoxygenation-induced necroptosis in endothelial cells using the *in vitro* cold hypoxia-reoxygenation injury model.

To date, no effective pharmacological inhibitor of AIF has been recognized [147, 148]. Therefore, to study the role of AIF in hypoxia/reoxygenation-induced necroptosis in endothelial cells, *Aifm1* was silenced in WT B6 endothelial cells using siRNA. AIF silencing was confirmed by RT-qPCR and Western Blot (Figure 12). AIF-silenced endothelial cells were subjected to the *in vitro* cold hypoxia-reoxygenation injury model. Compared to scrambled siRNA-transfected endothelial cells, AIF-silenced endothelial cells show a significant reduction in cell death in all treatment groups, indicating inhibition of necroptosis in the AIF-silenced cells. The level of cell death in the AIF-silenced hTNFα + IFNγ + z-VAD-fmk group is similar to the level of cell death in the WT hTNFα + IFNγ + z-VAD-fmk + Nec-1s group (Figure 13A). This finding indicates that AIF has a critical role in the necroptotic pathway.

Recent studies have established that AIF translocation to the nucleus requires CypA and is inhibited by HSP-70 [147, 148, 152]. Since there are no known AIF inhibitors, CypA inhibition can be used to indirectly evaluate the role of AIF. Alisporivir is a non-immunosuppressive cyclophilin binding molecule that binds to CypA, an essential co-factor for Hepatitis C virus replication [221, 222]. Several *in vitro* and *in vivo* studies have explored the therapeutic potential of Alisporivir in patients with chronic hepatitis C viral infection [148, 221, 222]. To evaluate the role of AIF in hypoxia/reoxygenation-induced necroptosis in endothelial cells, we used Alisporivir. The addition of Alisporivir to the hTNFα + IFNγ + z-VAD-fmk treatment group considerably reduces the level cell death in WT endothelial cells following the *in vitro* cold hypoxia-reoxygenation injury (Figure 13B). This finding establishes that AIF has a critical role in hypoxia/reoxygenation-induced necroptosis in endothelial cells.

A

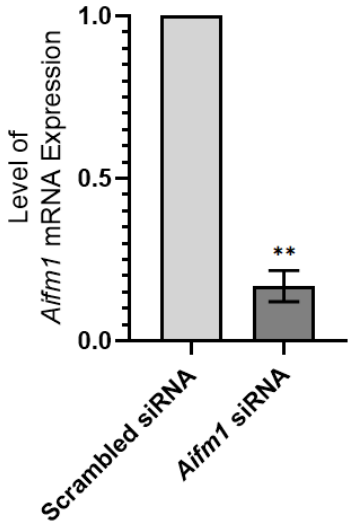
Level of
Aifm1 mRNA Expression
1.0
0.5
0.0
**
Scrambled siRNA
Aifm1 siRNA

B

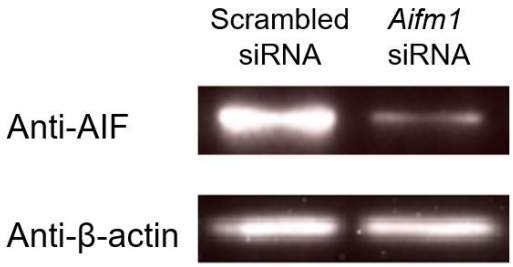
Scrambled siRNA
Aifm1 siRNA
Anti-AIF
Anti-β-actin

C

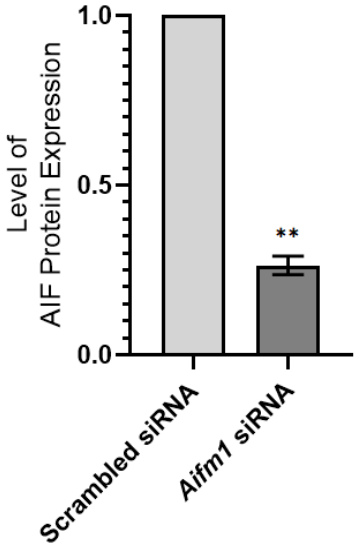
Level of
AIF Protein Expression
1.0
0.5
0.0
**
Scrambled siRNA
Aifm1 siRNA

Figure 12 – siRNA-Induced Silencing of *Aifm1*

WT B6 endothelial cells were transfected with 200 nM ON-TARGETplus Mouse *Aifm1* using EndoFectin™ Max transfection reagent in Opti-MEM® media. Transfected cells were harvested for *in vitro* cold hypoxia-reoxygenation injury experiments at 48 hours post-transfection. **(A)** siRNA-induced silencing of *Aifm1* was confirmed by RT-qPCR at 48 hours post-transfection. *β-actin* was used as endogenous control for gene expression analysis. Data at 48 hours post-transfection are shown as mean ± SD and representative of 3 independent RT-qPCR experiments. n = 3; **p ≤ 0.05; Student's t test for paired values. **(B)** The reduction in the protein expression of AIF-silenced cells was confirmed by Western Blot analysis at 72 hours post-transfection. β-actin was used as loading control. **(C)** The reduction in the level of AIF protein expression at 72 hours following siRNA-induced silencing of *Aifm1* was measured in 3 independent experiments. n = 3; **p ≤ 0.05; Student's t test for paired values.

A

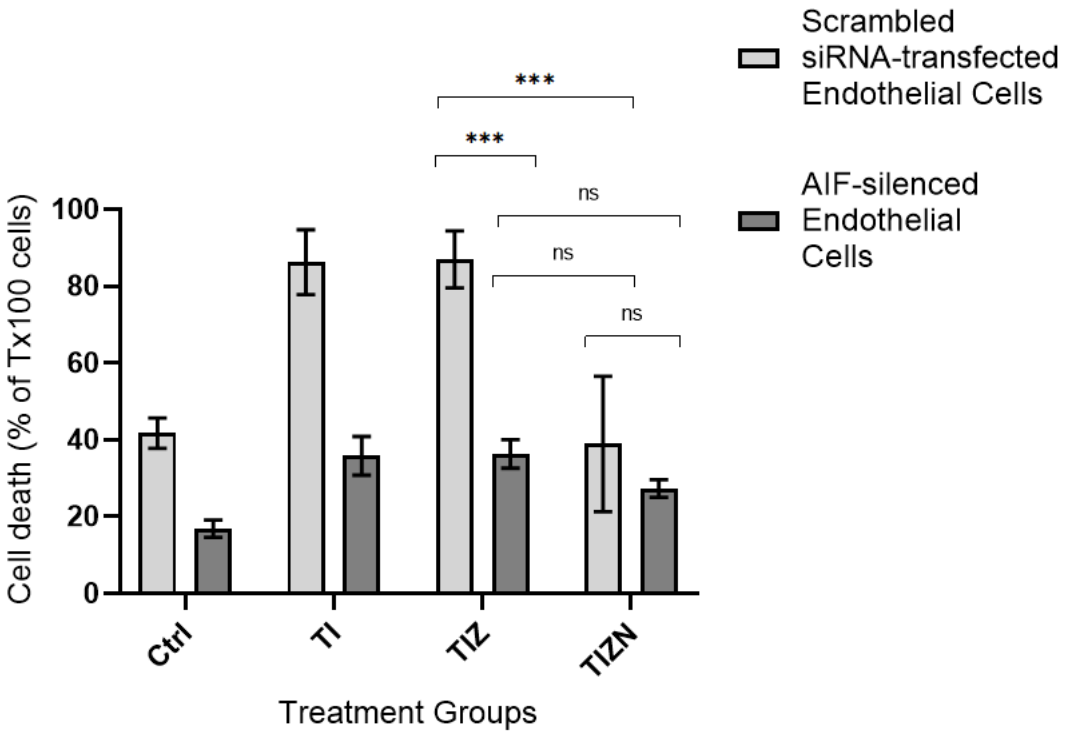
Scrambled siRNA-transfected Endothelial Cells
AIF-silenced Endothelial Cells
***
***
ns
ns
ns
Cell death (% of Tx100 cells)
100
80
60
40
20
0
Ctrl
TI
TIZ
TIZN
Treatment Groups

B

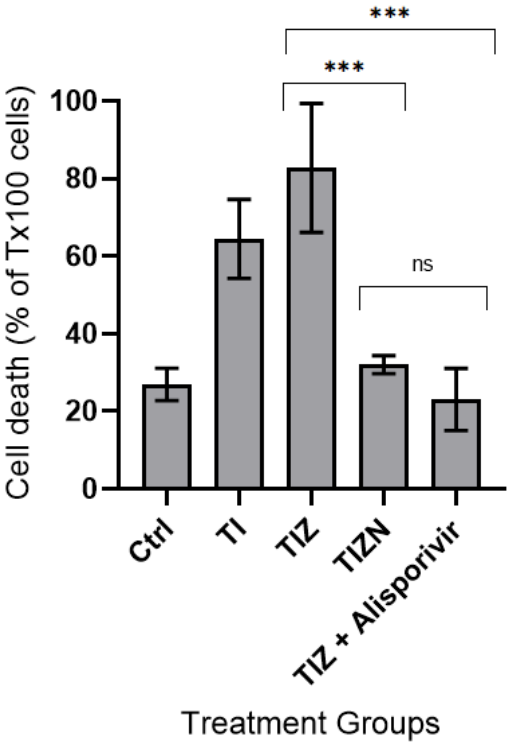
***
***
ns
Cell death (% of Tx100 cells)
100
80
60
40
20
0
Ctrl
TI
TIZ
TIZN
TIZ + Alisporivir
Treatment Groups

Figure 13 – AIF Silencing Prevents Hypoxia/Reoxygenation-Induced Necroptosis in Endothelial Cells

WT, scrambled siRNA-transfected cells and AIF-silenced (*Aifm1* siRNA-transfected) B6 endothelial cells were subjected to the *in vitro* cold hypoxia-reoxygenation injury model and cell death was detected and quantified as described earlier in Figure 9. Data at 36 hours post-reperfusion are shown as mean ± SD and representative of at least 3 independent experiments. **(A)** Scrambled siRNA-transfected and AIF-silenced B6 endothelial cells were harvested 48 hours post-transfection and subjected to the *in vitro* cold hypoxia-reoxygenation injury model. n = 3; ***p ≤ 0.001, **p ≤ 0.002, *p ≤ 0.033, ns = non-significant (p value ≥ 0.05); 2-way ANOVA; Tukey's multiple comparisons test. **(B)** CypA inhibitor – Alisporivir at 1 μM was added during both the hypoxia and the reoxygenation phases to inhibit CypA-mediated AIF translocation to the nucleus. n = 3; ***p ≤ 0.001, **p ≤ 0.002, *p ≤ 0.033, ns = non-significant (p value ≥ 0.05); 1-way ANOVA; Tukey's multiple comparisons test.

3.5 – AIF Translocation to the Nucleus in Hypoxia/Reoxygenation-Induced Necroptosis in Endothelial Cells

Following its release into the cytosol from the mitochondria, AIF translocates to the nucleus and induces DNA degradation [147, 148]. To confirm the role of AIF in necroptosis, WT endothelial cells were subjected to the *in vitro* cold hypoxia-reoxygenation injury model and immunocytochemistry was used to observe AIF translocation to the nucleus in various treatment groups. In untreated cells, AIF localizes to the mitochondria in the cytoplasm (Figure 14). AIF translocation to the nucleus is observed in the hTNFα + IFNγ and hTNFα + IFNγ + z-VAD-fmk treatment groups. AIF translocation and overall cell death (necroptosis) is considerably reduced in the hTNFα + IFNγ + z-VAD-fmk + Nec-1s and hTNFα + IFNγ + z-VAD-fmk + Alisporivir treatment groups (Figure 14). Inhibition of AIF translocation to the nucleus following treatment with Nec-1s indicates that AIF is the downstream mitochondrial mediator involved in hypoxia/reoxygenation-induced necroptosis in endothelial cells.

A

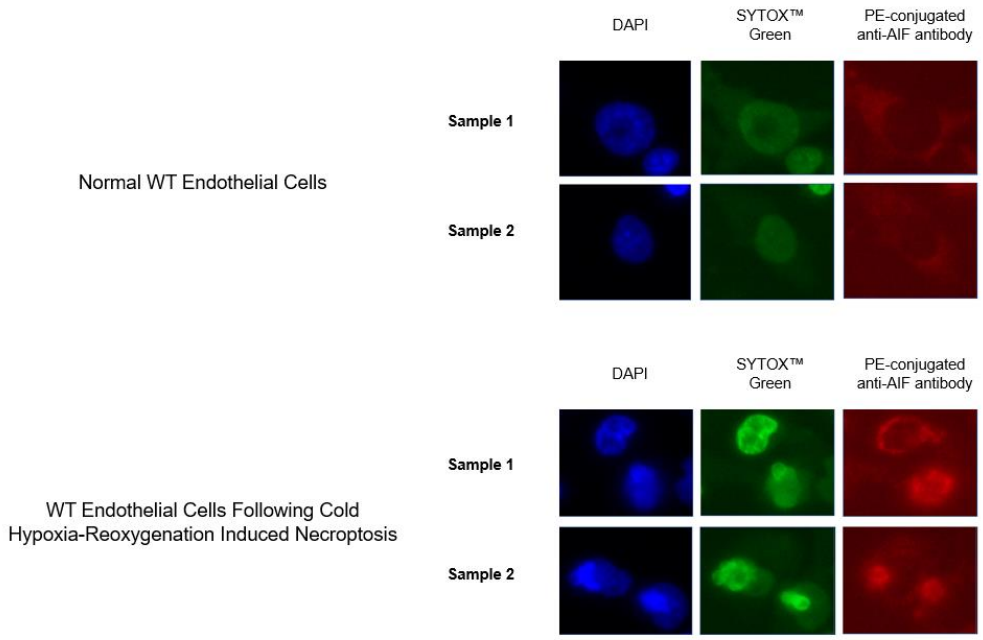
DAPI
SYTOX™ Green
PE-conjugated anti-AIF antibody
Sample 1
Sample 2
Normal WT Endothelial Cells
DAPI
SYTOX™ Green
PE-conjugated anti-AIF antibody
Sample 1
Sample 2
WT Endothelial Cells Following Cold Hypoxia-Reoxygenation Induced Necroptosis

B

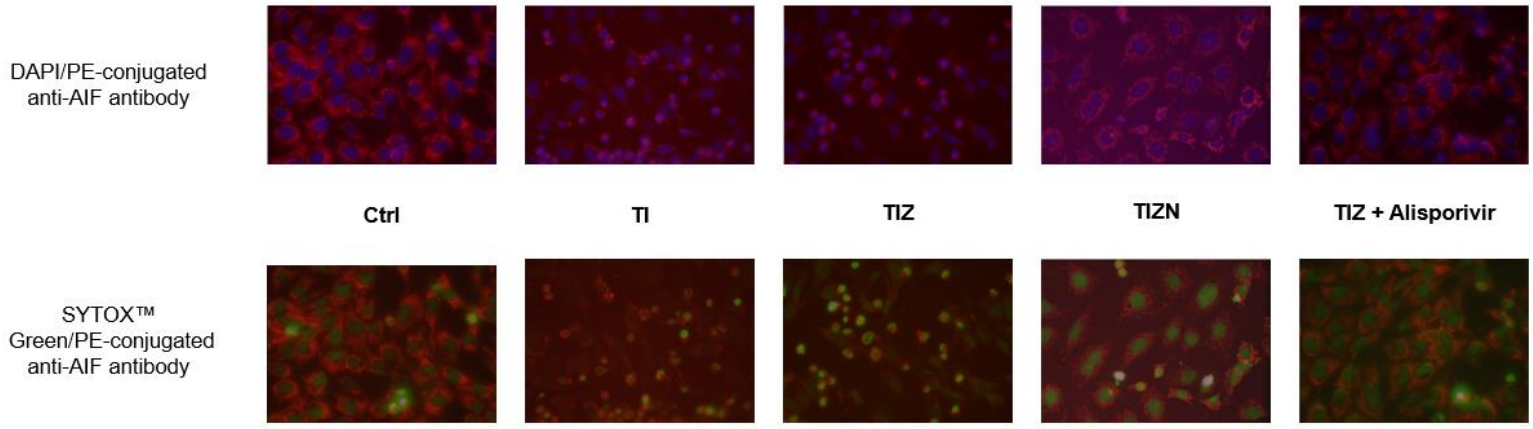
DAPI/PE-conjugated anti-AIF antibody
Ctrl
TI
TIZ
TIZN
TIZ + Alisporivir
SYTOX™ Green/PE-conjugated anti-AIF antibody

Figure 14 – AIF Translocation to the Nucleus in Hypoxia/Reoxygenation-Induced Necroptosis in Endothelial Cells

WT B6 endothelial cells were subjected to the *in vitro* cold hypoxia-reoxygenation injury model described earlier in Figure 9. Alisporivir at 1 μM was added during both the hypoxia and the reoxygenation phases. The reoxygenation phase was limited to 24 hours at which point the cells were fixed with 4% formaldehyde solution and permeabilized with 0.1-0.25% Triton™ X-100 non-ionic surfactant. To reduce non-specific antigen binding and background fluorescence, the cells were incubated with a blocking solution comprised of 1% BSA, 22.52 mg/mL glycine and 0.1% Tween 20 in D-PBS. The cells were incubated with primary rabbit anti-murine AIF antibody diluted in 1% BSA in D-PBS with 0.1% Tween 20 at 1:1000 concentration ratio for 1 hour at room temperature in a humidified chamber. The cells were then incubated with secondary donkey anti-rabbit PE-conjugated antibody diluted in 1% BSA in D-PBS at 1:60 concentration ratio for 1 hour at room temperature in a dark humidified chamber for immunofluorescence. For DAPI counterstaining, the cells were incubated with 300 nM DAPI staining solution for 5 minutes at room temperature in a humidified chamber. Nikon Inverted Research Microscope ECLIPSE Ts2R was used to capture images at 20-40X magnification. **(A)** Representative individual cell images at 80X magnification are shown. Cells undergoing hypoxia/reoxygenation-induced necroptosis (hTNFα + IFNγ + z-VAD-fmk treatment group) are shown. **(B)** Representative microscopic field images at 40X magnification are shown. All treatment groups are shown.

3.6 – AIF Induces Large-Scale DNA Degradation in Hypoxia/Reoxygenation-Induced Necroptosis in Endothelial Cells

To further confirm the role of AIF in hypoxia/reoxygenation-induced necroptosis, WT endothelial cells were subjected to the *in vitro* cold hypoxia-reoxygenation injury model and DNA degradation was characterized by gel electrophoresis. A distinct ~50 kbp band is observed in the hTNFα + IFNγ + z-VAD-fmk treatment group. The intensity of the 50 kbp band is considerably decreased in the hTNFα + IFNγ + z-VAD-fmk + Nec-1s and hTNFα + IFNγ + z-VAD-fmk + Alisporivir groups (Figure 15). This finding indicates that hypoxia/reoxygenation-induced necroptosis in endothelial cells involves AIF-mediated DNA degradation into ~50 kbp fragments.

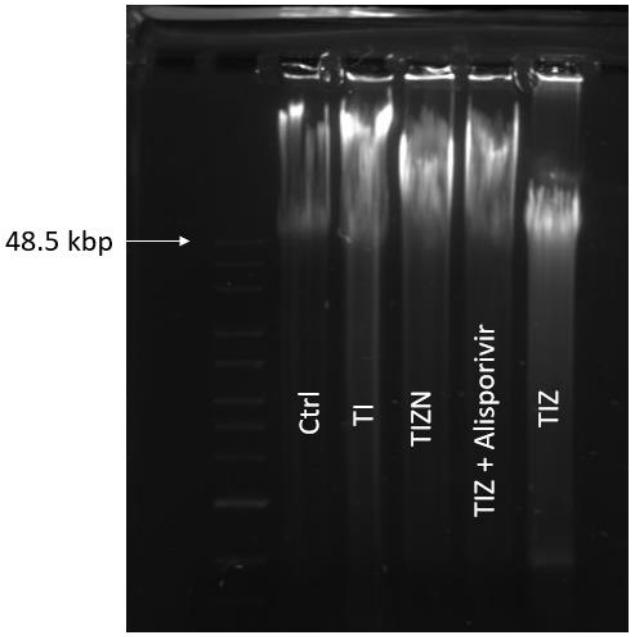
48.5 kbp
Ctrl
TI
TIZN
TIZ + Alisporivir
TIZ

Figure 15 – AIF Induces Large-Scale DNA Degradation During Hypoxia/Reoxygenation-Induced Necroptosis in Endothelial Cells

WT B6 endothelial cells were subjected to the *in vitro* cold hypoxia-reoxygenation injury model described earlier in Figure 9. Alisporivir at 1 μM was added during both the hypoxia and the reoxygenation phases. The reoxygenation phase was limited to 12-18 hours at which point, DNA was isolated using the QIAGEN Blood & Cell Culture DNA Mini Kit. The size of the isolated DNA fragments was characterized by electrophoretic separation using 0.3% agarose gel run at 3-4 V/cm.

3.7 – Parthanatos Does Not Contribute to Hypoxia/Reoxygenation-Induced Endothelial Cell Death

ROS-mediated oxidative damage to DNA in the setting of IRI induces PARP-1 activation [106, 149, 180, 181, 182]. PARP-1 activation causes ADP ribosylation of 'damaged' chromatin, modulating its structure and facilitating its interaction with DNA repair enzymes. However, if the DNA damage is severe, the excessive PAR moieties in the nucleus translocate to the mitochondria and mediate AIF release, ultimately leading to a form of regulated necrosis termed parthanatos [149]. We investigated the role of parthanatos in endothelial cell death using our *in vitro* cold hypoxia-reoxygenation injury model. The addition of the PARP-1 inhibitor, 3-ABA to hTNFα + IFNγ + z-VAD-fmk treated cells, did not reverse the hypoxia/reoxygenation-induced necroptosis (Figure 16). This indicates that parthanatos does not contribute to hypoxia/reoxygenation-induced endothelial cell death.

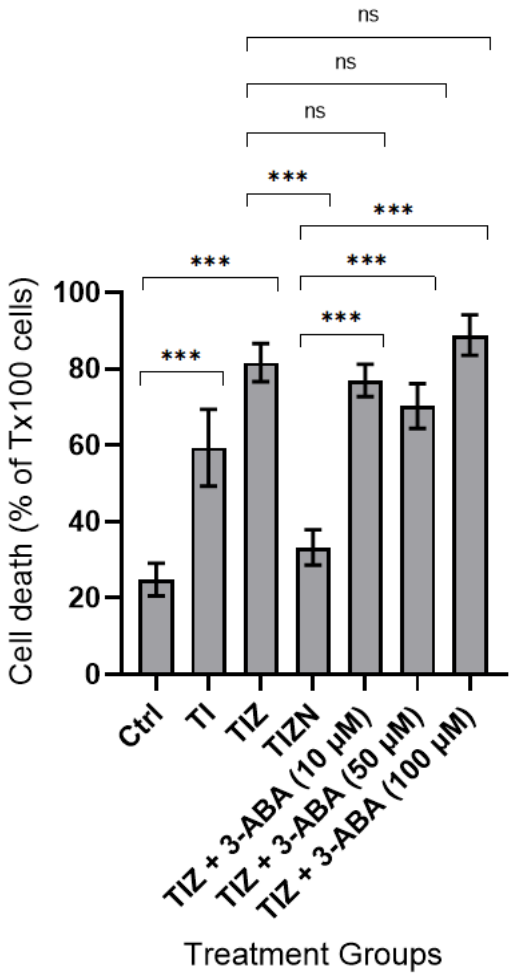
ns
ns
ns
***
***
***
***
***
Cell death (% of Tx100 cells)
100
80
60
40
20
0
Ctrl
TI
TIZ
TIZN
TIZ + 3-ABA (10 µM)
TIZ + 3-ABA (50 µM)
TIZ + 3-ABA (100 µM)
Treatment Groups

Figure 16 – Hypoxia/Reoxygenation-Induced AIF Release Does Not Contribute to Parthanatos

WT B6 endothelial cells were subjected to the *in vitro* cold hypoxia-reoxygenation model and cell death was detected and quantified as described earlier in Figure 9. PARP-1 inhibitor, 3-ABA at 10 μM, 50 μM and 100 μM were added during both the hypoxia and the reoxygenation phases. Data at 36 hours post-reperfusion are shown as mean ± SD and representative of at least 3 independent experiments. n = 3; ***$p \leq 0.001$, **$p \leq 0.002$, *$p \leq 0.033$, ns = non-significant (p value ≥ 0.05); 1-way ANOVA; Tukey's multiple comparisons test.

3.8 – CypD Ablation in Donor Hearts Attenuates IRI-Induced Allograft Injury and Promotes Long-Term Graft Survival

Static cold (4°C) storage is the most commonly used strategy in donor organ preservation [218, 219, 220]. Myocardial tissue is particularly sensitive to ischemia, and donor heart preservation is limited to 4-6 hours in clinical transplantation [4, 5, 6, 7, 8, 9, 10, 12]. Our *in vitro* data strongly supported the role of CypD inhibition and ablation in protecting endothelial cells from hypoxia/reoxygenation-induced necroptosis. We wanted to extend our findings to a clinically relevant model of cardiac transplantation. To study the *in vivo* efficacy of CypD ablation in promoting graft survival, donor hearts from WT and $CypD^{-/-}$ B6 mice were subjected to ischemic storage at 4°C for 4 hours and then transplanted into BALB/c mice. Our data show that ischemia aggravates graft rejection and significantly reduces graft survival time compared to non-ischemic grafts (Figure 17A). Interestingly, CypD ablation in donor hearts attenuates ischemia-induced rejection and promotes graft survival (Figure 17B).

Histomorphological evaluation of WT and $CypD^{-/-}$ allografts at 28 days post-transplantation indicated significant damage to the microvasculature, with neointima formation and fibrosis in the WT allografts (Figure 18A&B). These changes indicated severe inflammatory damage and were accompanied with T cell and monocyte/macrophage infiltration into the graft as assessed by CD3 and CD68 staining (Figure 18C). Allograft injury to the microvasculature, inflammatory damage and lymphocyte infiltration into the graft were significantly decreased in the $CypD^{-/-}$ allografts (Figure 18D).

A

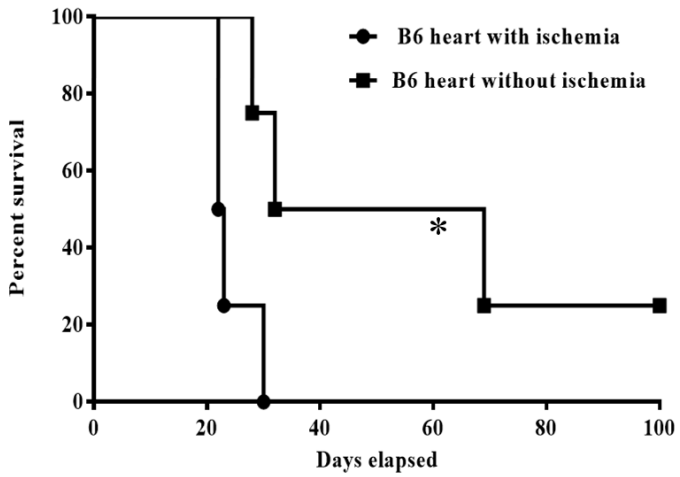
B6 heart with ischemia
B6 heart without ischemia
Percent survival
Days elapsed
100
80
60
40
20
0
0
20
40
60
80
100
*

B

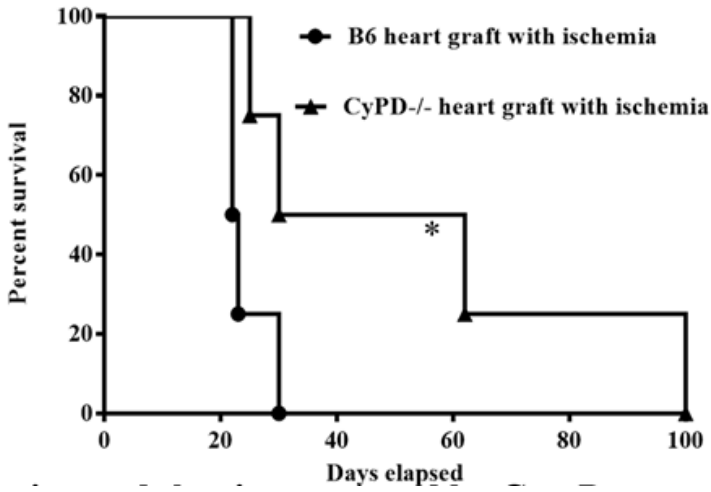
B6 heart graft with ischemia
CyPD-/- heart graft with ischemia
Percent survival
Days elapsed
100
80
60
40
20
0
0
20
40
60
80
100
*

Figure 17 – CypD Ablation Attenuates IRI-Induced Allograft Injury and Promotes Long-Term Graft Survival

Heart grafts from WT and CypD$^{-/-}$ B6 mice were subjected to ischemic storage at 4°C for 4 hours before being transplanted into BALB/c mice followed by anti-CD40L injection. Graft survival was monitored twice a week. Cessation of beating was considered as rejection. **(A)** Ischemia aggravates graft rejection and reduces graft survival time. n = 4; *p ≤ 0.05; Log-Rank test. **(B)** CypD deficiency in donor hearts attenuates ischemia-aggravated graft rejection and prolongs graft survival time. n = 4/group; *p ≤ 0.05; Log-Rank test.

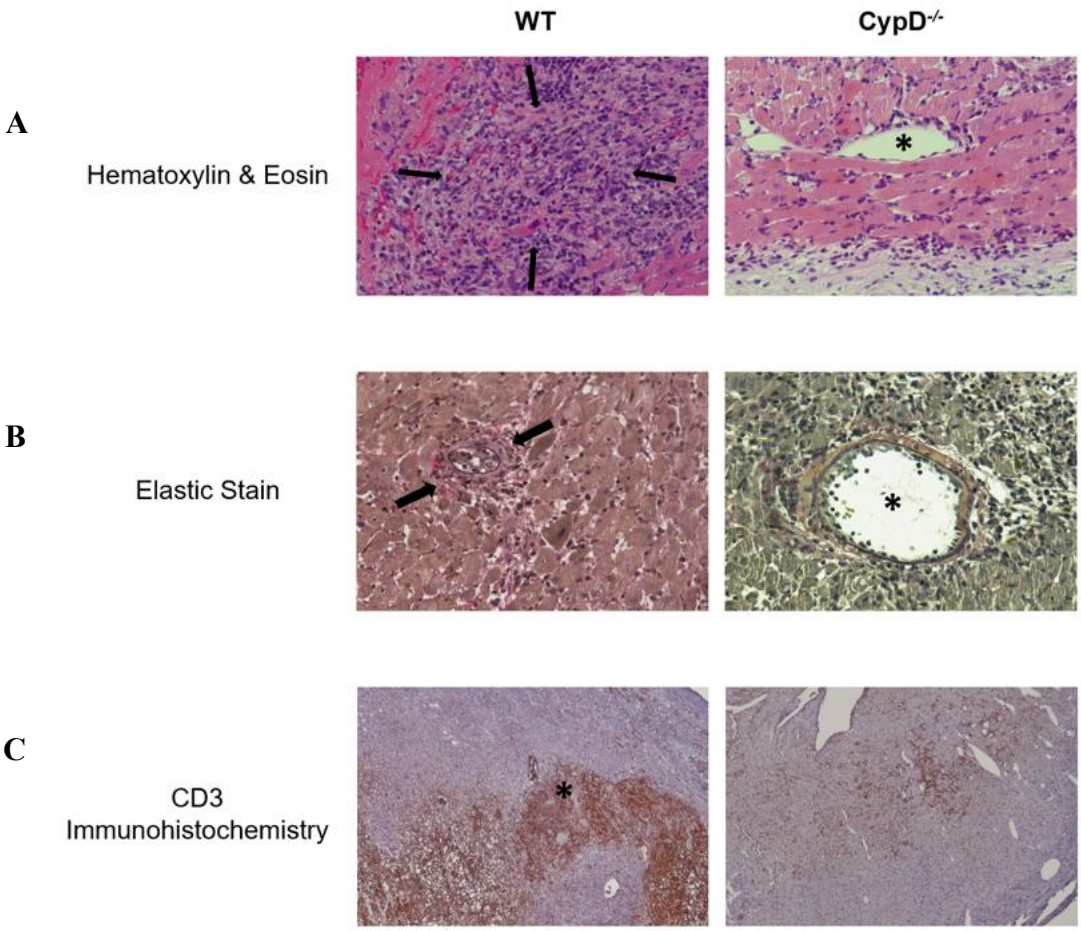
WT
CypD-/-
A
Hematoxylin & Eosin
B
Elastic Stain
C
CD3
Immunohistochemistry

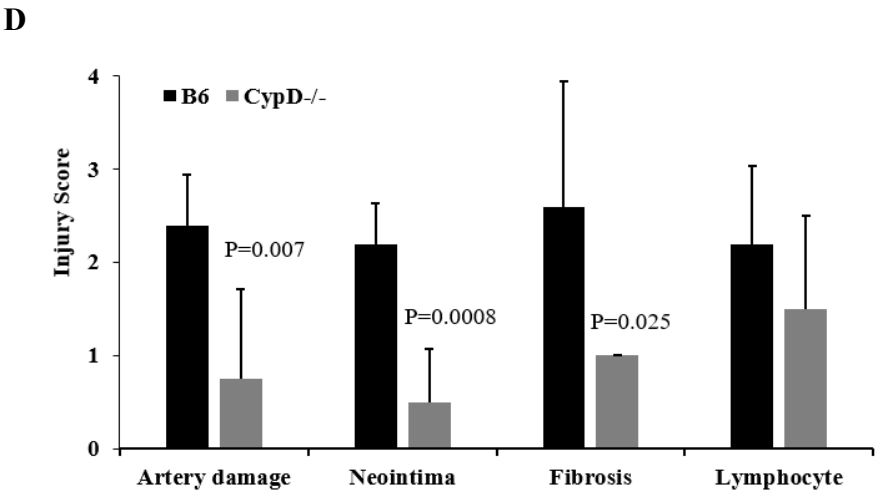
D
B6
CypD-/-
Injury Score
4
3
2
1
0
P=0.007
P=0.0008
P=0.025
Artery damage
Neointima
Fibrosis
Lymphocyte

Figure 18 – CypD Ablation Attenuates IRI-Induced Allograft Injury, Inflammatory Damage and Alloimmune Response

Heart grafts from WT and CypD$^{-/-}$ B6 mice were subjected to ischemic storage at 4°C for 4 hours before being transplanted into BALB/c mice as described in Figure 17. Recipient mice (n = 4/group) were euthanized 28 days post-transplantation and the cardiac allografts were isolated, fixed with 10% neutral buffered formalin and embedded in paraffin for sectioning. The tissue sections were then stained with H&E, Verhoeff–Van Gieson Elastic Stain and CD3 & CD68 Immunohistochemistry. Nikon ECLIPSE E200 microscope was used to capture images at 20X and 4X magnification. Allograft injury was evaluated and quantified based on damage to microvasculature, neointima formation, fibrosis and lymphocytic infiltration compared to naïve tissue by a pathologist in a blinded manner. The criteria used scored the injury on a scale of 0-4 as follows – 0: no change, 1: 0-24% change, 2: 25-49% change, 3: 50-74% change, and 4: >75% change. Representative slide images are shown. **(A)** Hematoxylin & Eosin staining of tissue sections from cardiac grafts isolated from WT and CypD$^{-/-}$ mice, indicating damage to the endothelium. **(B)** Elastic staining of tissue sections from cardiac grafts isolated from WT and CypD$^{-/-}$ mice, indicating damage to the microvasculature. **(C)** CD3 and CD68 Immunohistochemistry of tissue sections from cardiac grafts isolated from WT and CypD$^{-/-}$ mice, indicating graft infiltration by T cells and monocytes/macrophages, respectively. **(D)** Quantification of WT and CypD$^{-/-}$ cardiac graft injury in WT and CypD$^{-/-}$ mice, evaluating arterial damage, neointima formation, fibrosis and lymphocytic infiltration. n = 3; ***$p \leq 0.001$, **$p \leq 0.002$, *$p \leq 0.033$, ns = non-significant (p value ≥ 0.05); 2-way ANOVA; Tukey's multiple comparisons test.

Chapter 4

DISCUSSION

4.1 – Study Summary

A growing body of evidence indicates that necroptosis plays an important role in the pathogenesis of numerous clinical conditions and diseases [102, 103, 104, 105, 106, 109, 110]. The pathological relevance of necroptosis in the context of organ transplantation is particularly significant. Necroptosis is an inflammatory form of cell death that contributes to graft injury and triggers alloimmunity, which adversely affects graft survival and function [102, 103, 104, 105, 109, 110]. Studies by our group have demonstrated the role of necroptosis in inducing inflammation and tissue injury in donor heart and kidney grafts [103, 104]. We have previously demonstrated that RIPK1 and RIPK3 contribute to necroptosis and that RIPK3 ablation attenuates graft rejection [103, 104]. While the upstream pathways of necroptosis are well-established, the role of mitochondria and the downstream mechanisms involved remain controversial [102, 106]. A recent study by our group demonstrated that the downstream pathway of necroptosis involves CypD-mediated mPTP formation and that CypD-deficient donor hearts exhibit prolonged survival [104].

In this study, we investigated the role of necroptosis in cell death induced by cold hypoxia-reoxygenation injury, which modeled *in vivo* IRI. Our data indicate that necroptosis plays a significant role in hypoxia/reoxygenation-induced cell death in endothelial cells, indicating its relevance in IRI and organ transplantation. Inhibition of caspases prevents hypoxia/reoxygenation-induced apoptosis but promotes necroptosis and significantly increases overall cell death (Figure 9A&B). We were able to corroborate findings from our previous

study indicating the role of CypD in necroptosis using the *in vitro* cold hypoxia-reoxygenation injury model. We found that CypD inhibition (and ablation) significantly attenuates hypoxia/reoxygenation-induced necroptosis (Figure 11). We then extended our findings to a clinically relevant model of cardiac transplantation. Donor hearts from WT and $CypD^{-/-}$ mice were subjected to static cold storage (ischemic injury) followed by heterotopic transplantation into BALB/c mice (reperfusion injury). We found that pre-transplant ischemia aggravates cardiac allograft rejection and that $CypD^{-/-}$ cardiac allografts survive significantly longer than WT cardiac allografts (Figures 17 and 18). Our *in vitro* and *in vivo* studies confirmed that CypD plays an essential role in the necroptotic pathway and that inhibiting CypD confers protection against IRI and attenuates alloimmunity.

Subsequently, we investigated the roles of various potential mediators downstream of CypD-mediated mPTP formation. We first ruled out the roles of ROS (oxidative damage) and the PGAM5-Drp1 axis (mitochondrial fragmentation) in hypoxia/reoxygenation-induced necroptosis (Figure 10). We observed the translocation of AIF to the nucleus and AIF-mediated DNA degradation into ~50 kbp fragments following cold hypoxia-reoxygenation injury (Figures 14 and 15). We found that AIF silencing significantly decreases hypoxia/reoxygenation-induced necroptosis (Figure 13A). Since no known pharmacological inhibitors of AIF exist, we confirmed our results by restricting AIF translocation to the nucleus via CypA inhibition, since CypA is required for the translocation of AIF to the nucleus [148, 152, 153]. CypA inhibition also decreases hypoxia/reoxygenation-induced necroptosis (Figure 13B). We found that disrupting the upstream pathway of necroptosis via RIPK1 inhibition prevents AIF translocation to the nucleus and DNA degradation into ~50 kbp fragments (Figures 14 and 15). These findings suggest that AIF may be the downstream mediator in necroptosis.

4.2 – The Endothelium in Organ Transplantation

The endothelium is critical in maintaining the vascular homeostasis and constitutes the first barrier between the recipient's immune system and the allograft. Substantial injury to the endothelium results in loss of vascular integrity and tone, increased vascular permeability and intravascular thromboses, which disrupts blood flow, promotes inflammation and alloimmunity and ultimately, contributes to graft injury and necrosis [65, 66, 67, 77, 90, 95, 96]. Endothelial cells are susceptible to the different forms of PCD induced by IRI [8, 10, 65, 66, 67, 77, 90, 103, 104]. Given the central role of the endothelium in initiating and promoting the alloimmune response, preventing endothelial cell death is particularly important.

4.3 – Necroptosis in IRI and Organ Transplantation

IRI is an inevitable consequence of organ transplantation (Figure 1) with life-threatening consequences in the immediate postoperative period, such as PGD. IRI has also been shown to have deleterious long-term effects on graft survival and contributes to graft rejection (Figure 3) [4, 8, 12]. Improvements in organ preservation processes and post-transplantation immunosuppressive protocols have not diminished the impact of IRI on graft survival and function; therefore, current research efforts are focused on minimizing IRI itself. IRI is associated with unregulated necrosis and various forms of PCD (Figures 2, 4 and 5). A thorough understanding of the mechanisms involved in PCD can aid in the designing of targeted therapies that disrupt IRI and promote graft survival [8, 12, 13, 18].

Historically, apoptosis was considered the sole form of PCD, with essential roles in homeostasis, development and numerous disease processes, including IRI. However, evidence now indicates that necrosis, which was previously regarded as an unregulated form of cell

death, can occur in a regulated manner [102, 105, 154]. There are many different forms of regulated necrosis (Figure 4) [101]. Amongst the different forms of regulated necrosis induced by IRI, the best characterized and clinically relevant in the context of organ transplantation is necroptosis [13, 102, 103, 104, 105, 109, 110, 154, 155, 156, 157, 158]. Necroptosis is a highly inflammatory form of cell death that triggers robust alloimmune responses due to the release of cDAMPs and cytosolic contents [102, 103, 104, 154, 155, 156, 157, 158]. Thus, inhibiting IRI-induced necroptosis will minimize the loss of functional cells and limit the inflammatory and alloimmune injuries in organ transplantation [102, 103, 104, 156, 157, 158].

In a recent study by our group, we showed that endothelial cells are susceptible to TNFα-induced necroptosis [104]. Considering the role of endothelial dysfunction in augmenting graft injury and promoting alloimmunity, we investigated the role of hypoxia/reoxygenation-induced necroptosis in endothelial cells. Our findings indicate that necroptosis plays a significant role in hypoxia/reoxygenation-induced endothelial cell death and that the inhibition of caspases decreases apoptosis but increases necroptosis and overall cell death (Figure 9A). To develop a better understanding of the necroptotic pathway, we designed this study to investigate the putative mediators and downstream mechanisms activated following the upstream signaling.

4.4 – Role of Mitochondria in Hypoxia/Reoxygenation-Induced Necroptosis

In necroptosis, the sequence of events downstream of the RIPK1/RIPK3 necrosome formation and phosphorylation of MLKL is a subject of scientific controversy (Figure 5) [102, 104, 106]. Specifically, the evidence for the role of mitochondria in necroptosis is conflicting [102, 104, 106]. While the majority of the studies support a role for mitochondria in necroptosis, a few studies suggest that the mitochondria may be dispensable for this process

[106]. This was best argued by Tait *et al.* who showed that widespread mitochondrial depletion via mitophagy in SVEC and 3T3 cells did not disrupt necroptosis [128]. One proposed pathway that does not involve the mitochondria implicates the translocation of oligomerized pMLKL to the plasma membrane, followed by its rupture. Although inconclusive, evidence for this pathway was presented by Cai *et al.* and Chen *et al.* using multiple cell types [133, 134].

The earliest studies investigating the downstream mechanisms of necroptosis indicated a shift in metabolism leading to ROS production following necrosome translocation to the mitochondria (Figure 5) [106]. In a study done by Lin *et al.* using MEFs, TNFα signaling increased ROS levels and necroptosis and the use of the ROS scavenger, butylated hydroxyanisole, efficiently blocked necroptosis following TNFα stimulation [115]. Furthermore, the ablation of critical necroptotic mediators, RIPK1, TRAF2 and FADD, led to decreased ROS levels and resistance against TNFα-induced necroptosis. Vanlangenakker *et al.* later demonstrated that the RIPK1/RIPK3-mediated ROS generation following TNFα stimulation in L929 cells were mitochondrially derived [116]. These findings were corroborated by Ardestani *et al.*, who used two different cell lines, L929 and RAW 264.7, to demonstrate the mitochondrial origin of ROS generated following TNFα stimulation [117]. The strongest evidence indicating the role of mitochondrial ROS in necroptosis was provided by Davis *et al.*, who showed the translocation of RIPK3 to the mitochondria following TNFα stimulation and inhibition of necroptosis with the mitochondrial antioxidant MnSOD in endothelial cells [122].

The earlier studies strongly implicating a role for mitochondrial ROS in necroptosis were later disputed by findings from other studies, which indicated that ROS were not 'absolutely' essential for necroptosis. He *et al.* suggested that the downstream mechanism of

necroptosis may be cell-type specific [159]. While establishing the role of RIPK3, they showed that ROS scavenging in HT-29 cells did not attenuate TNFα-induced necroptosis. This observation was supported by a study by Temkin *et al.*, which precluded the role of antioxidants (ascorbic acid, glutathione and NAC) in rescuing THP-1 cells from TNFα-induced necroptosis [120]. Hence, the role of ROS in mediating necroptosis requires further investigation.

IRI is associated with significant production of ROS, including ROS generated secondary to mitochondrial damage and ETC disruption (Figure 2) [13, 18]. We, therefore, decided to investigate the role of ROS in hypoxia/reoxygenation-induced necroptosis. In our study, treatment with the ROS scavengers, TEMPOL and NAC, did not result in a significant reduction of hypoxia/reoxygenation-induced necroptosis (Figure 10 B&C). The use of the mitochondria-specific ROS scavenger, mito-TEMPOL, also did not inhibit hypoxia/reoxygenation-induced necroptosis (Figure 10D). Although unexpected, our findings are not entirely surprising. Endothelial cells have low-energy turnover and generate most of their ATP molecules via anaerobic glycolysis [95, 160, 161, 162]. A significant mechanism of ROS production following reperfusion injury is associated with ischemia-induced ETC dysfunction. While speculative, it is possible that since the endothelial cells rely primarily on anaerobic glycolysis, ROS production secondary to ETC dysfunction is minimal and, unlike with other cell types, does not contribute to hypoxia/reoxygenation-induced necroptosis in endothelial cells.

Another potential mediator of necroptosis involves the PGAM5-Drp1 axis (Figure 5). According to a study by Wang *et al.*, following its formation, the necrosome translocates to the mitochondria and interacts with PGAM5. Activated PGAM5, in turn, activates Drp1 and

induces mitochondrial fragmentation. Data from this study indicate a direct interaction between RIPK1/RIPK3 and PGAM5 indicated by coimmunoprecipitation assays. Furthermore, Drp1 silencing and treatment with the PGAM5 inhibitor, MDivi-1, inhibited TNFα-induced necroptosis [123]. These findings were later supported by Zhang *et al.*, who showed that Drp1 depletion in NRK-52E cells resisted TNFα-induced cell death [124]. Drp1 inhibition has also been shown to be protective against IRI and recommended as a novel therapeutic strategy for cardioprotection [163].

The role of mitochondrial PGAM5-Drp1 axis has been disputed by recent studies by several groups [128, 129, 130, 131]. These studies used PGAM5 and Drp1 silenced or deficient MEFs and L929 cells and did not find a reduction in cell death following TNFα stimulation [106, 131]. In our study, PGAM5-Drp1 axis inhibition in endothelial cells did not protect against hypoxia/reoxygenation-induced cell death (Figure 10A) and ruled out mitochondrial fragmentation as the mechanism responsible for cellular demise in hypoxia/reoxygenation-induced necroptosis. However, a recent study by Zhang *et al.* suggested that Drp1 modulates CypD-mediated mPTP formation and mitochondrial ROS production [163]. It remains to be established how this interaction relates to necroptosis.

We have previously shown that mitochondria critically participate in necroptosis and that inhibition of CypD mediated mPTP formation attenuated necroptosis in endothelial cells [104]. In this study, we ruled out the role of ROS and PGAM5-Drp1 axis in hypoxia/reoxygenation-induced necroptosis and then investigated the role of CypD-mediated mPTP formation in hypoxia/reoxygenation-induced necroptosis.

4.5 – Hypoxia/Reoxygenation-Induced Necroptosis in Endothelial Cells Involves CypD-Mediated mPTP Formation

The role of CypD-mediated mPTP formation in necroptosis has been the subject of considerable study (Figures 2, 4, 5 and 7). In studies conducted by Baines *et al.*, Nakagawa *et al.*, and Schinzel *et al.*, CypD-mediated mPTP formation was shown to be involved in necroptosis [125, 126, 127]. These studies indicated that CypD ablation provided resistance against necroptosis induced by ROS-mediated oxidative damage and mitochondrial calcium overload. In the setting of IRI, mPTP formation also provides a link to ROS production. While ROS-mediated oxidative damage promotes CypD-mediated mPTP formation by sensitizing mPTP to mitochondrial calcium, mPTP formation augments ROS production by contributing towards ETC dysfunction and incomplete oxygen reduction [20]. This was confirmed in a study by Roca and Ramakrishnan, which showed that TNFα-induced ROS production and necroptosis in macrophages were both blocked by CypD inhibition [164].

As with the other proposed mitochondrial mediators, the role of mPTP formation in necroptosis has also been questioned [106, 128]. The most compelling evidence against the involvement of mPTP formation in necroptosis was presented in studies by Tait *et al.*, and Ch'en *et al.* [128, 165]. These studies showed that although RIPK1 and RIPK3 ablation rescued caspase-8-deficient cells from necroptosis, CypD ablation did not. Linkermann *et al.* also argued against the involvement of mPTP formation by showing that simultaneous RIPK3 and CypD ablation provided greater protection against IRI-induced necroptosis than separate RIPK3 and CypD depletions [132]. The findings from these studies suggested that the proposed necroptotic pathway involving the upstream RIPK1/RIPK3/pMLKL and the downstream CypD-mediated mPTP formation pathways were divergent.

Gan *et al.* from our group, however, confirmed that the protection conferred by CypD ablation is not additive to that conferred by blocking the upstream signaling pathway of

necroptosis via RIPK1 inhibition in endothelial cells [104]. Our group also showed that the phosphorylation of MLKL, an established event in necroptosis, was suppressed by CypD inhibition and ablation. These findings confirmed that CypD-mediated mPTP formation was the downstream mechanism involved in TNFα-induced necroptosis in endothelial cells. In this study, we found that hypoxia/reoxygenation-induced necroptosis in endothelial cells was significantly reversed with CypD inhibition and ablation (Figure 11). Furthermore, the protection conferred by CypD inhibition was not additive to that conferred by RIPK1 inhibition. We, therefore, concluded that hypoxia/reoxygenation-induced necroptosis in endothelial cells is dependent on CypD-mediated mPTP formation.

While inconclusive, recent evidence also implicates CypD-mediated mPTP formation in apoptosis (Figure 6). The earliest evidence supporting this position was presented in a study by Murphy *et al.*, who showed that the overexpression of the anti-apoptotic protein BCL-2 suppresses calcium-induced mPTP formation [166]. Later, Crompton *et al.* and Green *et al.* reported that the use of the CypD inhibitor CsA blocked some forms of apoptosis [167, 168]. Most importantly, in its most current model, the OMM component of mPTP is formed by the pro-apoptotic proteins BAX and BAD [138, 143]. However, most evidence associating CypD-mediated mPTP formation to apoptosis is circumstantial and indirect. It is possible that the ROS generated secondary to mPTP formation in the setting of cellular injury trigger apoptosis. mPTP formation also dysregulates cytosolic calcium homeostasis, which can then activate calpains and calcineurin [138, 169]. Calpain-mediated BID cleavage promotes OMM permeabilization by BAX and BAK [170]. Similarly, calcineurin activates the pro-apoptotic protein BAD, which then antagonizes the anti-apoptotic activities of BCL-2 and BCL-XL [171]. Persistent mPTP formation also leads to mitochondrial swelling followed by OMM rupture, which may facilitate the release of the pro-apoptotic mediators [13, 18, 20].

In order to exclude the role of CypD-mediated mPTP formation in hypoxia/reoxygenation-induced apoptosis within this study, we used the pan-caspase inhibitor z-VAD-fmk in our *in vitro* cold hypoxia-reoxygenation injury model. The use of the pan-caspase inhibitor also indicates that the DNA degradation in necroptosis is not mediated by caspase-activated DNases (Figure 9A). In fact, our findings show that inhibition of caspases promotes DNA degradation into ~50 kbp fragments. Hence, it is likely that CypD-mediated mPTP formation leads to necroptosis without contributing to apoptosis.

4.6 – Downstream of CypD-Mediated Mitochondrial Damage, Hypoxia/Reoxygenation-Induced Necroptosis in Endothelial Cells Involves AIF

The scientific controversy involving the role of CypD-mediated mPTP formation in necroptosis has diverted attention from investigating the precise downstream mechanisms activated by its formation. As described earlier, mPTP augments ROS production, the role of which was supported by the earlier studies investigating the downstream mechanisms of necroptosis (Figure 2) [106, 115, 116, 117, 119, 119]. In this study, our findings suggested that the mitochondrial ROS generated secondary to mPTP did not contribute to hypoxia/reoxygenation-induced necroptosis since treatment with mito-TEMPOL did not confer any protection (Figure 10D). More importantly, however, our findings suggested that CypD-mediated mPTP formation was not dependent on ROS since the use of ROS scavengers, unlike CypD inhibition, did not attenuate necroptosis. This finding supports a 'direct' link between the upstream necroptotic pathway involving RIPK1/RIPK3/pMLKL and CypD-mediated mPTP formation.

After excluding the role of ROS and caspases downstream of CypD-mediated mPTP formation in hypoxia/reoxygenation-induced necroptosis, we investigated the role of AIF. The

dual and apparently paradoxical roles of AIF in cellular life and death can best be compared to Cyt C. AIF has an essential survival role as a mitochondrial oxidoreductase involved in the assembly and stabilization of the ETC components, Complex I and Complex III [147, 148, 150]. However, once released into the cytosol, it quickly translocates to the nucleus and induces DNA degradation (Figure 8) [145, 146, 147, 148]. Since its discovery by Susin *et al.* 20 years ago, several studies have reported the involvement of AIF in various clinical conditions and diseases [147, 148]. The role of AIF in IRI is well-established [147, 148, 172, 173, 174, 175, 176]. Soon after its discovery, Plesnila *et al.* and Kim *et al.* published studies supporting a role for AIF in cerebral and myocardial IRI-induced cell death, respectively [174, 175]. Culmsee *et al.* later demonstrated that compared to WT mice, Hq mice displayed smaller infarct volumes and significantly reduced neuronal death after transient cerebral artery occlusion [176]. More recent studies have shown the role of AIF in non-ischemic pathological conditions as well [145, 146, 147, 148, 172, 177, 178].

The mechanism regulating the processing and translocation of AIF to the nucleus is complex and not fully understood. The release of AIF from the mitochondria involves two essential steps: proteolytic cleavage yielding the truncated 'liberated' form of AIF and permeabilization of mitochondria that enables its exit. While not completely established, it is speculated that the cleavage of AIF to its liberated form is mediated by cysteine proteases such as calpains and cathepsins (Figure 8) [147, 148]. Several studies, including one from the group that discovered AIF, have shown that the dissipation of $\Delta\Psi m$ accompanies the release of AIF from mitochondria [147, 148, 172]. These studies are supported by experiments in which treatment with CsA blocks the release of AIF from the mitochondria suggesting that mPTP may be the channel through which AIF is released into the cytosol [145, 177, 178].

Our findings from this study clearly support a role for AIF in hypoxia/reoxygenation-induced necroptosis in endothelial cells. In cells undergoing necroptosis, translocation of AIF to the nuclei (Figure 14) and DNA degradation into ~50 kbp fragments was observed (Figure 15). These changes were associated with the phosphorylation of MLKL, a crucial event in necroptosis. Interruption of the upstream necroptotic pathway via RIPK1 inhibition reversed these changes. Furthermore, AIF-silenced cells, like CypD-ablated cells, were resistant to hypoxia/reoxygenation-induced necroptosis. Our findings, coupled with studies indicating a role for mPTP in necroptosis and AIF release, indicate that hypoxia/reoxygenation-induced necroptosis in endothelial cells involves the release of AIF from CypD-mediated mPTP formation following RIPK1/RIPK3/pMLKL translocation to the mitochondria. While there is considerable evidence supporting a role for mPTP in necroptosis and studies suggesting its role in the release of AIF, our findings connecting the established upstream pathway of necroptosis involving RIPK1/RIPK3/pMLKL to AIF release via CypD-mediated mPTP formation is novel.

Genomic stress leading to PARP-1 activation has been strongly implicated in various diseases [149, 179]. In the setting of IRI, ROS-mediated oxidative damage to DNA and subsequent activation of PARP-1 has been reported in various tissues, including the brain, heart, intestine and retina [149, 179, 180, 181, 182]. PARP-1 activation causes ADP ribosylation of 'damaged' chromatin, modulating its structure and facilitating its interaction with DNA repair enzymes. However, if the DNA damage is severe, the excessive PAR moieties in the nucleus translocate to the mitochondria and mediate AIF release, ultimately leading to a form of cell death termed parthanatos (Figure 4) [147, 149].

In this study, neither treatment with the ROS scavengers nor PARP-1 inhibition decreased hypoxia/reoxygenation-induced cell death (Figure 16). This finding indicated that

the ROS-mediated DNA damage following cold hypoxia-reoxygenation injury, if present, was not sufficiently severe to induce the accumulation of excessive PAR moieties in the nucleus. The failure to attenuate cell death with direct inhibition of PARP-1 confirmed that the AIF release following cold hypoxia-reoxygenation injury was unrelated to PARP-1 activation and parthanatos. While targeting AIF to disrupt necroptosis is a promising prospect, it presents two problems. Firstly, no pharmacological inhibition of AIF currently exists, and secondly, AIF has an essential pro-survival role in cellular bioenergetics. The translocation of AIF to the nucleus is facilitated by CypA and suppressed by HSP-70 [147, 148, 172]. As with the silencing of AIF, CypA inhibition protected endothelial cells from hypoxia/reoxygenation-induced necroptosis. Our findings showed that CypA inhibition blocked AIF translocation to the nucleus and DNA degradation into ~50 kbp fragments. CypA inhibition, therefore, represents an effective therapeutic strategy to disrupt AIF-mediated necroptosis. Our findings are supported by recent studies indicating a protective role for CypA inhibition in IRI [147, 148, 153, 172, 183].

4.7 – CypD Ablation Attenuates Cardiac Allograft Injury and Transplant Rejection

CypD inhibition has been shown to protect against IRI and neurodegenerative disorders. The protection conferred by pharmacological inhibition of CypD against IRI has been confirmed with CypD ablation in every organ tested, including heart, kidneys, intestine and liver [18, 137, 138, 141, 184, 185, 186, 187, 188, 189, 190, 191, 192]. Inhibition of CypD-mediated mPTP formation underlies the cardioprotection elicited by the endogenous phenomenon of ischemic conditioning and has been recommended as a potential therapeutic target in the management of myocardial infarction [184, 185]. These studies strongly indicate

that CypD-mediated mPTP formation can be used as an effective strategy in organ preservation as well. More recently, Tran *et al.* have shown that mPTP formation promotes endothelial cell immunogenicity in the setting of IRI that can be negated by CypD inhibition [193]. While their study focuses on the role of mPTP formation in transplant immunity, it is plausible that the increase in endothelial cell immunogenicity is the result of necroptotic cell death. Our group has previously shown that interrupting necroptosis via RIPK3 ablation attenuates allograft injury and transplant rejection in cardiac and renal transplantation models [103, 104]. CypD deficiency in donor hearts conferred the same protection [104].

In this study, we extended our findings to a clinically relevant model of donor heart preservation involving cold ischemic storage followed by transplantation. Our findings showed that pre-transplant ischemia aggravates cardiac allograft rejection. Donor hearts subjected to ischemia had shorter survival times compared to non-ischemic hearts (Figure 17A). Interestingly, CypD deficiency in donor hearts attenuated graft rejection and promoted allograft survival dramatically (Figure 17B).

4.8 – Therapeutic Strategies to Disrupt Necroptosis

Pharmacological and genetic inhibition of necroptosis has been shown to ameliorate several diseases with an inflammatory component [102, 105, 194, 195, 196]. The first pharmacological inhibitor investigated for use in clinical practice was Nec-1, an allosteric inhibitor of RIPK1 [102, 197, 198]. However, limited half-life, poor pharmacokinetic properties and off-target activity precluded its use [102, 197, 199, 200, 201, 202, 203]. Optimization of Nec-1 generated Nec-1s, which enhanced its specificity, but the poor pharmacokinetic properties associated with Nec-1 persist and a clinical trial is yet to be completed [102, 197, 200, 203]. The newer RIPK1 kinase inhibitors developed by

GlaxoSmithKline, including GSK'963 and GSK'2982772, have shown efficacy against necroptosis in human cells [204, 205, 206]. However, the results were not replicated in mouse and rat cells, limiting explorations of their *in vivo* therapeutic value with animal disease models [206]. RIPK3 kinase inhibitor GSK'872 and MLKL inhibitor necrosulfonamide have also been developed, but *in vivo* data using animal models are lacking [206, 207, 208, 209, 210]. The interconnected pathways involving the various forms of PCD and essential cellular functions is a limiting factor in the use of all these drugs [197, 203, 206].

Since it was first discovered in 1972, the CypD inhibitor CsA has been crucial in achieving improved survival rates in patients following organ transplantation [211, 212]. While the current use of CsA in the post-transplantation setting is aimed at suppressing the immune system by repressing the IL-2 -mediated activation of T cells, it is possible that the beneficial effects of CsA in organ transplantation involves its inhibitory effect on CypD and prevention of mPTP formation [104, 211, 212]. In fact, although the immunosuppressive capacity of CsA is less potent than other immunosuppressive agents such as tacrolimus, mycophenolate-mofetil and rapamycin, it provides greater protection against graft loss compared to these compounds [211, 213, 214, 215, 216, 217]. As with several other studies, findings from this study have shown that the use of CsA in organ transplantation results in a reduced inflammatory response and significantly improved graft survival and function. Our study is unique because we have provided evidence indicating that this is due to the reduction in cell death via the highly inflammatory necroptotic death pathway. A more intriguing challenge with the use of CsA (or alternative pharmacological agents) to block necroptosis in organ transplantation is its targeted and sustained delivery to the donor organ [211].

In this study, inhibiting AIF translocation to the nucleus provided a more significant benefit than inhibiting CypD-mediated mPTP formation with CsA. This might be due to the presence of an AIF splice-variant located outside the mitochondria that is equally capable of translocating to the nucleus and inducing DNA degradation as the mitochondrial AIF [147, 148]. Inhibition of AIF translocation targets both the mitochondrial and the extra-mitochondrial AIF, while the use of CsA prevents only the mitochondrial AIF from translocating to the nucleus. Although more extensive testing needs to be done, our data explain why Hq mice show resistance against IRI [147, 148, 152, 153, 172, 173, 174, 175, 176]. Since AIF deficiency is associated with severe adverse effects, a better approach would be inhibition of AIF translocation to the nucleus with the use of pharmacological agents such as Alisporivir. Inhibition of AIF translocation may promote graft survival and attenuate alloimmunity by inhibiting necroptosis while preserving the vital functions of AIF. As such, it represents a potent therapeutic strategy in organ transplantation.

More recently, research investigating better organ preservation strategies have gained a lot of attention [218, 219]. This includes the development of perfusion systems and the 'engineering' of organ preservation solutions to enhance the functional preservation of donor organs [218, 219, 220]. Our *in vitro* data from this study showed that combined intervention strategies during the hypoxia and reperfusion phases conferred greater protection than intervention at any one stage. For this study, our *in vivo* experiments used the current model of organ preservation involving static cold storage. It would be interesting to evaluate the efficacy of CsA and Alisporivir in preserving graft viability when used as pharmacological additives in organ preservation solutions used in perfusion pumps.

4.9 – Future Directions

Our *in vitro* data shows the role of AIF in inducing necroptosis in endothelial cells following cold hypoxia-reoxygenation injury. We are currently studying the role of AIF in *in vivo* cardiac transplantation models using endothelium-specific AIF knockout mice generated by Cre-LoxP recombinase system. We plan on investigating the role of AIF in inducing necroptosis in other cell types such as renal tubular epithelial cells and believe that evaluating cellular function following IRI is as important as evaluating cellular survival. In addition to preserving cellular survival, it would be worthwhile investigating the role of the potential therapeutic strategies in maintaining cellular function as well. This is important because organ function is ultimately dependent on the integrated activities of its cells. Finally, we would like to investigate the most suitable delivery and administration methods of the identified pharmacological agents.

4.10 – Limitations

As with all *in vitro* experiments, a limitation of this study is that the *in vitro* cold hypoxia-reoxygenation injury model used may not accurately represent the *in vivo* and clinical conditions. For the *in vitro* cold hypoxia phase, anaerobic GENbags were used. The GENbags use a chemical generator sachet to induce hypoxia. Although the results of the *in vitro* cold hypoxia-reoxygenation injury were repeated with hypoxia induction in the Hypoxystation, the results may not reflect physiological hypoxia. The GENbags also generate heat in the first 30-60 minutes of the chemical reaction that induces hypoxia while the Hypoxystation can only be set as low as 10°C, which does not reflect clinical conditions involved in organ transplantation. *In vitro* experiments using a single cell-type, as is the case with this study, also do not take into account the complex physiological and pathological cellular responses triggered by the cell's external environment. The cells may also react differently in *in vivo* and clinical settings

depending on their interaction with leukocytes. Furthermore, the pathways involved in one cell-type may not be activated/involved in other cell types. In this study, endothelial cells were used to study the effects of IRI in the context of organ transplantation. Endothelial cells represent only one component of IRI. They are also relatively resistant to hypoxia due to low-energy turnover compared to cardiomyocytes (cardiac transplantation) or kidney tubular epithelial cells (renal transplantation). Finally, the concentration of the proinflammatory cytokines used in the *in vitro* settings may not be reflective of their physiological levels. In this study, these problems were addressed by repeating *in vivo* experiments involving a clinically relevant model cardiac transplantation.

To study the various pathways involved in necroptosis, several drugs were used. The drugs used may have off-target effects and may influence other pathways involved. The use of the drugs studied in the *in vitro* as well as *in vivo* studies may not be clinically applicable and may have toxic effects at the concentrations used. This study did not address adverse effects related to drug concentrations. This is particularly true for Alisporivir, which was discontinued due to severe adverse effects (e.g., pancreatitis) following late stage clinical development as a combination therapy for the treatment of HCV infection [221, 222]. Both CsA and Alisporivir are cyclophilin-binding molecules and may bind non-specifically to other cyclophilins [104, 147, 148, 211, 212]. This problem was addressed by using gene knock-out and siRNA interference silencing. However, these techniques may not be truly effective due to substantial genetic variability, and siRNA interference silencing is limited to a few days. These problems may be overcome by the use of shRNA interference silencing and CRIPSPR/Cas9 genome editing.

While data from this study indicate that AIF-silencing in endothelial cells confers protection against hypoxia/reoxygenation-induced necroptosis, AIF is a physiologically vital molecule essential in cellular bioenergetics, and its inhibition in cells with high-energy turnover such as cardiomyocytes (cardiac transplantation) or kidney tubular epithelial cells (renal transplantation) may exacerbate graft injury [147, 148]. A potential strategy may be to inhibit AIF translocation to the nucleus rather than its inhibition. A therapeutic strategy aimed at preventing AIF translocation globally in the context of organ transplantation is yet to be designed.

4.11 – Conclusion and Study Significance

In this study, we corroborated findings from our previous study and presented evidence indicating that targeting CypD-mediated mPTP formation presents a comprehensive therapeutic strategy in organ transplantation [104]. We showed the role of CypD-mediated mPTP formation in necroptosis using *in vitro* and *in vivo* experiments and investigated the putative mechanisms activated downstream of mPTP formation. Our findings established the role of AIF in necroptosis in endothelial cells and indicated that targeting AIF translocation yields even greater protection than targeting CypD-mediated mPTP formation in organ transplantation.

It is important to note that while the role of IRI-induced necroptosis in organ transplantation is well-established, the development of clinically applicable pharmacological agents in disrupting it represents a significant obstacle [102, 104, 202, 203, 206]. The ‘ideal’ pharmacological inhibitor will disrupt necroptosis without perturbing the vital pro-survival physiological functions of the mediators involved. The goal of this study was to identify and develop a better understanding of the downstream mechanisms of IRI-induced necroptosis. We

believe that this will enable the generation of therapeutic strategies aimed at mitigating IRI and the subsequent inflammatory and alloimmune responses, ultimately promoting graft survival and function. Furthermore, the use of these pharmacological agents during donor organ storage will enhance the functional preservation of organs and enable the use of marginal donors, thereby addressing donor organ shortage.

REFERENCES

1. Ziaeian B, Fonarow GC. Epidemiology and aetiology of heart failure. *Nat Rev Cardiol.* 2016;13(6):368–378. doi:10.1038/nrcardio.2016.25.

2. Vos T, Flaxman AD, Naghavi M, et al. Years lived with disability (YLDs) for 1160 sequelae of 289 diseases and injuries 1990-2010: a systematic analysis for the Global Burden of Disease Study 2010 [published correction appears in Lancet. 2013 Feb 23;381(9867):628. AlMazroa, Mohammad A [added]; Memish, Ziad A [added]]. *Lancet*. 2012;380(9859):2163–2196. doi:10.1016/S0140-6736(12)61729-2.

3. Bui AL, Horwich TB, Fonarow GC. Epidemiology and risk profile of heart failure. *Nat Rev Cardiol*. 2011;8(1):30–41. doi:10.1038/nrcardio.2010.165.

4. Angela Felicia Sunjaya and Anthony Paulo Sunjaya. Combating Donor Organ Shortage: Organ Care System Prolonging Organ Storage Time and Improving the Outcome of Heart Transplantations. *Cardiovascular Therapeutics*. Vol. 2019, Article ID 9482797, 7 pages, 2019. https://doi.org/10.1155/2019/9482797.

5. Wittwer T, Wahlers T. Marginal donor grafts in heart transplantation: lessons learned from 25 years of experience. *Transpl Int*. 2008;21:113-25. 10.1111/j.1432-2277.2007.00603.x.

6. Harris C, Cao C, Croce B, Munkholm-Larsen S. Heart transplantation. *Ann Cardiothorac Surg*. 2018;7(1):172. doi:10.21037/acs.2018.01.11.

7. Kittleson MM, Kobashigawa JA. Cardiac transplantation: current outcomes and contemporary controversies. *JACC Heart Fail*. 2017;5:857–868. doi: 10.1016/j.jchf.2017.08.021.

8. Kim IC, Youn JC, Kobashigawa JA. The Past, Present and Future of Heart Transplantation. *Korean Circ J*. 2018;48(7):565–590. doi:10.4070/kcj.2018.0189.

9. Lund LH, Edwards LB, Dipchand AI., et al; International Society for Heart and Lung Transplantation. The Registry of the International Society for Heart and Lung Transplantation: thirty-third adult heart transplantation report-2016; focus theme: primary diagnostic indications for transplant. *J Heart Lung Transplant*. 2016. October;35(10):1158-1169. doi: 10.1016/j.healun.2016.08.017.

10. Tonsho M, Michel S, Ahmed Z, Alessandrini A, Madsen JC. Heart transplantation: challenges facing the field. *Cold Spring Harb Perspect Med*. 2014;4(5):10.1101/cshperspect.a015636 a015636. Published 2014 May 1. doi:10.1101/cshperspect.a015636.

11. Potena, L., Zuckermann, A., Barberini, F. *et al.* Complications of Cardiac Transplantation. *Curr Cardiol Rep* 20, 73 (2018). https://doi-org.proxy1.lib.uwo.ca/10.1007/s11886-018-1018-3.

12. Khush KK, Menza R, Nguyen J, Zaroff JG, Goldstein BA. Donor predictors of allograft use and recipient outcomes after heart transplantation. *Circ Heart Fail*. 2013;6(2):300–309. doi:10.1161/CIRCHEARTFAILURE.112.000165.

13. Kalogeris T, Baines CP, Krenz M, Korthuis RJ. Cell biology of ischemia/reperfusion injury. *Int Rev Cell Mol Biol*. 2012;298:229–317. doi:10.1016/B978-0-12-394309-5.00006-7.

14. Sanada S., Komuro I., Kitakaze M. Pathophysiology of myocardial reperfusion injury: preconditioning, postconditioning, and translational aspects of protective measures. *American Journal of Physiology. Heart and Circulatory Physiology*. 2011;301(5):H1723–H1741. doi: 10.1152/ajpheart.00553.2011.

15. Holger K. Eltzschig, Charles D. Collard, Vascular ischaemia and reperfusion injury, *British Medical Bulletin*, Volume 70, Issue 1, 2004, Pages 71–86, https://doi.org/10.1093/bmb/ldh025.

16. Chen M, Won DJ, Krajewski S, Gottlieb RA. Calpain and mitochondria in ischemia/reperfusion injury. *J. Biol. Chem*. 2002;277:29181–29186.

17. Wu MY, Yiang GT, Liao WT, et al. Current mechanistic concepts in ischemia and reperfusion injury. *Cell Physiol Biochem*. 2018;46:1650–1667. doi:10.1159/000489241.

18. Carden DL, Granger DN. Pathophysiology of ischaemia-reperfusion injury. *J Pathol*. 2000;190:255–266.

19. Granger DN, Korthuis RJ. Physiologic mechanisms of postischemic tissue injury. *Annu Rev Physiol* 1995; 57: 311–332.

20. Baines CP. The mitochondrial permeability transition pore and ischemia-reperfusion injury. *Basic Res Cardiol*. 2009;104(2):181–188. doi:10.1007/s00395-009-0004-8.

21. Slegtenhorst BR, Dor FJ, Rodriguez H, Voskuil FJ, Tullius SG. Ischemia/reperfusion Injury and its Consequences on Immunity and Inflammation. *Curr Transplant Rep*. 2014;1(3):147–154. doi:10.1007/s40472-014-0017-6.

22. Land W, Schneeberger H, Schleibner S, Illner WD, Abendroth D, Rutili G, et al. The beneficial effect of human recombinant superoxide dismutase on acute and chronic

rejection events in recipients of cadaveric renal transplants. *Transplantation*. 1994 Jan;57(2):211–217.

23. Matzinger P. Tolerance, danger, and the extended family. *Annu Rev Immunol.* 1994;12:991–1045.

24. Gross O, Thomas CJ, Guarda G, Tschopp J. The inflammasome: An integrated view. *Immunol Rev*. 2011 Sep;243(1):136–151.

25. Tschopp J, Schroder K. NLRP3 inflammasome activation: The convergence of multiple signalling pathways on ROS production? *Nat Rev Immunol*. 2010 Mar;10(3):210–215.

26. Chen GY, Nunez G. Sterile inflammation: Sensing and reacting to damage. *Nat Rev Immunol*. 2010 Dec;10(12):826–837.

27. Frangogiannis NG. Chemokines in ischemia and reperfusion. *Thromb Haemost*. 2007 May;97(5):738–747.

28. Nathan C. Neutrophils and immunity: Challenges and opportunities. *Nat Rev Immunol*. 2006 Mar;6(3):173–182.

29. Lee S, Huen S, Nishio H, Nishio S, Lee HK, Choi BS, et al. Distinct macrophage phenotypes contribute to kidney injury and repair. *J Am Soc Nephrol*. 2011 Feb;22(2):317–326.

30. Schofield ZV, Woodruff TM, Halai R, Wu MC, Cooper MA. Neutrophils—a key component of ischemia-reperfusion injury. *Shock*. 2013;40(6):463–70. Epub 2013/10/04. 10.1097/SHK.0000000000000044.

31. Gordon S, Martinez FO. Alternative activation of macrophages: Mechanism and functions. *Immunity*. 2010 May 28;32(5):593–604.

32. Locati M, Mantovani A, Sica A. Macrophage activation and polarization as an adaptive component of innate immunity. *Adv Immunol*. 2013;120:163–184.

33. Schlaepfer E, Rochat MA, Duo L, Speck RF. Triggering TLR2, -3, -4, -5, and -8 reinforces the restrictive nature of M1- and M2-polarized macrophages to HIV. *J Virol*. 2014;88(17):9769–9781. doi:10.1128/JVI.01053-14.

34. Quero L, Hanser E, Manigold T, Tiaden AN, Kyburz D. TLR2 stimulation impairs anti-inflammatory activity of M2-like macrophages, generating a chimeric M1/M2 phenotype. *Arthritis Res Ther*. (2017) 19:245. 10.1186/s13075-017-1447-1.

35. Atri C, Guerfali FZ, Laouini D. Role of Human Macrophage Polarization in Inflammation during Infectious Diseases. *Int J Mol Sci*. 2018;19(6):1801. Published 2018 Jun 19. doi:10.3390/ijms19061801.

36. Beyer M., Mallmann M.R., Xue J., Staratschek-Jox A., Vorholt D., Krebs W., Sommer D., Sander J., Mertens C., Nino-Castro A., et al. High-resolution transcriptome of human macrophages. *PLoS ONE*. 2012;7:e45466. doi: 10.1371/journal.pone.0045466.

37. Vogel D.Y., Glim J.E., Stavenuiter A.W., Breur M., Heijnen P., Amor S., Dijkstra C.D., Beelen R.H. Human macrophage polarization in vitro: Maturation and activation methods compared. *Immunobiology*. 2014;219:695–703. doi: 10.1016/j.imbio.2014.05.002.

38. Italiani P., Mazza E.M., Lucchesi D., Cifola I., Gemelli C., Grande A., Battaglia C., Bicciato S., Boraschi D. Transcriptomic profiling of the development of the inflammatory response in human monocytes in vitro. *PLoS ONE*. 2014;9:e87680. doi: 10.1371/journal.pone.0087680.

39. Martinez F.O., Gordon S., Locati M., Mantovani A. Transcriptional profiling of the human monocyte-to-macrophage differentiation and polarization: New molecules and patterns of gene expression. *J. Immunol*. 2006;177:7303–7311. doi: 10.4049/jimmunol.177.10.7303.

40. Zhang Z-X, Huang X, Jiang J, Lau A, Yin Z, Liu W, et al. . Natural killer cells mediate long-term kidney allograft injury. *Transplantation*. (2015) 99:916–24. 10.1097/TP.0000000000000665.

41. Benichou G, Yamada Y, Aoyama A, Madsen JC. Natural killer cells in rejection and tolerance of solid organ allografts. *Curr Opin Organ Transplant*. 2011;16(1):47–53. doi:10.1097/MOT.0b013e32834254cf.

42. Al-Lamki RS, Bradley JR, Pober JS. Endothelial cells in allograft rejection. *Transplantation*. 2008;86(10):1340–1348. doi:10.1097/TP.0b013e3181891d8b.

43. Pratschke J, Stauch D, Kotsch K. Role of NK and NKT cells in solid organ transplantation. *Transpl Int*. 2009;22:859–868. doi: 10.1111/j.1432-2277.2009.00884.x.

44. Kitchens WH, Uehara S, Chase CM, Colvin RB, Russell PS, Madsen JC. The changing role of natural killer cells in solid organ rejection and tolerance. *Transplantation*. 2006;81:811–817. doi: 10.1097/01.tp.0000202844.33794.0e.

45. Langer HF, Chavakis T. Leukocyte-endothelial interactions in inflammation. *J Cell Mol Med*. 2009;13(7):1211–1220. doi:10.1111/j.1582-4934.2009.00811.x.

46. Liao JK. Linking endothelial dysfunction with endothelial cell activation. *J Clin Invest*. 2013;123(2):540–541. doi:10.1172/JCI66843.

47. Tuuminen R, Syrjala S, Krebs R, Keranen MA, Koli K, Abo-Ramadan U, et al. Donor simvastatin treatment abolishes rat cardiac allograft ischemia/reperfusion injury and chronic rejection through microvascular protection. *Circulation*. 2011 Sep 6;124(10):1138–1150.

48. Rezkalla SH, Kloner RA. No-reflow phenomenon. *Circulation*. 2002 Feb 5;105(5):656–662.

49. Yang Q, He GW, Underwood MJ, Yu CM. Cellular and molecular mechanisms of endothelial ischemia/reperfusion injury: perspectives and implications for postischemic myocardial protection. *Am J Transl Res*. 2016;8(2):765–777. Published 2016 Feb 15.

50. Cai H, Harrison DG. Endothelial dysfunction in cardiovascular diseases: the role of oxidant stress. *Circ Res*. 2000;87:840–844.

51. Hirase T., Node K. Endothelial dysfunction as a cellular mechanism for vascular failure. *Am. J. Physiol*. Circ. Physiol. 2012;302:H499–H505. doi: 10.1152/ajpheart.00325.2011.

52. Devan AE, Umpierre D, Harrison ML, et al. Endothelial ischemia-reperfusion injury in humans: association with age and habitual exercise. *Am J Physiol Heart Circ Physiol*. 2011;300(3):H813–H819. doi:10.1152/ajpheart.00845.2010.

53. De Caterina R, Libby P, Peng HB, et al. Nitric oxide decreases cytokine-induced endothelial activation. Nitric oxide selectively reduces endothelial expression of adhesion molecules and proinflammatory cytokines. *J Clin Invest*. 1995;96(1):60–68. doi:10.1172/JCI118074.

54. Tousoulis D, Kampoli AM, Tentolouris C, Papageorgiou N, Stefanadis C. The role of nitric oxide on endothelial function. *Curr Vasc Pharmacol*. 2012;10:4–18.

55. Jin RC, Loscalzo J. Vascular Nitric Oxide: Formation and Function. *J Blood Med*. 2010;2010(1):147–162. doi:10.2147/JBM.S7000.

56. Kuzkaya N, Weissmann N, Harrison DG, Dikalov S. Interactions of peroxynitrite, tetrahydrobiopterin, ascorbic acid, and thiols: implications for uncoupling endothelial nitric-oxide synthase. *J Biol Chem*. 2003;278:22546–22554.

57. Vinson AJ, Rose C, Kiberd BA, et al. Factors Associated With Prolonged Warm Ischemia Time Among Deceased Donor Kidney Transplant Recipients. *Transplant Direct*. 2018;4(5):e342. Published 2018 Apr 18. doi:10.1097/TXD.0000000000000781.

58. Banner NR, Thomas HL, Curnow E, Hussey JC, Rogers CA, Bonser RS. The importance of cold and warm cardiac ischemia for survival after heart transplantation. *Transplantation*. 2008;86(4):542–547.

59. Singh SSA, Dalzell JR, Berry C, Al-Attar N. Primary graft dysfunction after heart transplantation: a thorn amongst the roses. *Heart Fail Rev*. 2019;24(5):805–820. doi:10.1007/s10741-019-09794-1.

60. Kobashigawa J, Zuckermann A, Macdonald P., et al; Consensus Conference participants. Report from a consensus conference on primary graft dysfunction after cardiac transplantation. *J Heart Lung Transplant*. 2014. April;33(4):327-340. doi: 10.1016/j.healun.2014.02.027.

61. George TJ, Arnaoutakis GJ, Beaty CA, Shah AS, Conte JV, Halushka MK. A novel method of measuring cardiac preservation injury demonstrates University of Wisconsin solution is associated with less ischemic necrosis than Celsior in early cardiac allograft biopsy specimens. *J Heart Lung Transplant*. 2012;31(4):410–418. doi:10.1016/j.healun.2011.11.023.

62. Patel JK, Kittleson M, Kobashigawa JA. Cardiac allograft rejection. *Surgeon*. 2011;9:160-7. 10.1016/j.surge.2010.11.023.

63. Weil R 3rd, Clarke DR, Iwaki Y, et al. Hyperacute rejection of a transplanted human heart. *Transplantation*. 1981;32(1):71–72.

64. Kaczorowski DJ, Datta J, Kamoun M, Dries DL, Woo YJ. Profound hyperacute cardiac allograft rejection rescue with biventricular mechanical circulatory support and plasmapheresis, intravenous immunoglobulin, and rituximab therapy. *J Cardiothorac Surg*. 2013;8:48. Published 2013 Mar 16. doi:10.1186/1749-8090-8-48.

65. Kittleson MM, Patel JK, Kobashigawa JA. Chapter 72: cardiac transplantation. In: Fuster V, Harrington RA, Narula J, Eapen ZJ, editors. Hurst's the Heart. 14th ed. New York (NY): *McGraw-Hill*; 2017.

66. Kobashigawa J. Clinical Guide to Heart Transplantation. Los Angeles (CA): *Springer.* 2017.

67. Costanzo MR, Dipchand A, Starling R, et al. The International Society of Heart and Lung Transplantation guidelines for the care of heart transplant recipients. *J Heart Lung Transplant*. 2010;29:914–956.

68. Labarrere CA, Jaeger BR. Biomarkers of heart transplant rejection: the good, the bad, and the ugly! *Transl Res*. 2012;159:238–251.

69. Musick A, Kim A, Glass C. Acute cellular rejection. *PathologyOutlines.com website*. http://www.pathologyoutlines.com/topic/heartacutecellularrejection.html. Accessed March 4th, 2020.

70. Ingulli E. Mechanism of cellular rejection in transplantation. *Pediatr Nephrol*. 2010;25(1):61–74. doi:10.1007/s00467-008-1020-x

71. Tan CD, Baldwin WM, Rodriguez ER. Update on cardiac transplantation pathology. *Arch Pathol Lab Med*. 2007;131:1169–91. 10.1043/1543-2165(2007)131[1169:UOCTP]2.0.CO;2.

72. Auchincloss H, Sultan H. Antigen processing and presentation in transplantation. *Curr Opin Immunol*. (1996) 8:681–7.10.1016/S0952-7915(96)80086-0.

73. Azzawi M, Hasleton PS, Hutchinson IV. TNF-alpha in acute cardiac transplant rejection. *Cytokines Cell Mol Ther*. 1999;5:41–49.

74. Hummel M, Kurian SM, Lin S, et al. Intragraft TNF receptor signaling contributes to activation of innate and adaptive immunity in a renal allograft model. *Transplantation*. 2009;87(2):178–188.

75. Zhang T, Pierson RN 3rd, Azimzadeh AM. Update on CD40 and CD154 blockade in transplant models. *Immunotherapy*. 2015;7(8):899–911. doi:10.2217/IMT.15.54.

76. Weigt SS, Palchevskiy V, Belperio JA. Inflammasomes and IL-1 biology in the pathogenesis of allograft dysfunction. *J Clin Invest*. 2017;127(6):2022–2029. doi:10.1172/JCI93537.

77. Colvin MM, Cook JL, Chang P, et al. Antibody-mediated rejection in cardiac transplantation: emerging knowledge in diagnosis and management: a scientific statement from the American Heart Association. *Circulation*. 2015;131:1608–1639.

78. Berry GJ, Burke MM, Andersen C, et al. The 2013 International Society for Heart and Lung Transplantation Working Formulation for the standardization of nomenclature in the pathologic diagnosis of antibody-mediated rejection in heart transplantation. *J Heart Lung Transplant*. 2013;32:1147–1162.

79. Chih S, Chruscinski A, Ross HJ, Tinckam K, Butany J, Rao V. Antibody-mediated rejection: an evolving entity in heart transplantation. *J Transplant*. 2012;2012:210210. doi:10.1155/2012/210210.

80. Murata K, Baldwin WM., III Mechanisms of complement activation, C4d deposition, and their contribution to the pathogenesis of antibody-mediated rejection. *Transplantation Reviews*. 2009;23(3):139–150.

81. Tambur AR, Pamboukian SV, Costanzo MR, et al. The presence of HLA-directed antibodies after heart transplantation is associated with poor allograft outcome. *Transplantation*. 2005;80:1019–1025.

82. Coutance G, Ouldamar S, Rouvier P, et al. Late antibody-mediated rejection after heart transplantation: mortality, graft function, and fulminant cardiac allograft vasculopathy. *J Heart Lung Transplant*. 2015;34:1050–1057.

83. Skorić B, Čikeš M, Ljubas Maček J, et al. Cardiac allograft vasculopathy: diagnosis, therapy, and prognosis. *Croat Med J*. 2014;55(6):562–576. doi:10.3325/cmj.2014.55.562.

84. Lund LH, Edwards LB, Kucheryavaya AY, Dipchand AI, Benden C, Christie JD, et al. The Registry of the International Society for Heart and Lung Transplantation: thirtieth official adult heart transplant report – 2013; focus theme: age. *J Heart Lung Transplant*. 2013;32:951–64. doi: 10.1016/j.healun.2013.08.006.

85. Ramzy D, Rao V, Brahm J, Miriuka S, Delgado D, Ross HJ. Cardiac allograft vasculopathy: a review. *Can J Surg*. 2005;48(4):319–327.

86. Hiemann NE, Wellnhofer E, Knosalla C, Lehmkuhl HB, Stein J, Hetzer R, Meyer R. Prognostic impact of microvasculopathy on survival after heart transplantation: evidence from 9713 endomyocardial biopsies. *Circulation*. 2007;116(11):1274–1282.

87. Musick A, Glass C. Chronic allograft vasculopathy. *PathologyOutlines.com website*. https://www.pathologyoutlines.com/topic/heartchronicgraftvasculopathy.html. Accessed March 4th, 2020.

88. Weis M, von Scheidt W. Cardiac allograft vasculopathy: A review. *Circulation*. 1997;96:2069–2077. doi: 10.1161/01.CIR.96.6.2069.

89. Vassalli G, Gallino A, Weis M, von Scheidt W, Kappenberger L, von Segesser LK, et al. Alloimmunity and nonimmunologic risk factors in cardiac allograft vasculopathy. *Eur Heart J*. 2003;24(13):1180–8. Epub 2003/07/02. 10.1016/s0195-668x(03)00237-9.

90. Kobashigawa JA, Stevenson LW, Moriguchi JD, et al. Is intravenous glucocorticoid therapy better than an oral regimen for asymptomatic cardiac rejection? A randomized trial. *J Am Coll Cardiol*. 1993;21:1142–1144.

91. Schmauss D, Weis M. Cardiac allograft vasculopathy: recent developments. *Circulation*. 2008. Apr 22;117(16):2131-2141. doi: 10.1161/CIRCULATIONAHA.107.711911.

92. Jennings Douglas L., Lange Nicholas, Shullo Michael, Latif Farhana, Restaino Susan, Topkara Veli K., Takeda Koji, Takayama Hiroo, Naka Yoshifumi, Farr Maryjane, Colombo Paolo, Baker William L. Outcomes associated with mammalian target of rapamycin (mTOR) inhibitors in heart transplant recipients: A meta-analysis. *International Journal of Cardiology*. 2018;265:71–76.

93. Stoica SC, Goddard M, Large SR. The endothelium in clinical cardiac transplantation. *Ann Thorac Surg*. 2002;73:1002–1008.

94. Rifle G, Mousson C, Hervé P. Endothelial cells in organ transplantation: Friends or foes? *Transplantation*. 2006;82:S4–S5.

95. Singhal AK, Symons JD, Boudina S, Jaishy B, Shiu YT. Role of Endothelial Cells in Myocardial Ischemia-Reperfusion Injury. *Vasc Dis Prev*. 2010;7:1–14. doi:10.2174/1874120701007010001.

96. Weis M, Cooke JP. Cardiac allograft vasculopathy and dysregulation of the nitric oxide synthase pathway. *Arterioscler Thromb*. 2003;23:567–75.

97. Seino K, Azuma M, Bashuda H, Fukao K, Yagita H, Okumura K. CD86 (B70/B7-2) on endothelial cells co-stimulates allogeneic CD4+ T cells. *Int Immunol* (1995) 7(8):1331–7.10.1093/intimm/7.8.1331.

98. Jollow KC, Zimring JC, Sundstrom JB, Ansari AA. CD40 ligation induced phenotypic and functional expression of CD80 by human cardiac microvascular endothelial cells. *Transplantation* (1999) 68(3):430–9.10.1097/00007890-199908150-00016.

99. Tan PH, Chan C, Xue SA, Dong R, Ananthesayanan B, Manunta M, et al. Phenotypic and functional differences between human saphenous vein (HSVEC) and umbilical vein (HUVEC) endothelial cells. *Atherosclerosis* (2004) 173(2):171–83.10.1016/j.atherosclerosis.2003.12.011.

100. Pober JS, Merola J, Liu R, Manes TD. Antigen Presentation by Vascular Cells. *Front Immunol*. 2017;8:1907. Published 2017 Dec 22. doi:10.3389/fimmu.2017.01907.

101. Galluzzi L, Vitale I, Aaronson SA, et al. Molecular mechanisms of cell death: recommendations of the Nomenclature Committee on Cell Death 2018. *Cell Death Differ*. 2018;25(3):486–541. doi:10.1038/s41418-017-0012-4.

102. Linkermann A., Hackl M.J., Kunzendorf U., Walczak H., Krautwald S., Jevnikar A.M. Necroptosis in immunity and ischemia-reperfusion injury. *Am. J. Transpl*. 2013;13:2797–2804. doi: 10.1111/ajt.12448.

103. Lau A, et al. RIPK3-mediated necroptosis promotes donor kidney inflammatory injury and reduces allograft survival. *Am J Transplant*. 2013;13(11):2805–2818. doi: 10.1111/ajt.12447.

104. Gan, I, Jiang, J, Lian, D, et al. Mitochondrial permeability regulates cardiac endothelial cell necroptosis and cardiac allograft rejection. *Am J Transplant*. 2019; 19: 686– 698. https://doi.org/10.1111/ajt.15112.

105. Choi ME, Price DR, Ryter SW, Choi AMK. Necroptosis: a crucial pathogenic mediator of human disease. *JCI Insight*. 2019;4(15):e128834. Published 2019 Aug 8. doi:10.1172/jci.insight.128834.

106. Marshall KD, Baines CP. Necroptosis: is there a role for mitochondria?. *Front Physiol*. 2014;5:323. Published 2014 Aug 26. doi:10.3389/fphys.2014.00323.

107. Tsuchiya Y, Nakabayashi O, Nakano H. FLIP the Switch: Regulation of Apoptosis and Necroptosis by cFLIP. *Int J Mol Sci*. 2015;16(12):30321–30341. Published 2015 Dec 18. doi:10.3390/ijms161226232.

108. Safa AR. Roles of c-FLIP in Apoptosis, Necroptosis, and Autophagy. *J Carcinog Mutagen*. 2013;Suppl 6:003. doi:10.4172/2157-2518.S6-003.

109. Dhuriya YK, Sharma D. Necroptosis: a regulated inflammatory mode of cell death. *J Neuroinflammation*. 2018;15(1):199. Published 2018 Jul 6. doi:10.1186/s12974-018-1235-0.

110. Cho YS. The role of necroptosis in the treatment of diseases. *BMB Rep*. 2018;51(5):219–224. doi:10.5483/bmbrep.2018.51.5.074.

111. Wang C, Youle RJ. The role of mitochondria in apoptosis*. *Annu Rev Genet*. 2009;43:95–118. doi:10.1146/annurev-genet-102108-134850.

112. Parsons M.J., Green D.R. Mitochondria in cell death. *Essays Biochem*. 2010;47:99–114. doi: 10.1042/bse0470099.

113. Tait SW, Green DR. Mitochondrial regulation of cell death. *Cold Spring Harb Perspect Biol*. 2013;5(9):a008706. Published 2013 Sep 1. doi:10.1101/cshperspect.a008706.

114. Singh R., Letai A., Sarosiek K. Regulation of apoptosis in health and disease: the balancing act of BCL-2 family proteins. *Nature Reviews Molecular Cell Biology*. 2019;20(3):175–193. doi: 10.1038/s41580-018-0089-8.

115. Lin Y., Choksi S., Shen H. M., Yang Q. F., Hur G. M., Kim Y. S., et al. (2004). Tumor necrosis factor-induced nonapoptotic cell death requires receptor-interacting protein-mediated cellular reactive oxygen species accumulation. *J. Biol. Chem*. 279, 10822–10828 10.1074/jbc.M313141200.

116. Vanlangenakker N., Vanden Berghe T., Bogaert P., Laukens B., Zobel K., Deshayes K., et al. (2011). cIAP1 and TAK1 protect cells from TNF-induced necrosis by preventing RIP1/RIP3-dependent reactive oxygen species production. *Cell Death Differ*. 18, 656–665 10.1038/cdd.2010.138.

117. Ardestani S., Deskins D. L., Young P. P. (2013). Membrane TNF-alpha-activated programmed necrosis is mediated by Ceramide-induced reactive oxygen species. *J. Mol. Signal*. 8, 12 10.1186/1750-2187-8-12.

118. Schulze-Osthoff K., Bakker A. C., Vanhaesebroeck B., Beyaert R., Jacob W. A., Fiers W. (1992). Cytotoxic activity of tumor necrosis factor is mediated by early damage of mitochondrial functions. Evidence for the involvement of mitochondrial radical generation. *J. Biol. Chem*. 267, 5317–5323.

119. Goossens V., Stangé G., Moens K., Pipeleers D., Grooten J. (1999). Regulation of tumor necrosis factor-induced, mitochondria- and reactive oxygen species-dependent cell death by the electron flux through the electron transport chain complex I. *Antioxid. Redox Signal*. 1, 285–295.

120. Temkin V., Huang Q., Liu H., Osada H., Pope R. M. (2006). Inhibition of ADP/ATP exchange in receptor-interacting protein-mediated necrosis. *Mol. Cell. Biol*. 26, 2215–2225 10.1128/MCB.26.6.2215-2225.2006.

121. Zhang D. W., Shao J., Lin J., Zhang N., Lu B. J., Lin S. C., et al. (2009). RIP3, an energy metabolism regulator that switches TNF-induced cell death from apoptosis to necrosis. *Science* 325, 332–336 10.1126/science.1172308.

122. Davis C. W., Hawkins B. J., Ramasamy S., Irrinki K. M., Cameron B. A., Islam K., et al. (2010). Nitration of the mitochondrial complex I subunit NDUFB8 elicits RIP1- and RIP3-mediated necrosis. *Free Radic. Biol. Med*. 48, 306–317 10.1016/j.freeradbiomed.2009.11.001.

123. Wang Z., Jiang H., Chen S., Du F., Wang X. (2012). The mitochondrial phosphatase PGAM5 functions at the convergence point of multiple necrotic death pathways. *Cell* 148, 228–243 10.1016/j.cell.2011.11.030.

124. Zhang L., Jiang F., Chen Y., Luo J., Liu S., Zhang B., et al. (2013). Necrostatin-1 attenuates ischemia injury induced cell death in rat tubular cell line NRK-52E through decreased Drp1 expression. *Int. J. Mol. Sci*. 14, 24742–24754 10.3390/ijms141224742.

125. Baines C. P., Kaiser R. A., Purcell N. H., Blair N. S., Osinska H., Hambleton M. A., et al. (2005). Loss of cyclophilin D reveals a critical role for mitochondrial permeability transition in cell death. *Nature* 434, 658–662 10.1038/nature03434.

126. Nakagawa T., Shimizu S., Watanabe T., Yamaguchi O., Otsu K., Yamagata H., et al. (2005). Cyclophilin D-dependent mitochondrial permeability transition regulates some necrotic but not apoptotic cell death. *Nature* 434, 652–658 10.1038/nature03317.

127. Schinzel A. C., Takeuchi O., Huang Z., Fisher J. K., Zhou Z., Rubens J., et al. (2005). Cyclophilin D is a component of mitochondrial permeability transition and mediates neuronal cell death after focal cerebral ischemia. *Proc. Natl. Acad*. Sci.U.S.A. 102, 12005–12010 10.1073/pnas.0505294102.

128. Tait S. W., Oberst A., Quarato G., Milasta S., Haller M., Wang R., et al. (2013). Widespread mitochondrial depletion via mitophagy does not compromise necroptosis. *Cell Rep*. 5, 878–885 10.1016/j.celrep.2013.10.034.

129. Murphy J. M., Czabotar P. E., Hildebrand J. M., Lucet I. S., Zhang J. G., Alvarez-Diaz S., et al. (2013). The pseudokinase MLKL mediates necroptosis via a molecular switch mechanism. *Immunity* 39, 443–453 10.1016/j.immuni.2013.06.018.

130. Remijsen Q., Goossens V., Grootjans S., Van den Haute C., Vanlangenakker N., Dondelinger Y., et al. (2014). Depletion of RIPK3 or MLKL blocks TNF-driven necroptosis and switches towards a delayed RIPK1 kinase-dependent apoptosis. *Cell Death* Dis. 5, e1004 10.1038/cddis.2013.531.

131. Moujalled D. M., Cook W. D., Murphy J. M., Vaux D. L. (2014). Necroptosis induced by RIPK3 requires MLKL but not Drp1. *Cell Death Dis*. 5, e1086 10.1038/cddis.2014.18.

132. Linkermann A., Bräsen J. H., Darding M., Jin M. K., Sanz A. B., Heller J. O., et al. (2013). Two independent pathways of regulated necrosis mediate ischemia-reperfusion injury. *Proc. Natl. Acad. Sci. U.S.A*. 110, 12024–12029 10.1073/pnas.1305538110.

133. Cai Z., Jitkaew S., Zhao J., Chiang H. C., Choksi S., Liu J., et al. (2014). Plasma membrane translocation of trimerized MLKL protein is required for TNF-induced necroptosis. *Nat. Cell Biol*. 16, 55–65 10.1038/ncb2883.

134. Chen X., Li W., Ren J., Huang D., He W. T., Song Y., et al. (2014). Translocation of mixed lineage kinase domain-like protein to plasma membrane leads to necrotic cell death. *Cell Res*. 24, 105–121 10.1038/cr.2013.171.

135. Dondelinger Y., Declercq W., Montessuit S., Roelandt R., Goncalves A., Bruggeman I., et al. (2014). MLKL compromises plasma membrane integrity by binding to phosphatidylinositol phosphates. *Cell Rep*. 7, 971–981 10.1016/j.celrep.2014.04.026.

136. Wang H., Sun L., Su L., Rizo J., Liu L., Wang L. F., et al. (2014). Mixed lineage kinase domain-like protein MLKL causes necrotic membrane disruption upon phosphorylation by RIP3. *Mol. Cell* 54, 133–146 10.1016/j.molcel.2014.03.003.

137. Halestrap AP. What is the mitochondrial permeability transition pore? *J Mol Cell Cardiol*. 2009;46:821–31.

138. Karch J, Molkentin JD. Identifying the components of the elusive mitochondrial permeability transition pore. *Proc Natl Acad Sci U S A*. 2014;111(29):10396–10397. doi:10.1073/pnas.1410104111.

139. Morciano G., Bonora M., Campo G., Aquila G., Rizzo P., Giorgi C., et al. (2017). Mechanistic role of mPTP in ischemia-reperfusion injury. *Adv. Exp. Med. Biol.* 982 169–189. 10.1007/978-3-319-55330-6-9.

140. Hausenloy DJ, Duchen MR, Yellon DM. Inhibiting mitochondrial permeability transition pore opening at reperfusion protects against ischaemia-reperfusion injury. *Cardiovasc Res*. 2003;60(3):617–625. doi:10.1016/j.cardiores.2003.09.025.

141. Ong SB, Samangouei P, Kalkhoran SB, Hausenloy DJ. The mitochondrial permeability transition pore and its role in myocardial ischemia reperfusion injury. *J Mol Cell Cardiol*. 2015;78:23–34.

142. Karch J, et al. Bax and Bak function as the outer membrane component of the mitochondrial permeability pore in regulating necrotic cell death in mice. *eLife*. 2013;2:e00772.

143. Karch J, Kanisicak O, Brody MJ, Sargent MA, Michael DM, Molkentin JD. Necroptosis Interfaces with MOMP and the MPTP in Mediating Cell Death. *PLoS One*. 2015;10(6):e0130520. Published 2015 Jun 10. doi:10.1371/journal.pone.0130520.

144. Wong R, Steenbergen C, Murphy E. Mitochondrial permeability transition pore and calcium handling. *Methods Mol Biol*. 2012;810:235–242. doi:10.1007/978-1-61779-382-0_15.

145. Benítez-Guzmán A, Arriaga-Pizano L, Morán J, Gutiérrez-Pabello JA. Endonuclease G takes part in AIF-mediated caspase-independent apoptosis in Mycobacterium bovis-infected bovine macrophages. *Vet Res*. 2018;49(1):69. Published 2018 Jul 18. doi:10.1186/s13567-018-0567-1.

146. Marzetti E, Wohlgemuth SE, Lees HA, et al. Age-related activation of mitochondrial caspase-independent apoptotic signaling in rat gastrocnemius muscle. *Mechanisms of Ageing and Development*. 2008 Sep;129(9):542-549. DOI: 10.1016/j.mad.2008.05.005.

147. Bano D, Prehn JHM. Apoptosis-Inducing Factor (AIF) in Physiology and Disease: The Tale of a Repented Natural Born Killer. *EBioMedicine*. 2018;30:29–37. doi:10.1016/j.ebiom.2018.03.016.

148. Sevrioukova IF. Apoptosis-inducing factor: structure, function, and redox regulation. *Antioxid Redox Signal*. 2011;14(12):2545–2579. doi:10.1089/ars.2010.3445.

149. Fatokun AA, Dawson VL, Dawson TM. Parthanatos: mitochondrial-linked mechanisms and therapeutic opportunities. *Br J Pharmacol*. 2014;171(8):2000–2016. doi:10.1111/bph.12416.

150. Klein JA, et al. The harlequin mouse mutation downregulates apoptosis-inducing factor. *Nature*. 2002;419:367–374. doi: 10.1038/nature01034.

151. Zhang W, Li D, Mehta JL. Role of AIF in human coronary artery endothelial cell apoptosis. *American Journal of Physiology: Heart and Circulatory Physiology*. 2004;286(1):H354–H358.

152. Zhu C, Wang X, Deinum J, et al. Cyclophilin A participates in the nuclear translocation of apoptosis-inducing factor in neurons after cerebral hypoxia-ischemia. *J Exp Med*. 2007;204(8):1741–1748. doi:10.1084/jem.20070193.

153. Doti, N., Reuther, C., Scognamiglio, P. *et al.* Inhibition of the AIF/CypA complex protects against intrinsic death pathways induced by oxidative stress. *Cell Death Dis* 5, e993 (2014) doi:10.1038/cddis.2013.518.

154. Zhao H, Jaffer T, Eguchi S, Wang Z, Linkermann A, Ma D. Role of necroptosis in the pathogenesis of solid organ injury. *Cell Death Dis*. 2015;6(11):e1975. Published 2015 Nov 19. doi:10.1038/cddis.2015.316.

155. Han J, Zhong CQ, Zhang DW. Programmed necrosis: Backup to and competitor with apoptosis in the immune system. *Nat Immunol*. 2011; 12: 1143–1149.

156. Kaczmarek A, Vandenabeele P, Krysko DV. Necroptosis: The release of damage-associated molecular patterns and its physiological relevance. *Immunity*. 2013; 38: 209–223.

157. Linkermann A, Green DR. Necroptosis. *N Engl J Med*. 2014;370(5):455–465. doi:10.1056/NEJMra1310050.

158. Mannon RB. Necroptosis in solid organ transplantation: a missing link to immune activation. *Am J Transplant*. 2013;13:2785–2786.

159. He S., Wang L., Miao L., Wang T., Du F., Zhao L., et al. (2009). Receptor interacting protein kinase-3 determines cellular necrotic response to TNF-alpha. *Cell* 137, 1100–1111 10.1016/j.cell.2009.05.021.

160. Culic O., Gruwel M. L., Schrader J. (1997). Energy turnover of vascular endothelial cells. *Am. J. Physiol. Physiol.* 273 C205–C213. 10.1152/ajpcell.1997.273.1.C205.

161. Quintero M, Colombo SL, Godfrey A, Moncada S. Mitochondria as signaling organelles in the vascular endothelium. *Proc Natl Acad Sci U S A*. 2006;103(14):5379–5384. doi:10.1073/pnas.0601026103.

162. Davidson S. M., Duchen M. R. Endothelial mitochondria: contributing to vascular function and disease. *Circulation Research*. 2007;100(8):1128–1141. doi: 10.1161/01.RES.0000261970.18328.1d.

163. Zhang H, Wang P, Bisetto S, et al. A novel fission-independent role of dynamin-related protein 1 in cardiac mitochondrial respiration. *Cardiovasc Res*. 2017;113(2):160–170. doi:10.1093/cvr/cvw212.

164. Roca F. J., Ramakrishnan L. (2013). TNF dually mediates resistance and susceptibility to mycobacteria via mitochondrial reactive oxygen species. *Cell* 153, 521–534 10.1016/j.cell.2013.03.022.

165. Ch'en I. L., Tsau J. S., Molkentin J. D., Komatsu M., Hedrick S. M. (2011). Mechanisms of necroptosis in T cells. *J. Exp. Med*. 208, 633–641 10.1084/jem.20110251.

166. Murphy RC, Schneider E, Kinnally KW. Overexpression of Bcl-2 suppresses the calcium activation of a mitochondrial megachannel. *FEBS Lett*. 2001;497:73–76.

167. Crompton M. On the involvement of mitochondrial intermembrane junctional complexes in apoptosis. *Curr Med Chem*. 2003;10:1473–84.

168. Green DR, Kroemer G. The pathophysiology of mitochondrial cell death. *Science*. 2004;305:626–9.

169. Hurst S, Hoek J, Sheu SS. Mitochondrial Ca^{2+} and regulation of the permeability transition pore. *J Bioenerg Biomembr*. 2017;49(1):27–47. doi:10.1007/s10863-016-9672-x.

170. Tan Y, Wu C, De Veyra T, Greer PA. Ubiquitous calpains promote both apoptosis and survival signals in response to different cell death stimuli. *J Biol Chem*. (2006) 281:17689–98. 10.1074/jbc.M601978200.

171. Gabellini C, Trisciuoglio D, Del Bufalo D. Non-canonical roles of Bcl-2 and Bcl-xL proteins: relevance of BH4 domain. *Carcinogenesis*. 2017;38(6):579–587. doi: 10.1093/carcin/bgx016.

172. Delavallée L, Cabon L, Galán-Malo P, Lorenzo HK, Susin SA. AIF-mediated caspase-independent necroptosis: a new chance for targeted therapeutics. *IUBMB Life*. 2011;63: 221–232. 10.1002/iub.432.

173. Chen Q, Szczepanek K, Hu Y, Thompson J, Lesnefsky EJ. A deficiency of apoptosis inducing factor (AIF) in Harlequin mouse heart mitochondria paradoxically reduces ROS generation during ischemia-reperfusion. *Front Physiol*. 2014;5:271. Published 2014 Jul 22. doi:10.3389/fphys.2014.00271.

174. Plesnila N., Zhu C., Culmsee C., Groger M., Moskowitz M.A., Blomgren K. Nuclear translocation of apoptosis-inducing factor after focal cerebral ischemia. *J. Cereb. Blood Flow Metab*. 2004;24:458–466.

175. Kim G.T., Chun Y.S., Park J.W., Kim M.S. Role of apoptosis-inducing factor in myocardial cell death by ischemia-reperfusion. *Biochem. Biophys. Res. Commun*. 2003;309:619–624.

176. Culmsee C, Zhu C, Landshamer S, et al. Apoptosis-inducing factor triggered by poly(ADP-ribose) polymerase and Bid mediates neuronal cell death after oxygen-glucose deprivation and focal cerebral ischemia [published correction appears in *J Neurosci*. 2005 Nov 16;25(46):table of contents. Pellechia, Maurizio [corrected to Pellecchia, Maurizio]]. *J Neurosci*. 2005;25(44):10262–10272. doi:10.1523/JNEUROSCI.2818-05.2005.

177. Lan S LF, Zhao G, Zhou T, Wu C, Kou J, Fan R, Qi X, Li Y, Jiang Y, Bai T, Li P, Liu L, Hao D, Zhang L, Li Y, Liu JY. Cyclosporine A increases hair follicle growth by suppressing apoptosis-inducing factor nuclear translocation: a new mechanism. *Fundamental and Clinical Pharmacology.* 2015;29:191–203. doi: 10.1111/fcp.12100.

178. Hu WL, Dong HY, Li Y, Ojcius DM, Li SJ, Yan J. Bid-Induced Release of AIF/EndoG from Mitochondria Causes Apoptosis of Macrophages during Infection with *Leptospira interrogans*. *Front Cell Infect Microbiol*. 2017;7:471. Published 2017 Nov 14. doi:10.3389/fcimb.2017.00471.

179. Pacher P, Szabo C. Role of the peroxynitrite-poly(ADP-ribose) polymerase pathway in human disease. *Am J Pathol*. 2008;173:2–13.

180. Prado Spalm F. H., Vera M. S., Dibo M. J., Simón M. V., Politi L. E., Rotstein N. P. (2018). Ceramide induces the death of retina photoreceptors through activation of parthanatos. *Mol. Neurobiol.* 10.1007/s12035-018-1402-4.

181. Kim JH, Kim J, Roh J, Park CS, Seoh JY, Hwang ES. Reactive oxygen species-induced parthanatos of immunocytes by human cytomegalovirus-associated substance. *Microbiol Immunol*. 2018;62(4):229–242. doi:10.1111/1348-0421.12575.

182. Wen JJ, Yin YW, Garg NJ. PARP1 depletion improves mitochondrial and heart function in Chagas disease: Effects on POLG dependent mtDNA maintenance. *PLoS Pathog*. 2018;14(5):e1007065. Published 2018 May 31. doi:10.1371/journal.ppat.1007065.

183. Fuyu Cheng, Wei Yuan, Mengfei Cao, Rui Chen, Xiuli Wu, and Jinchuan Yan. Cyclophilin A Protects Cardiomyocytes against Hypoxia/Reoxygenation-Induced Apoptosis via the AKT/Nox2 Pathway. *Oxidative Medicine and Cellular Longevity,* vol. 2019, Article ID 2717986, 11 pages, 2019. https://doi.org/10.1155/2019/2717986.

184. Nighoghossian N, Ovize M, Mewton N, Ong E, Cho TH. Cyclosporine A, a potential therapy of ischemic reperfusion injury. A common history for heart and brain. *Cerebrovasc Dis*. 2016;42:309. doi: 10.1159/000446850.

185. Schneider, M. D. (2005). Cyclophilin D: Knocking On Deaths Door. *Science Signaling*,2005(287).

186. Matsumoto, S., Friberg, H., Ferrand-Drake, M., & Wieloch, T. (1999). Blockade of the Mitochondrial Permeability Transition Pore Diminishes Infarct Size in the Rat after Transient Middle Cerebral Artery Occlusion. *Journal of Cerebral Blood Flow & Metabolism*, 19(7), 736– 741. https://doi.org/10.1097/00004647-199907000-00002.

187. Waldmeier P.C., Zimmermann K., Qian T., Tintelnot-Blomley M., Lemasters J.J. Cyclophilin D as a drug target. *Curr. Med. Chem*. 2003;10:1485–1506. doi: 10.2174/0929867033457160.

188. Marc Fransen, Cyclophilin D: a therapeutic target to counteract reactive oxygen species–mediated damage in neurodegenerative disease?, *Brain*, Volume 135, Issue 12, December 2012, Pages 3525–3526, https://doi.org/10.1093/brain/aws304.

189. Rao VK, Carlson EA, Yan SS. Mitochondrial permeability transition pore is a potential drug target for neurodegeneration. *Biochim Biophys Acta*. 2014;1842(8):1267–1272. doi:10.1016/j.bbadis.2013.09.003.

190. Warne J, Pryce G, Hill JM, et al. Selective Inhibition of the Mitochondrial Permeability Transition Pore Protects against Neurodegeneration in Experimental Multiple Sclerosis. *J Biol Chem*. 2016;291(9):4356–4373. doi:10.1074/jbc.M115.700385.

191. Garbaisz D, Turoczi Z, Aranyi P, Fulop A, Rosero O, Hermesz E, et al. (2014) Attenuation of Skeletal Muscle and Renal Injury to the Lower Limb following Ischemia-Reperfusion Using mPTP Inhibitor NIM-811. *PLoS ONE* 9(6): e101067. https://doi.org/10.1371/journal.pone.0101067.

192. Theruvath TP, Snoddy MC, Zhong Z, Lemasters JJ. Mitochondrial permeability transition in liver ischemia and reperfusion: role of c-Jun N-terminal kinase 2. *Transplantation*. 2008;85(10):1500–1504. doi:10.1097/TP.0b013e31816fefb5.

193. Tran DT, Esckilsen S, Mulligan J, Mehrotra S, Atkinson C, Nadig SN. Impact of Mitochondrial Permeability on Endothelial Cell Immunogenicity in Transplantation. *Transplantation*. 2018;102(6):935–944. doi:10.1097/TP.0000000000002163.

194. Weinlich R, Oberst A, Beere HM, Green DR. Necroptosis in development, inflammation and disease. *Nat Rev Mol Cell Biol*. 2017;18:127–136. doi: 10.1038/nrm.2016.149.

195. Dhuriya, Y.K., Sharma, D. Necroptosis: a regulated inflammatory mode of cell death. *J Neuroinflammation* 15, 199 (2018) doi:10.1186/s12974-018-1235-0.

196. Newton K, Manning G. Necroptosis and inflammation. *Annu Rev Biochem*. (2016) 85:743–63. 10.1146/annurev-biochem-060815-014830.

197. Degterev A, Maki JL, Yuan J. Activity and specificity of necrostatin-1, small-molecule inhibitor of RIP1 kinase. *Cell Death Differ*. 2013;20(2):366. doi:10.1038/cdd.2012.133.

198. Degterev A, Ofengeim D, Yuan J. Targeting RIPK1 for the treatment of human diseases. *Proc Natl Acad Sci U S A*. 2019;116(20):9714–9722. doi:10.1073/pnas.1901179116.

199. Takahashi N, Duprez L, Grootjans S, et al. Necrostatin-1 analogues: critical issues on the specificity, activity and in vivo use in experimental disease models. *Cell Death Dis*. 2012;3(11):e437. Published 2012 Nov 29. doi:10.1038/cddis.2012.176.

200. Linkermann A, Brasen JH, De Zen F, et al. Dichotomy between RIP1- and RIP3-mediated necroptosis in tumor necrosis factor alpha-induced shock. *Mol Med*. 2012; 18: 577–586.

201. Degterev A, Huang Z, Boyce M, et al. Chemical inhibitor of nonapoptotic cell death with therapeutic potential for ischemic brain injury. *Nat Chem Biol*. 2005;1(2):112–119. doi:10.1038/nchembio711.

202. Degterev A, Hitomi J, Germscheid M, et al. Identification of RIP1 kinase as a specific cellular target of necrostatins. *Nat Chem Biol*. 2008;4(5):313–321. doi:10.1038/nchembio.83.

203. Teng X., Degterev A., Jagtap P., Xing X., Choi S., Denu R., Yuan J., Cuny G.D. Structure-activity relationship study of novel necroptosis inhibitors. *Bioorg Med. Chem Lett*. 2005;15:5039–5044. doi: 10.1016/j.bmcl.2005.07.077.

204. Berger SB, Harris P, Nagilla R, et al. Characterization of GSK'963: a structurally distinct, potent and selective inhibitor of RIP1 kinase. *Cell Death Discov*. 2015;1:15009. Published 2015 Jul 27. doi:10.1038/cddiscovery.2015.9.

205. Harris PA, et al. Discovery of a first-in-class receptor interacting protein 1 (RIP1) kinase specific clinical candidate (GSK2982772) for the treatment of inflammatory diseases. *J. Med. Chem*. 2017;60:1247–1261. doi: 10.1021/acs.jmedchem.6b01751.

206. Hou J, Ju J, Zhang Z, et al. Discovery of potent necroptosis inhibitors targeting RIPK1 kinase activity for the treatment of inflammatory disorder and cancer metastasis. *Cell Death Dis*. 2019;10(7):493. Published 2019 Jun 24. doi:10.1038/s41419-019-1735-6.

207. Chen T., Pan H., Li J., Xu H., Jin H., Qian C., et al. (2018). Inhibiting of RIPK3 attenuates early brain injury following subarachnoid hemorrhage: possibly through alleviating necroptosis. *Biomed. Pharmacother*. 107, 563–570. 10.1016/j.biopha.2018.08.056.

208. Mandal P, Berger SB, Pillay S, et al. RIP3 induces apoptosis independent of pronecrotic kinase activity. *Mol Cell*. 2014;56(4):481–495. doi:10.1016/j.molcel.2014.10.021.

209. Sun L, et al. Mixed lineage kinase domain-like protein mediates necrosis signaling downstream of RIP3 kinase. *Cell*. 2012;148:213–227. doi: 10.1016/j.cell.2011.11.031.

210. Dong W, Zhang M, Zhu Y, et al. Protective effect of NSA on intestinal epithelial cells in a necroptosis model. *Oncotarget*. 2017;8(49):86726–86735. Published 2017 Sep 30. doi:10.18632/oncotarget.21418.

211. Tedesco D, Haragsim L. Cyclosporine: a review. *J Transplant*. 2012;2012:230386. doi:10.1155/2012/230386.

212. Hariharan S, Johnson CP, Bresnahan BA, Taranto SE, McIntosh MJ, Stablein D. Improved graft survival after renal transplantation in the United States, 1988 to 1996. *The New England Journal of Medicine*. 2000;342(9):605–612.

213. Vincenti F, Ramos E, Brattstrom C, et al. Multicenter trial exploring calcineurin inhibitors avoidance in renal transplantation. *Transplantation*. 2001;71(9):1282–1287.

214. Larson TS, Dean PG, Stegall MD, et al. Complete avoidance of calcineurin inhibitors in renal transplantation: a randomized trial comparing sirolimus and tacrolimus. *American Journal of Transplantation*. 2006;6(3):514–522.

215. Ekberg H, Grinyó J, Nashan B, et al. Cyclosporine sparing with mycophenolate mofetil, daclizumab and corticosteroids in renal allograft recipients: the CAESAR study. *American Journal of Transplantation*. 2007;7(3):560–570.

216. Ekberg H, Tedesco-Silva H, Demirbas A, et al. Reduced exposure to calcineurin inhibitors in renal transplantation. *The New England Journal of Medicine*. 2007;357(25):2562–2575.

217. Baroja-Mazo A, Revilla-Nuin B, Ramírez P, Pons JA. Immunosuppressive potency of mechanistic target of rapamycin inhibitors in solid-organ transplantation. *World J Transplant*. 2016;6(1):183–192. doi:10.5500/wjt.v6.i1.183.

218. Guibert EE, Petrenko AY, Balaban CL, Somov AY, Rodriguez JV, Fuller BJ. Organ Preservation: Current Concepts and New Strategies for the Next Decade. *Transfus Med Hemother*. 2011;38(2):125–142. doi:10.1159/000327033.

219. Hameed AM, Hawthorne WJ, Pleass HC. Advances in organ preservation for transplantation. *ANZ J Surg*. 2017;87(12):976–980.

220. Van Raemdonck D, Neyrinck A, Rega F, et al. Machine perfusion in organ transplantation: a tool for ex-vivo graft conditioning with mesenchymal stem cells? *Curr Opin Organ Transplant*. 2013;18:24-33. 10.1097/MOT.0b013e32835c494f.

221. Zeuzem S, Flisiak R, Vierling JM, Mazur W, Mazzella G, Thongsawat S, Abdurakhmanov D, Van Kính N, Calistru P, Heo J, et al. ESSENTIAL II Study Group (2015) Randomised clinical trial: alisporivir combined with peginterferon and ribavirin in treatment-naive patients with chronic HCV genotype 1 infection (ESSENTIAL II). *Aliment Pharmacol Ther*. 42:829–844.

222. Stanciu C, Trifan A, Muzica C, Sfarti C. (2019) Efficacy and safety of alisporivir for the treatment of hepatitis C infection. *Expert Opin Pharmacother*. 20:379–384.

223. Faustman DL, Davis M. TNF Receptor 2 and Disease: Autoimmunity and Regenerative Medicine. *Front Immunol*. 2013;4:478. Published 2013 Dec 23. doi:10.3389/fimmu.2013.00478.

224. Pimentel-Muinos FX, Seed B. Regulated commitment of TNF receptor signaling: a molecular switch for death or activation. *Immunity*. (1999) 11:783–9310.1016/S1074-7613(00)80152-1.

225. Ando D, Inoue M, Kamada H, et al. Creation of mouse TNFR2-selective agonistic TNF mutants using a phage display technique. *Biochem Biophys Rep*. 2016;7:309–315. Published 2016 Jun 8. doi:10.1016/j.bbrep.2016.06.008.

226. Atretkhany KN, Mufazalov IA, Dunst J, et al. Intrinsic TNFR2 signaling in T regulatory cells provides protection in CNS autoimmunity. *Proc Natl Acad Sci USA*. 2018;115(51):13051–13056. doi:10.1073/pnas.1807499115.

227. Ameloot P, et al. Identification of tumor necrosis factor (TNF) amino acids crucial for binding to the murine p75 TNF receptor and construction of receptor-selective mutants. *J Biol Chem*. 2001;276:37426–37430.

CURRICULUM VITAE

Name: Adnan Qamar

Post-secondary Education and Degrees:

2017 – Present: MSc Pathology & Laboratory Medicine
University of Western Ontario – Canada

2014: ECFMG Certification
Educational Commission for Foreign Medical Graduates – USA

2012: Bachelor of Medicine; Bachelor of Surgery
University of Health Sciences – Pakistan

Publications:

Yau M., Khattab A., Qamar A., et al. (2018). Congenital Adrenal Hyperplasia. *BMJ Best Practice*, [http://bestpractice.bmj.com/topics/en-us/699].

Khattab A., Yau M., Qamar A., et al. (2017). Long term outcomes in 46, XX adult patients with congenital adrenal hyperplasia reared as males. *The Journal of Steroid Biochemistry and Molecular Biology*, Volume 165, Part A, p.12-17.

Conferences:

ABSTRACT TITLE: Mechanism of Mitochondria-Regulated Necroptosis in Heart Graft Ischemia-Reperfusion Injury and Transplant Rejection – *Adnan Qamar, Patrick McLeod, Jifu Jiang, Xuyan Huang, Anthony M Jevnikar and Zhu-Xu Zhang*.

- American Transplant Congress 2019 – Boston, MA
- Medical Resident Research Day 2019 – London, ON
- London Health Research Day 2019 – London, ON
- Pathology and Laboratory Medicine Research Day 2019 – London, ON
- Medical Resident Research Day 2018 – London, ON
- Pathology and Laboratory Medicine Research Day 2018 – London, ON

Platform Presentations:

Mitochondrial Permeability Regulates Heart Graft Ischemia-Reperfusion Injury and Allograft Rejection. Canadian Society of Transplantation 2019 Annual Scientific Meeting, Oct 18th, 2019, Banff, AB.